HOST UNIVERSITY: Ghent University

FACULTY: Faculty of Engineering

DEPARTMENT: Department of Flow, Heat and Combustion Mechanics

Academic Year 2017-2019

Accuracy of Numerical Simulations of Water Sprays in a Lagrangian-Eulerian Framework

Georgios Pakos

Promoters: Prof. Bart Merci, dr. Tarek Beji

Master thesis submitted in the Erasmus Mundus Study Programme

International Master of Science in Fire Safety Engineering

DISCLAIMER

This thesis is submitted in partial fulfilment of the requirements for the degree of *The International Master of Science in Fire Safety Engineering (IMFSE)*. This thesis has never been submitted for any degree or examination to any other University/programme. The author(s) declare(s) that this thesis is original work except where stated. This declaration constitutes an assertion that full and accurate references and citations have been included for all material, directly included and indirectly contributing to the thesis. The author(s) gives (give) permission to make this master thesis available for consultation and to copy parts of this master thesis for personal use. In the case of any other use, the limitations of the copyright have to be respected, in particular with regard to the obligation to state expressly the source when quoting results from this master thesis. The thesis supervisor must be informed when data or results are used.

Read and approved

Georgios Pakos

30.04.2019

Abstract

The thesis presents a detailed study on the accuracy of the water spray numerical simulations, concerning the statistical error that is induced by the number of Lagrangian particles (N_p), which is prescribed to represent the water spray pattern. A wide variety of nozzles that produce water droplets with mean diameters ($Dv_{0.5}$), ranging from 35 to 1000 μm, have been used to conduct a series of numerical simulations (experiments) with the Fire Dynamics Simulator (FDS). The simulation results were analyzed to derive prediction models that allow for the estimation of the appropriate number of particles that eliminates the statistical error (critical N_p or $N_{p,cr}$). The effect of the computational mesh on the $N_{p,cr}$ is also investigated. The N_p, as a simulation parameter, significantly affects the simulation results. In addition, the study proves that the FDS default value $N_p = 5 \times 10^3 s^{-1}$ fails to accurately represent any water spray within the aforementioned range and suggests a power law relation between the $N_{p,cr}$ and the $Dv_{0.5}$, which confirms the proportionality of the statistical error and the quantity $1/\sqrt{N_p}$, and reveals a homogeneous behavior of the $N_{p,cr}$ for $Dv_{0.5}$ higher than 400 μm. Finally, the present work illustrates that the CPU time increases either linearly or exponentially, as the N_p increases.

Abstract (Greek)

Η παρούσα διπλωματική εργασία μελετά την ακρίβεια των αριθμητικών προσομοιώσεων νέφους νερού, σε σχέση με το στατιστικό σφάλμα που προκύπτει εξαιτίας του αριθμού των Lagrangian σωματιδίων N_p που χρησιμοποιούνται για την αναπαράσταση του νέφους μιας μεγάλης ποικιλίας ακροφυσίων, τα οποία παράγουν σταγονίδια με μέσες διαμέτρους από 35 έως 1000 μm. Μελετάται επίσης η επίδραση του κανάβου στον απαιτούμενο N_p. Για τη διενέργεια των προσομοιώσεων χρησιμοποιήθηκε το λογισμικό FDS και τα αποτελέσματα αναλύθηκαν βάσει τριών προτεινόμενων μεθόδων, καθεμία από τις οποίες κατέληξε σε μοντέλα πρόβλεψης του απαιτούμενου για την απαλοιφή του σφάλματος κάθε φορά $(N_{p,cr})$, ως συνάρτηση της διαμέτρου και του μεγέθους των κελιών του κανάβου. Επιπλέον, τα συμπεράσματα της μελέτης κατέδειξαν, ότι ο προκαθορισμένος αριθμός $N_p = 5 \times 10^3 s^{-1}$ δεν είναι αρκετός για την ακριβή αναπαράσταση κανενός νέφους στο εύρος των διαμέτρων που μελετήθηκαν, το στατιστικό σφάλμα είναι ανάλογο του $1/\sqrt{N_p}$, η σχέση $N_{p,cr}$ και διαμέτρου συμφωνεί με την κατανομή νόμου δύναμης, η συμπεριφορά του $N_{p,cr}$ για διαμέτρους μεγαλύτερες των 400 μm είναι ομογενής και τέλος, ότι ο υπολογιστικός χρόνος των προσομοιώσεων αυξάνεται είτε γραμμικά είτε εκθετικά καθώς αυξάνεται ο αριθμός των N_p.

Table of Contents

List of Abbreviations

ADD	Actual Delivered Density
ANOVA	Analysis of Variance
C	Coarse
CFD	Computational Fluid Dynamics
CFL	Courant–Friedrichs–Lewy
CNF	Cumulative Number Fraction
CPU	Central Processing Unit
CVF	Cumulative Volume Fraction
dev	Deviation
D10	$Dv_{0.1}$, characteristic diameter (µm)
D32	Sauter Mean Diameter (µm)
F	Fine
FDS	Fire Dynamics Simulator
GB	Gigabyte
GHz	Gigahertz
HPC	High Performance Computer
IMFSE	International Master in Fire Safety Engineering
M	Medium
MC	Mass Concentration (kg/m^3)
NFD	Number Fraction Distribution
NFPA	National Fire Protection Association
PDF	Probability Density Function
PDPA	Phase Doppler Particle Analysis
PF	Particle Flux(lpm/m^2)
R&D	Research and Development
S	Simulation
SFPE	Society of Fire Protection Engineers
SMD	Sauter Mean Diameter (µm)
SPSS	Statistical Package for the Social Sciences
T	Time (min)
VMD	Volume Mean Diameter (µm)

List of Symbols

C	Global Weighting Constant
C_d	Friction Losses Factor
C_i	Computing Weighting Constants
cm	Centimeters
d_m	Mean diameter, (μm)
D_{32}	Sauter Mean Diameter, (μm)
$Dv_{0.1}$	10% Characteristic Diameter, (μm)
$Dv_{0.5}$	Volume Median Diameter or Mean Diameter, (μm)
$Dv_{0.9}$	90% Characteristic Diameter, (μm)
K	Nominal Discharge Coefficient. $\left(l/min\, bar^{1/2}\right)$
lpm	Liters per minute
m	Meter
$\bar{m}_d$	Average Mass of Water Droplets, (kg)
min	Minute
mm	Millimeter
$\dot{m}_w$	Water Mass Flow Rate (kg/s)
n	Representative Number of Droplets
N	Actual Number of Water Droplets
N_p	Number of Computational Particles (s^{-1})
$N_{p,cr}$	Critical Number of Computational Particles (s^{-1})
°C	Degrees Celsius
P	Nozzle Operating Pressure (bar)
Q	Volumetric Flow Rate (l/min)
R	Offset Distance (m)
R^2	Coefficient of Determination
s	second
u_0	Initial Droplet Velocity (m/s)
γ	Width of the Rosin-Rammler Distribution
ε	Error (%)
θ	Elevation Angle (°)
φ	Azimuthal Angle (°)
μm	Micrometer
ρ	Liquid Density (kg/m^3)
ρ_w	Water Density (kg/m^3)

List of Tables and Figures

List of Tables

List of Figures

1. Introduction & Objectives

1.1 Introduction

1.1.1 Water Mist Systems and the Need for Numerical Simulations

It is generally accepted that the water sprays have been one of the most reliable and effective methods to control or suppress a fire. Over the past decades, water-based fire suppression systems, such as sprinklers and water mists, have been proved, among other techniques, a favorable fire suppression system and have been widely used, as an effective method in the field of fire protection engineering, mainly because of the water's physical properties. The high heat capacity and latent heat of vaporization, enable water to absorb a significant quantity of heat from flames and fuels [1][2].

Even though fire sprinklers and water mist systems serve both the same goal, namely, to offer protection against fire, the mechanisms by which the aforementioned goal is achieved, differ in these two systems. Fire sprinklers are designed in principle to deliver water to the burning material, in order to reduce the burning rate of the fuel, to wet the surroundings combustibles and to prohibit the flame spread. This design objective is, not only achieved when the sprinkler spray has sufficient momentum to penetrate the fire plume and reach the burning combustibles, but also when it has sufficient heat absorption capability to lower the temperature of the fire environment [3]. The sprinkler systems, having relatively large water droplets, suppress a fire by direct cooling of the fire seat and the thermal plume [4].

Water mist systems, on the contrary, produce finer and significantly smaller water droplets and suppress or control the fire by heat removal, oxygen displacement and thermal radiation attenuation [5]. The heat extraction and the oxygen displacement are referred in [2] as primary suppression mechanisms, whereas the thermal radiation attenuation as a secondary mechanism. Either primary or secondary, all three mechanisms depend on the evaporation of the water droplets, which indicates that the evaporation of the water droplets plays a key role in the performance of such systems. For a given water volume, the smaller the water droplets, the larger the exchange surface between the droplets and the surrounding area [6].

Hence, it can be deduced that the main difference between the sprinkler and the water mist systems, which apparently results in the differences in the suppression mechanisms, is the water droplet size. The water mist systems generate very fine droplets. This is a key parameter that determines the performance of the water mist system, since it governs the suppression mechanisms [5]. According to NFPA 750 [7], systems that produce water sprays, for which the characteristic diameter $Dv_{0.99}$, for the flow-weighted cumulative volumetric distribution of water droplets, is less than 1000 microns, can be considered as water mists. Typically, the droplets of the water mist systems are much smaller, in the range of 20μm to 500μm, depending on the water pressure and the method used to create the droplets [8]. Correspondingly, the standard sprinkler-sprays contain droplet diameters larger than 1 mm.

The very fine dispersion of the water mist droplets allows them to perform gaseous-like behavior, which explains also why the water mist systems have become a very appealing substitute of traditional gaseous agents, such as the hydrogenated hydrocarbons (commonly known as halons), after they were restricted in 1987 [9][10][11][12].

The diversity of the suppression mechanisms and the gaseous-like behavior are the main reasons for the increasing popularity of the water mist systems in recent years. Water mist technology is emerging as an effective fire suppression agent, and, it is currently employed in residential, industrial, aeronautic and naval applications. The use of water mist systems has demonstrated various advantages, including limited water consumption, especially when compared to that of the conventional sprinkler systems [4][10][13], minimal property damage [11][13], no toxic and asphyxiation problems, limited environmental cost [2][4][10] and high efficiency in suppressing certain fires [2]. Despite the indisputable advantages, the application of water mists, as an active fire protection system, is hindered, due to their relatively high cost and the very strict reliability requirements.

The performance and the success of the application of the water mist systems, in terms of the goal that they are targeting, relies mainly on the nature of the spray pattern that is produced by the nozzles. The water mist nozzles are characterized by the volume flow rate, the spray cone angle, the size and the distribution of the water droplets, and, the spray momentum (discharging direction and water droplet velocity). These parameters have great and coupling effect on the suppression mechanisms, the effectiveness, and the reliability of the system. Additionally, there is an interaction between the water droplets and the fluid flow (momentum, mass and heat transfer), which governs the droplets' trajectory and their evaporation rate [1]. These phenomena are quite complex and difficult to be described quantitively.

For this reason, there is a lot of research and effort ongoing, in order to understand the spray dynamics and to characterize the spray produced by the water mist nozzles. It is only feasible by conducting experimental testing. Zhigang et al. conducted a series of full scale experiments in a mock-up commercial cooking area, to study extinguishing mechanisms and effectiveness of water mist against cooking oil fires [2] Kim et al. investigated quantitively the characteristics of fire suppression, using a water mist nozzle with certain specifications, through full scale experiments in an enclosure [4]. Santangelo, P. focused on characterizing the solid cone water mist spray produced by a typical atomizer at high operative pressure (in the range of 60-80 bar) [9]. Mahmud et al. investigated experimentally the distribution of water flux density emanating from a single and a multi-orifice high pressure water mist nozzle [10] and characterized the spray pattern of a single orifice nozzle, in terms of flux density distribution [13]. Ditch et al. describe in their paper the characterization of two selected nozzles to confirm the desired spray specifications, to validate PDPA mist flux measurements and to use mathematical functions to describe the drop size distribution [14]. Yinshui et al. employed two groups swirl nozzles to find a more effective way of fire suppression by

changing characteristics of the nozzles, such as the flow rate and the spray angle [15]. Santangelo et al. provided a thorough characterization of the spray produced by a water mist injector, investigating the drop size and the flux distribution, the initial velocity of the droplets and the spray cone angle [16].

It is obvious that understanding the water mist spray dynamics and the underlying physics, by characterizing the spray pattern of certain water mist nozzles through testing, is resource intensive. In addition, we shall not forget that, currently, a water mist system must be designed and implemented after certification approvals, through tests that verify the applicability of the relevant setup. There are no guidelines available for dimensioning water mist systems The NFPA 750 standard [7] , states clearly that a water mist system should be listed for the specific purpose. Undoubtedly, experimental testing to that extend is not feasible, not only from the economic point of view, but also from the time perspective. This means that the use of water mist systems is drastically limited, since every new system has to be designed and tested separately. Husted, P. in his doctoral thesis elaborates illustratively the problem with dimensioning water mist systems [8].

The experimental testing demands in time and money can be significantly reduced by the use of numerical simulations, as part of the R&D process. The ever-growing progress of the numerical simulations, in conjunction with the increasing processing computational power, offer a valuable supporting tool for testing various water mist systems, under different conditions. It is important to understand that experimental testing and numerical simulations are not competitive with each other. The numerical simulations are not a substitute that came in life to take the place of the experimental testing. The simulations can only be useful, if they provide sufficiently accurate results (validation). Full scale experiments are absolutely necessary, among others, to substantiate the accuracy of numerical simulations.

The last two decades more and more researchers started to explore the capabilities of CFD packages to predict the dynamics of the water mist sprays, the fire extinction by using water mist systems and the interaction between water droplets and the fire. The reader may refer to literature to find several works, among which [3][6][8][10][17][18][19][20][21][22] are indicative of the range of CFD capabilities. There are, also, two additional papers that investigate the accuracy of the spray characterization numerical simulations with FDS and constitute the basis of the present work. For this reason, we will refer to them more thoroughly in the following section 1.1.5, on the accuracy of the water mist simulations.

First, for the shake of the clarity and the completeness, it is important to understand how the water mist nozzles form the water sprays and how the water sprays can be modelled by the CFD packages, and more specifically by the FDS package, since FDS will be used in the present work for conducting the numerical experiments. The fluid motion is simulated in FDS by using the basic conservation equations of mass, momentum and energy for a Newtonian fluid as a set of partial differential equations, which are solved numerically, through the finite difference method, while the water droplets are simulated as Lagrangian particles. The water

spray modelling in FDS consists mainly of three components, the nozzle modelling, the particle size distribution definition and the particle transport modelling.

1.1.2 Water Mist Nozzle Modelling in FDS

A spray is formed by breaking up a volume of liquid into smaller and smaller water droplets. This is referred in literature as the atomization process [23]. The atomization of a liquid jet or a liquid sheet can be done in various ways. Whatever the atomization technique, the basic principle of the water spray formation, is the presence of small disturbances, after the development of the jet or the sheet, which eventually lead to the disintegration of the bulk liquid into ligaments and droplets. The characteristics of the liquid jet or sheet, when it leaves the orifice exit of the nozzle, the aforementioned disturbances, the density of the spray, the drop velocity and the drop size distribution, as functions of time and space, are some of the features of the atomization process that are of paramount importance for the shape and the penetrating ability of the spray. These, however, are not the only ones [23]. Figure 1.1 illustrates a typical atomization process with all physics taking place. For more information the reader may refer to [23], which is a very analytical reading about the atomization technique and the atomizers.

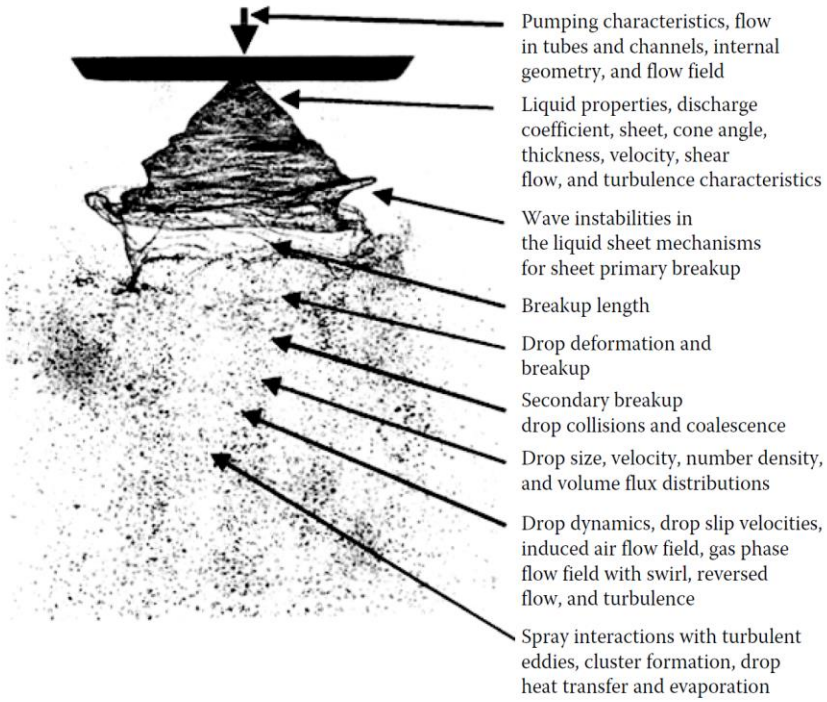

Figure 1.1. Example of the atomization process illustrating many features that need to be characterized (copied from Arrowsmisth, Atomization and Sprays, pg 7,1990, [23])

It is without any doubt that the atomization process is, on its own, exceptionally complex, and modeling it can be proved quite challenging, which, in its turn, can make the whole modelling of the water sprays in CFD packages an extremely difficult task. On grounds of that, most of the CFD packages do not attempt to model the atomization processes of the spray. Instead,

they describe the spray as a droplet inlet boundary condition. The droplets are injected randomly in the computational domain on a section of a spherical surface, at a certain distance from the nozzle orifice exit (offset). This implies that the atomization process has been terminated at the position of the boundary condition. By prescribing the physical parameters for the nozzle description, we assure that the correct amount of liquid phase momentum is introduced into the simulation. It remains then for the droplet size distribution and the particle transport modelling to be defined, so that to fully model a water spray in FDS. Both of them are analyzed in the following sections 1.1.3 and 1.1.4, since they are not straightforward and require more thought. In the present section, we will briefly talk about the physical parameters that are necessary for the water mist nozzle modelling in FDS.

The water mist nozzle modelling or more precisely the impact of the water mist nozzle characteristics on the produces spray is accomplished through the definition of physical parameters, such as the spray angle (pattern), the offset, the discharge flow rate, the operating pressure of the nozzle, the initial droplet velocity and the drop size. All of them are usually acquired with the aid of nozzle characterization experiments and the manufacturer's data. The physical parameters are typical of each nozzle, they are coupled with each other and they characterize the initial spray.

a. Spray Angle and Offset

The spray angle is a very important parameter, since, from the one side, it influences the distribution of water and governs the water coverage, and, from the other side, it determines the section of the surface, where the water droplets are launched inside the computational domain (Figure 1.2). FDS uses a pair of angles, through which the droplets are sprayed, namely, the inner and the outer angle [24]. They are defined via the parameter SPRAY_ANGLE (^{o}). The inner spray angle defines the spray area, inside which there is no water. The outer angle sets the outer boundaries of the spray. As for the OFFSET (m) parameter, it is defined as the radius of the sphere surrounding the sprinkler, across which the water droplets are initially placed in the simulation [24]. Figure 1.3 shows the sphere that is defined by the offset parameter, the inner angle (30^o) and the outer angle (80^o).

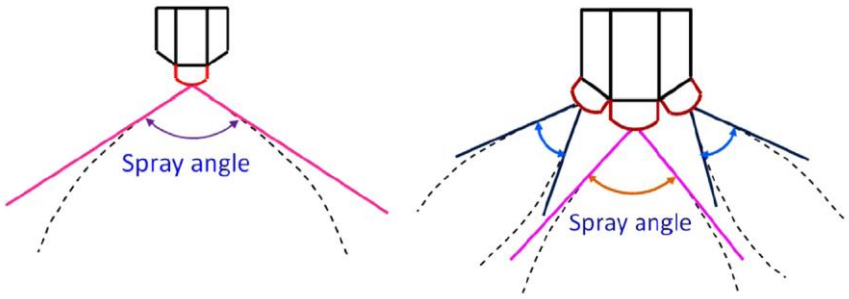

Figure 1.2. Measurement of spray angle for a single and a multi-orifice nozzle (copied from Mahmud et al. [10])

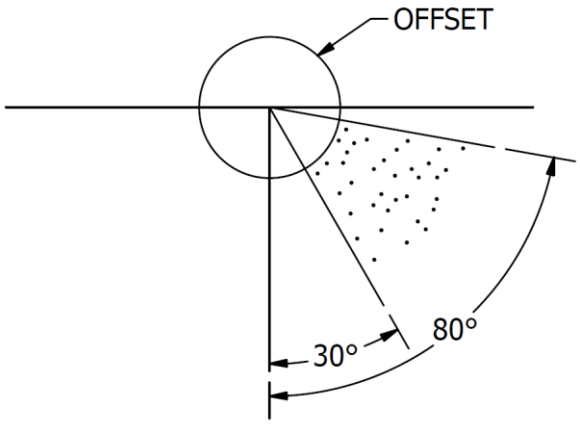

Figure 1.3. Sketch showing the role of the offset and the Spray_Angle parameters (copied from McGrattan et al. [24])

b. Volumetric flow rate and operating pressure

Water mist nozzles are designed to produce certain spray characteristics, most notable of which is the K-factor, showing the relationship between the volumetric flow rate and the operating pressure. Attempting to gain some commonality between various manufacturers, styles and capacities, it became readily accepted by the fire safety engineering community to use the nozzle discharge coefficient (or most commonly K-factor) for the system design, through the Eq. 1-1,

$$K = \frac{Q}{\sqrt{P}} \qquad \text{Eq. 1-1}$$

Where K, the nominal discharge coefficient ($l/minbar^{1/2}$)

Q, the volumetric flow rate (l/min)

P, the nozzle operating pressure (bar)

c. Initial droplet velocity

Initial droplet velocity is an important feature of the water mist system, especially when we assess the suppression capabilities of the system. The downward velocity of the water droplets is related with the momentum of the spray and its interaction with the fire plume. Higher drop velocities mean greater ability from the droplets to penetrate the fire plume and reach the fire base, while lower velocities usually result in higher times to penetrate the fire plume, and in higher chances for the droplet evaporation.

Of course, the drop velocities do not account on their own for the penetration capability of the spray. The drop size plays always a key role. Sheppard, D. in his doctoral thesis tested the spray characteristics of numerous sprinklers and, among others, he examined the initial and terminal velocities of droplets with various sizes [25]. When he tested water droplets of the

same size having though different initial velocities, he found that the vertical velocity does not alter the terminal velocity but affects only the vertical distance to reach the terminal velocity. This is very important to account for, when conducting experiments and taking measurements at a certain distance from the nozzle. The water droplets should have adequate initial velocity to reach the position of the measurement device.

The initial droplet velocity is usually provided by the manufacturer of the nozzle. It is dependent on the operating pressure, the volume flow rate and the nozzle orifice diameter. In fact, in case there are not any information about the initial droplet velocity, then it can be calculated with the flow rate and the nozzle orifice diameter, by dividing the first to the latter. This is practically what FDS does, when the particle velocity is missing, and the only input variables are the flow rate and the orifice diameter.

Alternatively, the initial droplet velocity can be calculated by the following correlation Eq. 1-2, which can be found in [5] and relates the initial velocity with the nozzle operating pressure, the density of the liquid and the friction losses.

$$u_0 = C_d \sqrt{\frac{2P}{\rho}} \qquad \text{Eq. 1-2}$$

Where u_0 = the initial droplet velocity (m/s)

P = the nozzle operating pressure (Pa)

ρ = the liquid density (kg/m^3)

C_d= 0.95, factor to account for the friction losses in the nozzle

The initial velocity of the water drops is defined in FDS as PARTICLE_VELOCITY (m/s).

d. Drop size

The mean droplet size is, basically, a measure of the overall surface area of the sprayed fluid. The smaller the droplet size, the greater the surface area of the spray for a certain volume of fluid. As it has already been mentioned, the importance of the droplet size lies in the ability of the spray to absorb or dissipate heat, as well as in its interaction with the gas flow. The droplet size is a function of the physical parameters that characterize the water mist nozzle. For any given flow rate, operating pressure, and spray angle corresponds a specific water droplet size. This is very important statement in a sense that the selection of the parameters for the nozzle description should have a physical meaning. In other words, the flow rate, the initial velocity (pressure) and the spray angle should be in complete agreement with the produced water droplet size.

The drop size is affected by the spray pattern, the spray angle, the nozzle geometry and, of course, by the pressure. Full cone sprays, hollow cone sprays, flat fans and solid stream sprays,

when working under similar conditions, produce different droplet sizes. Assuming constant flow rate, the wider the spray angle, the smaller the droplet size. Larger angle sprays denote that there is more space available for the droplets to be distributed and, therefore, there is a greater opportunity for atomization. The geometry of the nozzle determines the atomization process and, consequently, the resulting drop size.

The effect of the pressure on the drop size cannot be underestimated. A simple rule that holds for all nozzles signifies that the higher the fluid pressure, the smaller the droplet size. Even though there is not such an equation to calculate directly the mean diameter from the operating pressure, there are correlations in literature that describe the relation between droplet size and operating pressure and indicate, clearly, the connection between them. Fleming, R in the SFPE Handbook of Fire Protection Engineering [26] states that the median droplet diameter in the sprinkler spray is inversely proportional to the 1/3 power of water pressure and directly proportional the 2/3 of the sprinkler orifice diameter such that,

$$d_m \propto \frac{D^{2/3}}{P^{1/3}} \propto \frac{D^2}{P^{2/3}} \qquad \text{Eq. 1-3}$$

The FDS User's Guide [24] provides us with the following scaling correlation,

$$\frac{d_m(p)}{d_m(p_0)} = \left(\frac{p_0}{p}\right)^{1/3} \qquad \text{Eq. 1-4}$$

while Jayaweera et al. [11] and Heskestad, G, [27] ended up to two similar scaling correlations for the operating pressure and the drop size respectively,

$$\frac{d_2}{d_1} = \left(\frac{\Delta_{p2}}{\Delta_{p1}}\right)^{1/4} \qquad \text{Eq. 1-5}$$

$$\frac{d_2}{d_1} = \left(\frac{\Delta_{p2}}{\Delta_{p1}}\right)^{1/2} \qquad \text{Eq. 1-6}$$

A water mist system produces millions of droplets with various drop sizes, ranging between a maximum and a minimum drop size. The median drop diameter is a statistical quantity, which is indicative of the level of atomization and, apparently, of the drop size that is produced by the nozzle. It means in no case that all droplets are of that size. The water mist nozzle industry, in order to characterize the drop sizes, uses different diameter definitions and, according to the Spraying Systems Co. [28], the drop size terminology can be as follows:

- $Dv_{0.5}$: Volume Median Diameter (also known as VMD or MVD). It is the most common diameter definition and it is a mean of expressing drop size in terms of the volume of liquid sprayed. The VMD is a value where 50% of the total volume (or mass) of liquid sprayed is made up of drops with diameters larger than the median value and 50%

smaller than that. This diameter is used to compare the change in drop size on average between test conditions

- D_{32}: Sauter Mean Diameter (SMD) is a way of expressing the fineness of a spray in terms of the surface area produced by the spray. The Sauter Mean Diameter is the diameter of a drop having the same volume to surface area ratio as the total volume of all drops to the total surface area of all the drops.

- $Dv_{0.9}$: is a value where 90% of the total volume (or mass) of liquid sprayed is made up of drops with diameters smaller or equal to this value

- $Dv_{0.1}$: is a value where 10% of the total volume (or mass) of liquid sprayed is made up of drops with diameters smaller or equal to this value

FDS code uses as an input variable the median volumetric diameter $Dv_{0.5}$, which is defined via the parameter DIAMETER (μm). FDS uses this parameter to produce the size distribution of liquid droplets, by using a cumulative volume fraction (CVF)

1.1.3 Particle Size Distribution

By prescribing in FDS the parameters above, we are able to set up a device (water mist nozzle), which discharges a certain volume flow rate or mass (FLOW_RATE or MASS_FLOW_RATE), injected from a distance R (OFFSET) in the computational domain and distributed in a prescribed area, which is limited by the spray angle (SPRAY_ANGLE). The liquid volume is launched inside the computational domain in the form of liquid droplets, which in the language of a CFD package are called particles. The initial velocity of the particles is also predefined by the user (PARTICLE_VELOCITY). This is, in general, how the nozzle is modelled. As for the spray boundary surface, this is defined as a function of the offset distance and two angles, the azimuthal angle φ and the elevation angle θ ($\theta = 0$ for the vertical direction) (Figure 1.4).

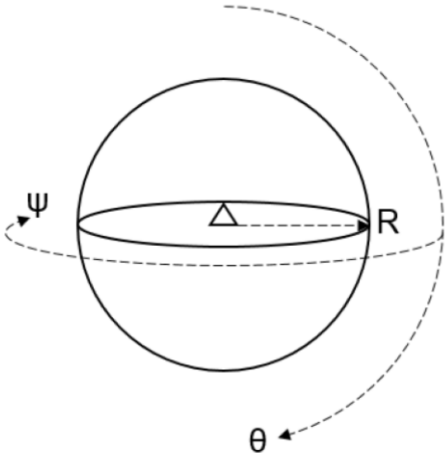

Figure 1.4. The initialization sphere with the radius R, the elevation angle ϑ and the azimuthal angle φ (copied from Takiedin, S. [20])

The question that arises now is, actually, on the way that the prescribed volume flux is distributed over the spherical surface. The volume flux distribution depends on the initial particle size and the position in the conical section of the sphere. If all droplets produced by the nozzle had the same size (diameter), then we would be certain about the volume fraction that each droplet brings in, and, consequently, about the volume fraction distribution. This is not the case whatsoever. We have mentioned that one water mist nozzle produces millions of droplets, at random positions, having diameters ranging within a minimum and a maximum size. Then how could the size droplet distribution be modelled in a precise and realistic way?

This is done stochastically, by defining Probability Density Functions (PDFs) for the volume fraction (VFD) and the droplet diameter (NFD), as well as their corresponding cumulative fractions (CVF and CNF). According to [5], the PDF for the volume fraction distribution is a joint probability (assumed independent) of the two angles, the azimuthal and the elevation. Due to the fact that the volume flux is uniformly distributed over φ and varies with θ the PDF is as follows [5],

$$p(\theta,\varphi) = p(\theta)p(\varphi) = \frac{1}{2\pi}\sin\theta\, f(\theta) \qquad \text{Eq. 1-7}$$

Figure 1.5 explains graphically all the previously mentioned.

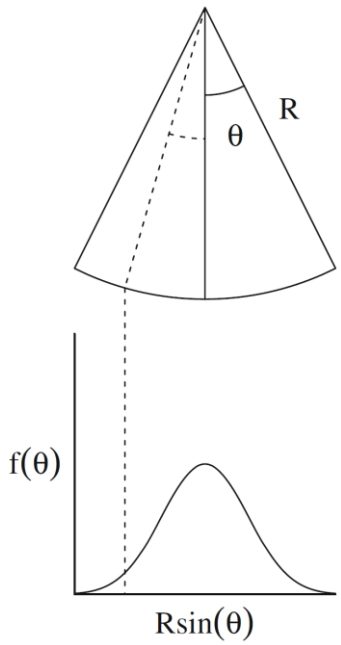

Figure 1.5. Illustration of the initial drop distribution with the use of a PDF (copied from Sikanen et al. [5])

The Cumulative Volume Fraction (CVF) is a function that relates the fraction of the water volume transported by droplets sized less than a given diameter [29]. In the FDS simulations, this function is represented very well by a combination of Rosin-Rammler and lognormal distributions [30], as follows,

$$F(d) = \begin{cases} \frac{1}{\sqrt{2\pi}} \int_0^d \frac{1}{\sigma\delta} e^{-\frac{[ln(\delta/d_m)]^2}{2\sigma^2}} d\delta \ (d \leq d_m) \\ 1 - e^{-0.693\left(\frac{d}{d_m}\right)^{\gamma}} \qquad (d_m < d) \end{cases} \qquad \text{Eq. 1-8}$$

where d_m is the median droplet diameter (DIAMETER) or $Dv_{0.5}$, and γ, σ are empirical constants equal to 2.4 and 0.48 respectively. Similarly, one can define the NFD and the CNF. The formulation of the definition for the VFD, NFD, CVF and CNF, as well as the calculation procedure that connects the droplet diameter distribution to the CVF are analytically described by Beji et al. in [31].

FDS uses the aforementioned definitions in order to select droplet sizes. The steps that the FDS follows are presented in the FDS Technical Reference Guide [30]. Very briefly what FDS does is, that once the user induces the parameter DIAMETER to the code, the numerical algorithm calculates immediately the CVF. The droplet diameters are then randomly selected (through the calculation procedure with the PDFs), in a way that the CVF is always satisfied, through a stratified sampling technique, to ensure that the droplets span the entire range of sizes, even with a relatively small number of droplets [30].

The FDS Technical Reference Guide talks about a stratified sampling technique, which indicates that the FDS code, like any other CFD package, cannot simulate and track every droplet that can be potentially produced by a water mist nozzle, since it is expensive and unnecessary. In the FDS calculations typically five to ten thousand droplets interact with the gas at any given time. This number of droplets represents the actual number of droplets that are produced by the nozzle, which brings us to the concept of the Lagrangian particles.

1.1.4 Lagrangian Particle Model

CFD packages can model the particle transport in two different ways. First with the Euler-Euler method, where the particles are modelled as a gas phase, having the properties of a given particle size and, in order to model a distribution of droplet sizes, several gas phases of droplets need to be used. The second approach is the Euler-Lagrangian method, where only a representative number of droplets is modelled and there is mass, momentum and energy interaction between the two phases, the gas and the liquid phase.

FDS uses the Euler-Lagrangian approach. The mass, momentum and energy conservation equations are described in detail in the FDS User's Manual [32] and the FDS Technical Reference Guide [30]. The particle transport model in FDS does not include droplet collision or break-up models, but it does include a model for the evaporation for the droplets. In [33] it is said that the droplet evaporation is calculated as a function of the droplet surface area, a mass transfer coefficient, the gas vapor fraction and the liquid equilibrium vapor mass fraction, evaluated using the Clausius-Clapeyron equation. In case of dense sprays, the drag effect is taken into account by the drag reduction coefficient, which can be assumed negligible in case of dilute sprays.

It is computationally prohibitive and unnecessary to track all the droplets that can be discharged from a nozzle. Instead, the actual number of droplets produced by a nozzle is divided in several sets, each of which is represented by one single computational droplet. The number of computational particles (N_p) that is used to represent the flow is user induced parameter and it is controlled in FDS via the parameter PARTICLES_PER_SECOND. The default value is $N_p = 5 \times 10^3 s^{-1}$, since it is believed that a number between $N_p = 5 \times 10^3 s^{-1}$ and $N_p = 10^4 s^{-1}$ is adequate to represent all types of water sprays that can be formed by various nozzles. The number of real droplets N (s^{-1}) that are produced by a certain nozzle can be calculated as follows,

$$N = \frac{\dot{m}_w}{\bar{m}_d} \qquad \text{Eq. 1-9}$$

where $\dot{m}_w$ is the mass flow rate of the water discharged at the nozzle, (kg/s), and $\bar{m}_d$ is the average mass of a droplet (kg) which can be calculated according to [29] as,

$$\bar{m}_d = \frac{4}{3}\pi\rho_w \int_0^\infty f(\delta)\left(\frac{\delta}{2}\right)^3 d\delta \qquad \text{Eq. 1-10}$$

where $f(\delta)$ is the probability density function for the droplet dimeter (NFD), mentioned in 1.1.3. The number of real droplets represented by the single simulated droplet is calculated as [33],

$$n = \frac{\dot{m}_w}{N_p \bar{m}_d} \qquad \text{Eq. 1-11}$$

At this point, it is of paramount importance to understand that the number of computational droplets does not affect or change the flow rate of the nozzle. This is solely determined by the nozzle parameter FLOW_RATE. The computational droplets or the PARTICLES_PER_SECOND define how uniformly the liquid mass is distributed over the computational area. They affect the mass that is transported by each of the computational droplets, which, on its turn, affects the water flux distribution over a surface, as well as the evaporation rate of the droplets and, consequently, the suppression capabilities of the mists. A certain number of computational droplets, each of which has a certain diameter, as it is calculated through the drop size distribution explained earlier, has a limited mass transfer capability. The numerical code, once the user defines the nozzle flow rate and the number of computational particles (N_p), understands the deficit between the mass that can be carried by the computational particles and the mass that is brought in the computational domain by the nozzle. This deficit is due to the limited number of computational droplets. In order to maintain the overall mass balance in the simulations, the code compensates for that deficit by computing weighting constants Ci for each droplet individually, as well as a global weighting constant C. The mass and the heat transferred from each droplet is then multiplied

by the weighting factor C. The complete procedure is described in the FDS Technical Reference Guide [30].

The weighting constants are nothing more than a mathematical trick that keeps the effectiveness of the conservation equations and enables the code to provide scientifically well documented numerical solutions. It makes it possible to get correct solutions, in a sense that the conservation laws are valid, but how accurate are really these solutions? The accuracy of the water mist simulations are of vital importance. Imagine a numerical simulation, where the task is to represent an ADD apparatus test or even a simulation that accompanies a certification approval for the suppression ability of a water mist nozzle system, where the evaporation rate of the droplet really matters. The importance of simulating the correct amount of liquid mass delivered over a certain surface is critical for both cases.

All the above indicate that the number of computational particles (N_p) is a very important parameter for the accuracy level of a numerical simulation, in terms of the volume and mass distribution of the water droplets. In fact, the significance of that parameter is not downgraded by the FDS User Manual itself [32]. We quote, "note that the PARTICLES_PER_SECOND can be a very important parameter. In some simulations, it is a good idea to increase this number so that the liquid mass is distributed more uniformly over the droplets. If this parameter is too small, it can lead to a non-physical evaporation pattern, sometimes even to the point of causing a numerical instability. If you encounter a numerical instability shortly after the activation of a sprinkler or nozzle, consider increasing the PARTICLES_PER_SECOND to produce a smoother evaporation pattern that is more realistic. Keep in mind that for a sprinkler or nozzle, there are many more droplets created per second than the number that can be simulated". This is why there is research, which focuses on studying the effect of the N_p on the simulation results and the reason for conducting the present study.

1.1.5 The Accuracy of the Water Mist Simulations in FDS

The procedure that needs to be followed, in order to simulate water mist sprays in FDS is not an easy one. It comprises various steps, simplifications, assumptions, input variables, modelling and numerical methods, each of which contains a certain degree of induced errors that reduce the level of accuracy of the simulation results. While some of these sources or errors can be found in almost any CFD simulations, there are some that can be met only in water spray simulations. The water spray modelling errors relate to the water mist nozzle modelling (input variables), the drop size distribution and the flow realization level, which depends on the distribution functions and the number of computational droplets N_p (PARTICLES_PER SECOND). As it has been already mentioned, there are in the literature two works in particular, which study the importance of several sources of water spray modelling errors and inspired the present thesis.

Sikanen et al. [5] assessed the ability of FDS to predict the drop size, velocity, mist flux and number concentration profiles within the spray cone, by modelling single and multi-orifice

high pressure water mist nozzles. The goal was to validate the FDS particle model for use in modelling water mist systems based on a series of validation experiments. The ability of the numerical code to predict the validation experiments was quantified in terms of a simulation error, expressing the deviation between the experimental and simulation results. They performed two series of simulations, both in cold conditions, with and without the presence of entrained air, so that to evaluate the contribution of the aerodynamic force as well. For the single orifice nozzle characterization simulations, without air entrainment, they checked the effect of the turbulence model on the results and they performed a sensitivity analysis to study model parameters, namely the spray angle and the initial velocity, and numerical parameters, such as the cell size, the CFL parameter, the offset distance R and the number of particles insertion rate (PARTICLES_PER_SECOND). The sensitivity study revealed a strong influence of the grid resolution and the spray angle parameter on the results, whereas the effect of the offset parameter R, the CFL and the initial velocity was shown negligible. Finally, doubling the number of particles from $N_p = 2 \times 10^5 s^{-1}$to $N_p = 4 \times 10^5 s^{-1}$resulted in larger velocity profiles, but it didn't affect otherwise the results. Keep though in mind, that the number of particles ($N_p = 2 \times 10^5 s^{-1}$) that they used for their base simulations are already a lot higher that the default value of the FDS code ($N_p = 5 \times 10^3 s^{-1}$).

Beji et al. [31] went one step further, by presenting a very detailed sensitivity analysis study on the effect of the particle injection rate, the droplet size distribution, the angular probability distribution, the turbulent viscosity and the cell size on the simulation results and the computational time of a water mist spray nozzle. They used water mist nozzle characterization experiments, which provided local measurements of the water volume flux, the droplet velocity and droplet diameters within the spray, to assess the numerical code performance by changing the aforementioned parameters. Similar to the previous study, the validation of the numerical simulations is held by calculating the deviation (error) between the experimental and the numerical results of the measured quantities. The study underlines the applicability of the uniform angular distribution and the lognormal-Rosin-Rammler against the gaussian and the Rossin-Rammler respectively and revealed that the dynamic Smagorinsky turbulence model is more sensitive than the modified Deardorf model to the cell size.

What is more, the sensitivity study for the particle injection rate has shown that there is a proportionality between the deviation the numerical simulations and the water volume flux measurements and the number of computational particles (N_p). It was found that the error originated by the limited N_p is proportional to $1/\sqrt{N_p}$, which denotes that it could be theoretically eliminated for an infinitely high number of computational droplets. On the contrary, the computational time of the simulations increases linearly with increasing the number of computational droplets. The authors consider this as a methodology for the modeler to quantify the previously mentioned error and to distinguish it from other sources of errors.

In fact, their finding is in complete agreement with what is described in [34] about the accuracy of the Lagrangian-Eulerian simulations. It is stated there that most of the numerical studies of the Lagrangian-Eulerian particle simulations seek convergence by increasing the number of computational particles and that for a fixed number of particles there exists an optimal choice of grid size that minimizes the total numerical error. These two statements make necessary a complete characterization of the individual contributions of the total error through an error decomposition technique. The main components of the total error are therefore the statistical error, which is due to the limited number of computational particles and converges as $N_p^{-1/2}$, and the deterministic error, further decomposed to bias and discretization errors, due to the magnitude of bias for a given N_p and due to spatial and temporal discretization techniques.

All the above indicate that the accuracy of the numerical simulations of water mist nozzles, which involves Lagrangian particles modelling, is highly dependent on the number of computational particles and the grid resolution of the numerical scheme. The present study is based on the findings of those papers and examines in detail the effect of the number of computational droplets and the grid size on the numerical simulations of a set of water mist nozzles, producing a wide range of droplet diameters.

1.2 Objectives

Sprinklers and water mist nozzles are very often used as active fire protection systems in various types of buildings such as warehouses, shopping malls and tunnels. The efficiency of such systems (with respect to a specific application) depends on the water spray pattern delivered by the sprinkler head or water mist nozzle. In design calculations that are based on Computational Fluid Dynamics (CFD), the water spray needs to be modelled accurately in order to assess the efficiency of the system in fire-driven flows. The most common approach is to track the motion, mass and heat transfer of water droplets on an individual basis. This is called the Lagrangian approach. However, because it would be computationally too prohibitive to track all the droplets one by one, a smaller number of droplets is used to describe the spray in the simulations.

In the literature, there are no clearly defined 'rules' or guidelines for the selection of the number of computational droplets that would lead to the convergence of the simulations (i.e., reduced statistical error). For example, in the FDS CFD package, the default number of computational particles per second is $N_p = 5 \times 10^3 s^{-1}$. Whilst this number may be appropriate for sprinklers with droplet diameters between 500 and 1000 μm, it has shown to be very insufficient for water mist sprays with characteristic droplet diameters of about 50 μm.

The goal of the thesis is to carry out a substantial number of 'numerical experiments' with FDS for a wide variety of water sprays and analyze the results, in order to provide guidelines to future users on the appropriate number of computational droplets per second (N_p),

depending on the water spray type (dimeter) and the computational mesh, that is necessary to eliminate the N_p statistical error.

2. Methodology

2.1 Introduction

In order to study the accuracy of the water mist sprays numerical simulations and to provide guidance, concerning the number of computational droplets N_p that are necessary for reaching a certain level of accuracy, a wide variety of water mist nozzles needed to be tested. An experimental setup in FDS was used to simulate various water mist nozzles, each of which produced different spray pattern and, more importantly, different median drop diameters. A series of numerical simulations was performed for every nozzle type tested, in order to specify the number of particles that provide the acceptable accuracy, which in our case is to eliminate the error induced by the limited number of computational droplets (zero statistical error). The number of computational particles that eradicates the statistical error is defined, as the critical number of computational particles $(N_{p,cr})$. This chapter describes the experimental setup, the input and the output variables for modelling water mist nozzles in FDS, as well as the methodologies that were used to analyze the results of the simulations.

2.2 The Experimental Setup (FDS simulations)

The experimental setup is based on the setup described in [5]. The numerical experiments were modeled in FDS by using a rectangular computational area. The dimensions of the computational area are 1.0 m wide, 1.0 m deep and 1.5 m high. The computational area was open to flow on all sides and on the bottom of the computational domain as well. The upper part of the domain has been modelled as an inert vent, which means that the solid boundary temperature is fixed at ambient temperature (20^{o}C default parameter).

The water mist nozzles were placed at a distance of 0.1 m from the top of the computational domain and the local measurements were taken by a PDPA device, which was placed 1.0 m below the nozzle head, across its centerline axis. Two additional devices were placed at 0.8 m, and 1.2 m to verify the sensitivity of the results, with regard to the measured location. The measurement locations follow the instructions of the NFPA 750 standard [7], and they were selected to be located at the far field region of the nozzle head, where it is believed that the spray will have been formed, without anymore the effect of the nozzle, as well as at the centerline of the nozzle axis, because otherwise the dense core of the sprays would have been missed. The offset distance, which, according to the introductory section, indicates the atomization length, was kept equal to the default FDS value (0.05 m). Figure 2.1 shows the experimental setup with the computational domain, the measurement devices placement and a typical spray pattern.

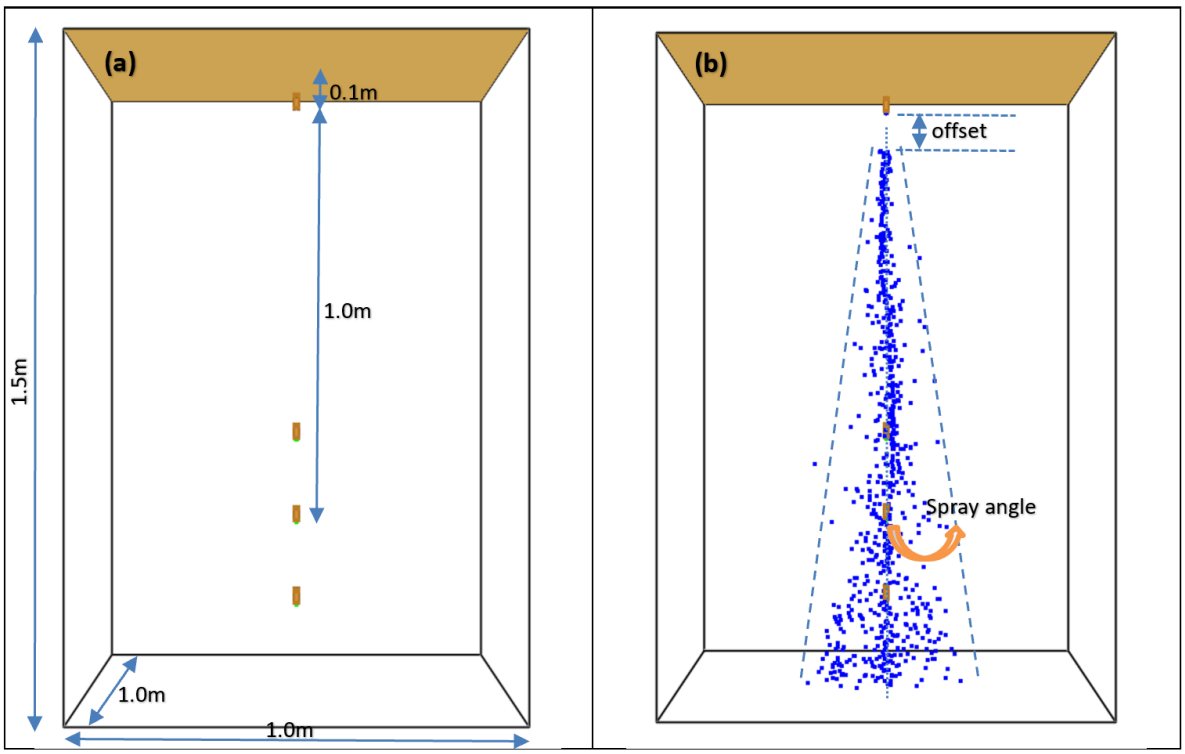

Figure 2.1. Smokeview visualization of the (a) experimental setup and (b) of a typical spray pattern

FDS, like all CFD packages, performs its calculations within a computational domain, which is made up of rectilinear volumes that are called meshes. Each mesh is divided in rectangular cells, the number of which depends on the desired resolution of the flow dynamics equations [32]. In order to study the effect of the computational grid on the statistical error, the numerical experiments took place under four different spatial discretization scenarios (cell size campaigns). Each campaign uses one single mesh, which was consisted of cubic cells sizing 10 cm, 5 cm, 2.5 cm and 1.25 cm respectively. Following the degree of the resolution they offer, the four meshes are called and abbreviated in the present work as Coarse (C), Medium (M), Fine (F) and Very Fine (VF) accordingly. The turbulent motion of the gas phase was simulated by using the Deardorff turbulent viscosity model, which is the default model in FDS.

All numerical experiments were performed in cold conditions. There is no interaction between the water sprays and a fire plume or any induced jet of hot air. The sprays, though, are evaporating, meaning that the evaporation model, as it is described in the FDS Technical Reference Guide [30], is active. Nevertheless, the evaporation of the water droplets is not expected to be important, since only cold sprays were simulated. Furthermore, the residence times of the particles in the simulations were very short, as well as the simulation time. No secondary breakup model was used in the framework of the present study.

The water mist nozzles were activated at the beginning of the simulations ($t = 0$ sec) and they were allowed to discharge water for the next ten seconds ($t = 10$ sec, simulation time). The droplet statistics were collected for the last five seconds of the simulation time, when the vast majority of the experiments had reached steady state conditions. The measurement devices

were activated and, consequently, started to record measurements after the first two seconds of simulation ($t = 2$ sec). The first two seconds of each simulation were therefore ignored, to avoid measuring nozzle start anomalies.

It has been noticed though that there were a few simulations, especially those run with the coarser grids (C and M), where ten seconds of simulation time was inadequate to reach steady state conditions. Due to the large number of simulations that needed to be performed and the underlying availability of the computational power and time, and, in order to be able to compare the experimental results among each other, we decided to keep the simulation time up to ten seconds, as a very decent compromise between the accuracy and the computational time. It is recommended that the future researchers investigate this issue, before executing the numerical experiments.

Finally, the simulations were running on one of the UGent HPC computer clusters (named golett) consisted of 200 nodes each of 64GB memory, with 2.5GHz, 2 × 12-core Intel E5-2680v3 processors and 2GB of memory per core. The simulations were inserted in the HPC as serial jobs, with one processor handling one single simulation, which was consisted of one computational mesh. The computational time was recorded and used for the evaluation of the results.

2.3 Water Mist Nozzles Modelling Input Data

Water mist nozzle modelling requires the knowledge of the physical parameters that are described in section 1.1.2. It was mentioned that the physical parameters that characterize the nozzle head are connected and coupled with each other and their selection should be coherent to the water spray that they produce. Usually the nozzle characteristics are available through the nozzle manufacturer. This is partly true. A typical nozzle manufacturers' technical specification table provides information about the material that the nozzle is made of, its orifice diameter, the volumetric flow rate, the nozzle operating pressure and the K-factor, and the spray angle. These tables lack any information about the volume median diameter of the droplets or any other characteristic diameter that is produced by a specific nozzle type.

Water spray characterization requires characterization experiments, which cost a lot of time and money. If you consider the variety of the products that exist in the market and need to be tested, you will shortly figure out that, characterizing them, is almost a mission impossible. The recent years, more and more companies either avoid carrying out such experiments, or they conduct just a few of them, so as to characterize some nozzles that are representative of their product range. The information that is provided by the mean diameter of the droplets is absolutely necessary for the present research, since we want to investigate the connection, if any, between the nozzle diameter and the number of computational droplets that diminishes the statistical error.

In order to do that we had to create a list of nozzles that produce median drop diameters between 35 μm and 1000 μm. Attaching nozzle technical specifications with random

diameters was not an option. The combination of the nozzle physical parameters should have a physical meaning. Hence, we retrieved the nozzle modelling input data, first, from nozzle characterization experiments that are available in the literature and, second, from a nozzle diameter chart that was provided to us by the Spraying Systems Co. (Appendix A). Table 2-1 presents the full range of water mist nozzles that were used in our numerical experiments, showing the physical parameters that characterize each nozzle (diameter), as well as the source of data that was used, namely the reference paper or the Spraying Systems Co. nozzle type.

Nozzle	***$Dv_{0.5}$ (μm)***	***Flow rate (l/min)***	***Operating Pressure (bar)***	***K^c ($l/minbar^{1/2}$)***	***Initial Velocity (m/s)***	***Spray angle (°)***	***Reference Paper /Spraying Systems Co. Type***
Nozzle 1	35	0.15	60	0.019	74	77	[35]
Nozzle 2	50	0.42	100	0.042	60	24	[36]
Nozzle 3	70	3.6	70	0.430	112[a]	12	[5]
Nozzle 4	80	0.4	7	0.151	35[b]	40	1/4LNSS4
Nozzle 5	100	0.6	7	0.227	35[b]	40	1/4LNSS6
Nozzle 6	125	5.7	56	0.762	72[a]	14	[5]
Nozzle 7	150	0.1	7	0.038	27.1[b]	60	TPU500017SS
Nozzle 8	200	0.1	7	0.038	27.1[b]	30	1/4LNSS18
Nozzle 9	250	1.5	13	0.416	34[a]	18	[37]
Nozzle 10	300	2.62	7	0.990	35.0[b]	70	TPU500050SS
Nozzle 11	350	1.32	10	0.417	30[a]	19	[37]
Nozzle 12	400	0.9	7	0.340	25.0[b]	20	TPU5001SS
Nozzle 13	500	0.3	7	0.113	30.1[b]	26	TPU150050SS
Nozzle 14	600	3.6	7	1.361	35.0[b]	50	TPU5006SS
Nozzle 15	700	0.6	7	0.227	29.2[b]	24	TPU1501SS
Nozzle 16	800	1.2	7	0.454	32.1[b]	22	TPU1502SS
Nozzle 17	900	3.6	7	1.361	29.8[b]	21	TPU1506SS
Nozzle 18	1000	5.5	7	2.079	29.2[b]	59	1/8GSS5

[a] initial velocity calculated according to Eq. 1-2
[b] initial velocity calculated through the flow rate and the orifice diameter
[c] K- factor calculated according to Eq. 1-1

Table 2-1. The input nozzle modelling parameters for the numerical experiments in FDS

2.4 Simulation Output Data

We mentioned previously, describing the experimental setup (section 2.2), that local measurements were taken at a distance of 1.0 m on the downstream of the centerline axis of the nozzle head by a PDPA measurement device. FDS is capable of providing detailed experimental measurements of sprays using Phase Doppler Particle Analysis (PDPA), giving information on the droplet size distribution, speed and concentration. This can be accomplished by the so-called PDPA devices. The PDPA device is nothing more than a sphere, which is centered at the measurement location and has a size that is user defined. The role of that sphere is to sample a number of particles that are produced by the nozzle head and to provide results, in terms of size, velocity and concentration, which correspond to droplet

properties averaged over the volume of the sphere. In other words, the sphere works like a filter, through which the particles pass, and as long as they pass, the device takes measurements with regard to their size, their velocity and concentration measurements.

This is a sample technique, because the device doesn't measure the total number of computational droplets that is released in the domain but limits that number to the particles that pass through a certain volume, placed at a certain location as well. The sampling number is, therefore, dependent on the size and the location of the sphere within the water spray. The larger the size of the sphere, the higher the number of droplets that are sampled, and as result the closer the results to the reality. All numerical experiments of this work were ran with the same sphere, having a radius of 1.0 cm. FDS User's Manual [32] and the Technical Reference Guide [30] describe in detail the mathematical formulation of the equations that the code uses to calculate the output quantities.

Concerning the output quantities that the device was prescribed to measure, these are the particle flux in the vertical direction (PF), the mass concentration (MC) or spray volume density, the Sauter Mean Diameter (D32) and the $Dv_{0.1}$(D10). Note here that the VMD is not an output quantity in FDS and cannot be directly predicted by the FDS code, since it is used as an input variable that defines the PDFs and CVFs described earlier. The particle flux and the mass concentration are representative of the ability of the FDS to compute mass related variables, whereas the SMD and the $Dv_{0.1}$ demonstrate its ability to compute mean diameters.

The particle flux (PF) refers to the amount of water spray in a unit volume (lpm/m^3) or applied to a unit area (lpm/m^2). In the numerical experiments performed, the PF output is given in the latter units. The mass concentration (MC) units are kg/m^3. They are very important quantities, since they are measured by many devices in experimental testing. On a compartment scale, the increase in the flux density will reduce the compartment temperature, whilst on a localized scale the fire is extinguished, only when water sprays achieve a minimum flux density. Without sufficient flux density, so that the heat is removed, and the fuel is cooled, it is very likely that the fire will sustain itself. Similarly, the gaseous properties of the water mist systems depend on a critical concentration of water droplets, measured by the MC quantity. It can be easily understood that these four output quantities are of great importance for the effectiveness of a water spray. The ability of the FDS to predict the quantities adequately determines the effectiveness of the system as well, and it is the reason why we chose these output variables. The FDS code that describes a typical numerical experiment is provided in Appendix B.

2.5 The Numerical Experiments Methodology

The accuracy of almost all the nozzle characterization numerical experiments is evaluated by comparing them with the results acquired from the experimental testing. The modeler or the researcher tries to quantify how far are the simulation results from the reality, taking also into account the uncertainties that stem from the measurement instruments and techniques,

on the one hand, and the modelling assumptions on the other hand. This distance between the experimental and the numerical results very often is expressed in terms of a deviation, commonly held as the error of the numerical experiments which is calculated as follows,

$$\varepsilon = \frac{numerical\ value - experimental\ value}{experimental\ value} \qquad \text{Eq. 2-1}$$

This error by definition implies that the experimental results are the basis, upon which the numerical simulations are assessed. The idea is to verify how well can the reality be represented by the numerical simulations. This is not the case in the present work. Even though we are conducting nozzle characterization numerical experiments, in order to improve their accuracy, the second element of that methodology is missing. There is no experimental testing to allow for the assessment of the numerical experiments. The intention here is not to find the appropriate parameters that best mimic the reality, that best mimic a particular experimental setting or a specific application. On the contrary, we focus on investigating the effect of the limited number of computational droplets on the numerical results (statistical error), which are expressed through the four output quantities mentioned previously, and at the same time, on providing guidance over the appropriate number of droplets that eliminates the error.

However, the methodology that quantifies the error of the numerical simulations against the experimental testing, inspired us to define a similar deviation, an error, that establishes the level of inaccuracy between a certain simulation and the error free simulation which, in this way, enabled us to set up the analysis methodology. Based on the theory assumption that the error induced by the limited number of computational droplets is proportional to the $1/\sqrt{N_p}$ and that this error becomes negligible for an infinitely large number of computational droplets, we define as an error free simulation, the simulation that was ran with the number of computational droplets that diminished the error. The error free simulation constitutes the basis of the accuracy assessment of every other simulation that was performed by a lower number of computational droplets. In other words, the error free simulation plays the role of the experimental testing for our methodology.

Moreover, we can also quantify the level of the error induced by the limited number of computational droplets, by defining a deviation between the error free simulation and the simulations ran with lower numbers of particles. Let us explain this with an example. Suppose that we want to simulate the water spray that is produced by a certain water mist nozzle and that we want to find the appropriate number of computational droplets that should be prescribed, so that to get an error free simulation. We set up the modelling parameters and we start running consecutive simulations, by keeping all modelling parameters constant, except for the number of computational droplets, which is increased, until we observe no variation of the output quantities. The simulation before the one that there is no variation of the measured quantities is considered to be as the error free simulation. If we indicate as S_N the error free simulation results of a particular output quantity and as S_i the simulation results

of the same output quantity of any other simulation ran by a lower number of computational droplets, then we can define a deviation among them as,

$$dev = \frac{S_i - S_N}{S_N} \qquad \text{Eq. 2-2}$$

This is, according to our methodology, the definition of the N_p statistical error, and what was described in the previous paragraph, is the methodology that we followed, in order to conduct the numerical experiments. More specifically, in section 2.3, we described the physical parameters of the eighteen nozzles that were used in the numerical experiments. Each nozzle represents one diameter and the whole set of nozzles bounds the range of diameters that was studied. Every nozzle was basically simulated eleven times using FDS code. The eleven basic simulations correspond to different user defined numbers of computational droplets (N_p), starting from the default parameter, which in FDS is $N_p = 5 \times 10^3 s^{-1}$, and they are progressively increased to $N_p = 10^4 s^{-1}$, $N_p = 2 \times 10^4 s^{-1}$, $N_p = 5 \times 10^4 s^{-1}$, $N_p = 10^5 s^{-1}$, $N_p = 2 \times 10^5 s^{-1}$, $N_p = 4 \times 10^5 s^{-1}$, $N_p = 8 \times 10^5 s^{-1}$, $N_p = 1.2 \times 10^6 s^{-1}$, $N_p = 1.6 \times 10^6 s^{-1}$ and $N_p = 2 \times 10^6 s^{-1}$ respectively. The number of particles is the only parameter that differentiates the simulations, all the other parameters have been kept constant. We call this bunch of 11 simulations as basic simulations, in order to distinguish them from the supplementary. The supplementary simulations were run, because there were either cases where $N_p = 2 \times 10^6 s^{-1}$ were not enough to put out the error, or cases that we had to make the spaces between two consecutive simulations thicker, so that to decide on the number of droplets that faints the error. What is more, each set of basic or supplementary simulations was run four times, under the four different meshes described in earlier section 2.2.

Nozzle $N_{i_{i=1}}^{18}$				
$\boldsymbol{N_p}$ $(\boldsymbol{s^{-1}})$	*Mesh*			
	C	***M***	***F***	***VF***
5000	S1	S12	S23	S34
10000	S2	S13	S24	S35
20000	S3	S14	S25	S36
50000	S4	S15	S26	S37
100000	S5	S16	S27	S38
200000	S6	S17	S28	S39
400000	S7	S18	S29	S40
800000	S8	S19	S30	S41
1200000	S9	S20	S31	S42
1600000	S10	S21	S32	S43
2000000	S11	S22	S33	S44

Table 2-2. The number of basic simulations run for each of the tested nozzles

Table 2-2 presents the number of basic simulations, ran for each of the tested nozzles. The total number of the simulations, basic and supplementary, that were ran for all meshes came up to 990. The results of the simulations are presented in Chapter 3 and the total raw FDS

simulation results are listed in Appendix C. What follows next is the result analysis presentation.

2.6 The Result Analysis Methodologies

After we determined the experimental methodology, which was followed in the context of the present work, the question that arises now is about the methodology that should be used to specify the critical number of computational droplets ($N_{p,cr}$). This is the result analysis, and, in order to answer the question before, we applied two different methodologies, the graphical and the statistical analysis. The statistical analysis of the results was applied for each of the nozzles separately, as well as for the total number of the experiments (global analysis).

I. The graphical analysis (Method A)

The first method is simple and fast, but it can give us a very good estimation of the area (number of droplets), where the error originating from the computational particles is starting to be negligible. After we ran the basic and the supplementary simulations (if needed) for a certain nozzle and mesh size, we collect the averaged results in tables like the one follows (Table 2-3).

N_p (s^{-1})	PF (lpm/m^2)	dev PF	MC (kg/m^3)	dev MC	D32 (μm)	dev D32	D10 (μm)	dev D10	T (min)
5000	8.4	*67.43%*	0.93	*70.00%*	96.5	*44.03%*	72.7	*38.74%*	0.1
10000	11.82	*54.17%*	1.26	*59.35%*	94.4	*40.90%*	69.7	*33.02%*	0.1
20000	13.17	*48.93%*	1.44	*53.55%*	87.9	*31.19%*	65.5	*25.00%*	0.2
50000	16.72	*35.17%*	1.93	*37.74%*	79.7	*18.96%*	60.3	*15.08%*	0.3
100000	20.24	*21.52%*	2.38	*23.23%*	73.5	*9.70%*	56	*6.87%*	0.6
200000	22.08	*14.39%*	2.62	*15.48%*	70.2	*4.78%*	54.2	*3.44%*	1.6
400000	24.29	*5.82%*	2.9	*6.45%*	68.5	*2.24%*	53	*1.15%*	3.3
500000	24.61	*4.58%*	2.95	*4.84%*	68	*1.49%*	52.9	*0.95%*	4.3
600000	25.21	*2.25%*	3.01	*2.90%*	67.9	*1.34%*	52.8	*0.76%*	5.5
800000	25.59	*0.78%*	3.07	*0.97%*	67.7	*1.04%*	52.7	*0.57%*	7.4
1000000	25.89	*0.39%*	3.11	*0.32%*	67.6	*0.90%*	52.7	*0.57%*	13.7
1200000	26.15	*1.40%*	3.14	*1.29%*	67.5	*0.75%*	52.7	*0.57%*	11.4
1400000	26.12	*1.28%*	3.14	*1.29%*	67.5	*0.75%*	52.6	*0.38%*	13.6
1600000	26.11	*1.24%*	3.13	*0.97%*	67.3	*0.45%*	52.6	*0.38%*	15.4
2000000	25.79	*0.00%*	3.1	*0.00%*	67	*0.00%*	52.4	*0.00%*	19.1

Table 2-3. Nozzle 7C simulation results. Letter C abbreviates the mesh (cell size 10cm)

Table 2-3 presents the post processing results of the Nozzle 7C, as they were tracked from simulating the nozzle fifteen times, under fifteen different number of computational particles (N_p). C stands for the Coarse mesh (10 cm cell). Each line of the table is the result of one individual simulation. The last simulation of the table ($N_p = 2 \times 10^6 s^{-1}$) is assumed as the error free simulation for that particular nozzle. The table columns include the N_p, the averaged (last 5 seconds) results of the four output quantities PF, MC, D32 and D10 and the evolution of their error, namely the dev PF, dev MC, dev D32 and dev D10 columns, as they

were defined in the previous section 2.5. Finally, the last column (T) reports the computational time in minutes, for each simulation performed. The increase in time is due to the higher number of computational droplets.

Back to the graphical approach, we plot next the number of particles N_p against the measured output quantities and we get the following scatter graphs (Figure 2.2 - Figure 2.5).

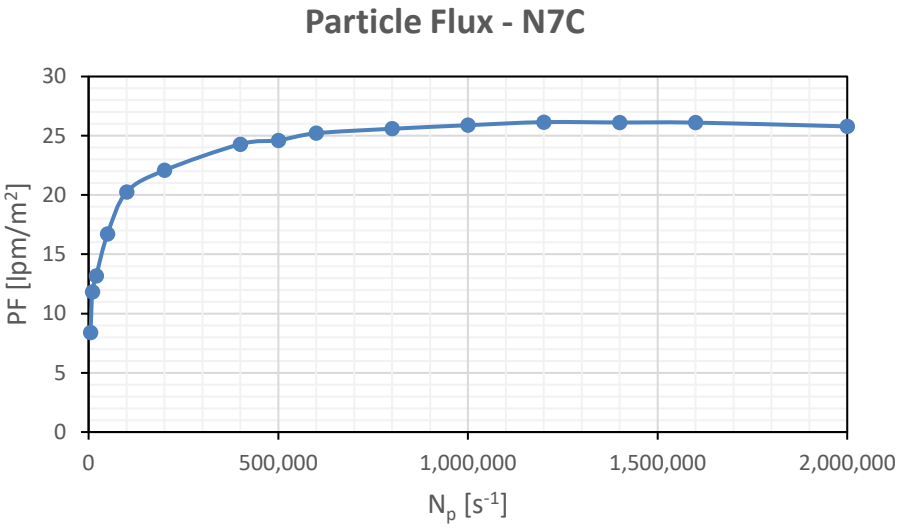

Figure 2.2 The particle flux (PF) simulation results (Nozzle7C)

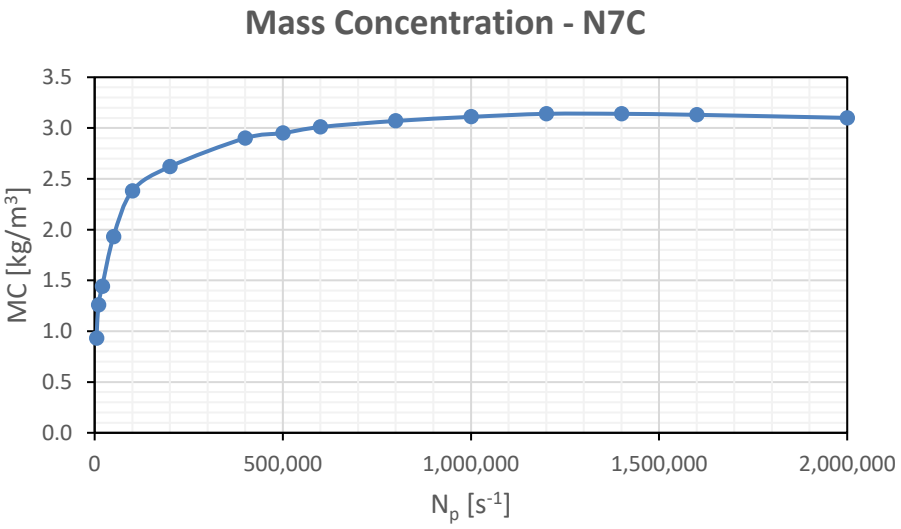

Figure 2.3. The mass concentration (MC) simulation results (Nozzle 7C)

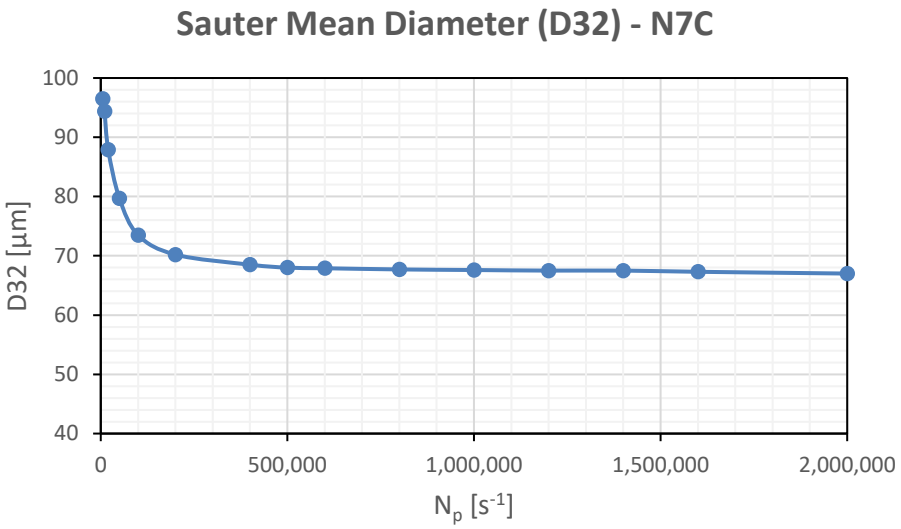

Figure 2.4. The Sauter Mean Diameter (D32) simulation results (Nozzle7C)

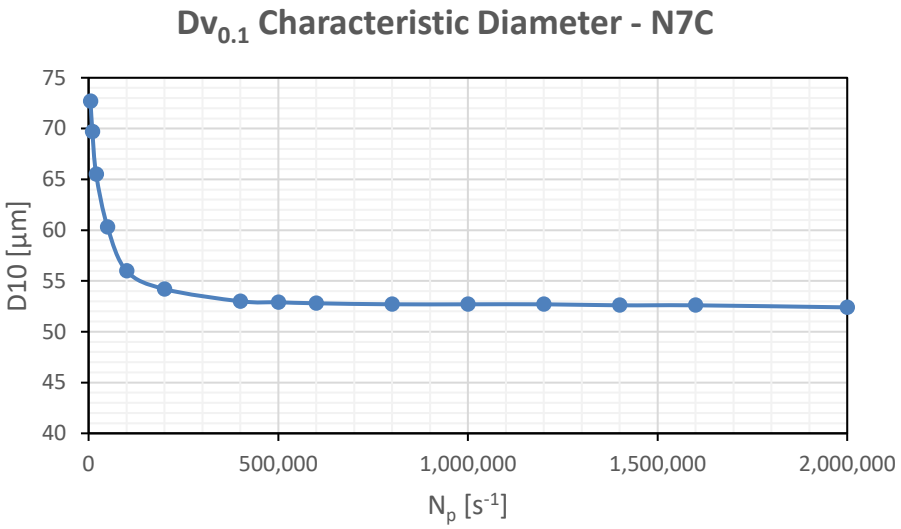

Figure 2.5. The $Dv_{0.1}$ simulation results (Nozzle7C)

By studying the graphs above, it can be seen that there is no significant variation of the output quantities for a number of computational droplets greater than $N_p = 8 \times 10^5 s^{-1}$. Therefore, according to the graphical analysis methodology, we assume that the critical number of droplets $(N_{p,cr})$, for that particular nozzle – diameter is $N_{p,cr} = 8 \times 10^5 s^{-1}$. This is the appropriate N_p that diminishes the error. The results of the implementation of this methodology for all nozzles are presented in section 3.2.

We used the verb diminish for the following reasons. First of all, because, the critical number of droplets $N_{p,cr}$ doesn't necessarily indicate that there is not any more change of the output values. As it can be observed from Table 2-3, the output results vary for N_p higher than the $N_{p,cr} = 8 \times 10^5 s^{-1}$, but the fluctuation of the values is quite small, moving in the range of ±1.5%. Consequently, and in order for this method to be applicable, we need to set a

threshold range, inside which the fluctuation of the resulting quantities is considered to be negligible. This threshold range has been set up to 3%. Besides, there are cases, where the output quantities, e.g. the PF, MC, D32 or D10, do not demand the same number of computational droplets, so that their corresponding error is minimized. In such cases the PF, due to its higher physical significance is the decisive quantity for determining the $N_{p,cr}$.

Another reason of using the verb diminish is linked to the uncertainty of the analysis methodologies, which is explained in section 2.7, concerning the error free simulation definition and the simulation with the highest number of computational droplets that could be reached. The quantification of the error depends on the simulation with the higher number of droplets that we performed, which on its turn depends on the availability of the time and the computational resources. This is the farthest point that we could get in the context of the present work. We have evidence that is adequate, but we didn't go any further to be absolutely certain.

For all these reasons, and despite the fact that the graphical analysis methodology stands out for its simplicity and its directness, there is always a kind of bias, mainly because of the threshold range and the error free simulation estimation. Therefore, we were looking for an approach that subsides these drawbacks and is able, from the one hand, to provide us with results that are outside the range of the simulations we performed and on the other hand, to involve less subjectivity. The statistical analysis of the results, in terms of finding a model to predict the number of droplets that extinguishes the error seems to be applicable for this case in particular.

II. <u>The curve fitting analysis (Method B)</u>

Method B is based on the theory assumption, concerning the proportionality between the error (deviation) generated by the limited number of computational droplets and the quantity $1/\sqrt{N_p}$. The analysis of the error of the output variables, as it is presented in the following section 4.2, indicated that, in most of the cases, there is a linear relationship between the error of an output variable and the former quantity. We are seeking, therefore, a model that describes the linear relationship between $1/\sqrt{N_p}$ and the errors, and particularly the error of the Particle Flux $(devPF)$, so that to predict the exact number of computational droplets, which makes the correspondent error equal to zero. For the shake of the completeness, we note also that the same methodology can be applied for each of the other output variables, e.g. the MC, the D32 and the D10. The analysis was conducted in excel, by plotting the calculated error of the PF output quantity against $1/\sqrt{N_p}$ and finding a linear model (equation) that best fits the results. The equation then was solved backwards for the quantity $1/\sqrt{N_p}$, from which the $N_{p,cr}$ was extracted.

The methodology is explained by the following example on the simulation results of the Nozzle 9C, which are presented in Table 2-4. Figure 2.6 - Figure 2.9 present the evolution of the error of the four measured output quantities as a function of the $1/\sqrt{N_p}$, as well as the

trendline that best fits the results along with the linear equation and the coefficient of determination R^2.

N_p (s^{-1})	$1/\sqrt{N_p}$	PF (lpm/m²)	dev PF	MC (kg/m³)	dev MC	D32 (μm)	dev SMD	D10 (μm)	dev D10	T (min)
5000	0.014142	3.06	*43.85%*	0.58	*50.00%*	139.1	*32.10%*	108.2	*35.76%*	0.1
20000	0.007071	4.25	*22.02%*	0.85	*26.72%*	123	*16.81%*	93	*16.69%*	0.1
50000	0.004472	4.86	*10.83%*	1	*13.79%*	113.4	*7.69%*	84.3	*5.77%*	0.3
100000	0.003162	5.22	*4.22%*	1.09	*6.03%*	108.9	*3.42%*	81.2	*1.88%*	1
200000	0.002236	5.41	*0.73%*	1.13	*2.59%*	107.6	*2.18%*	80.5	*1.00%*	1.6
300000	0.001826	5.39	*1.10%*	1.14	*1.72%*	106.8	*1.42%*	80.4	*0.88%*	2.1
400000	0.001581	5.45	*0.00%*	1.16	*0.00%*	106.1	*0.76%*	80	*0.38%*	3.1
600000	0.001291	5.45	*0.00%*	1.16	*0.00%*	105.3	*0.00%*	79.7	*0.00%*	4.9

Table 2-4. Nozzle 9C simulation results

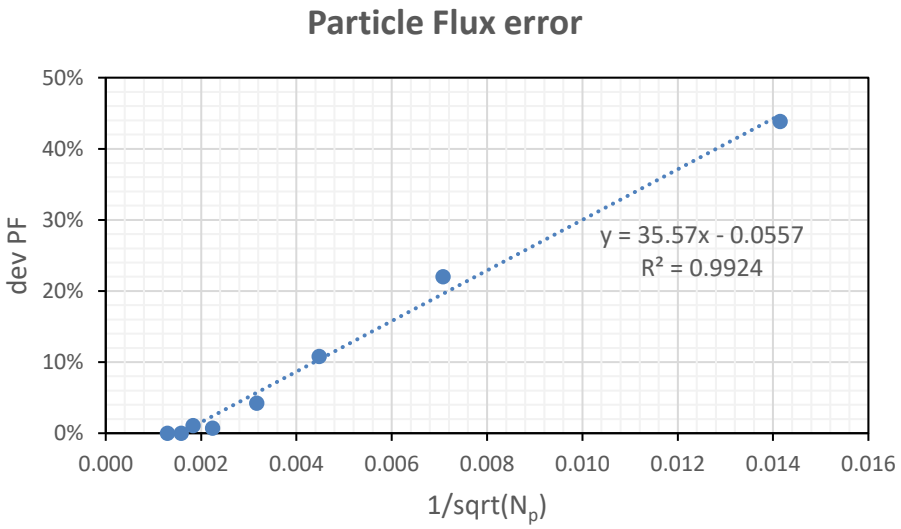

Figure 2.6. Evolution of the PF error with increasing number of computational droplets (Nozzle9C)

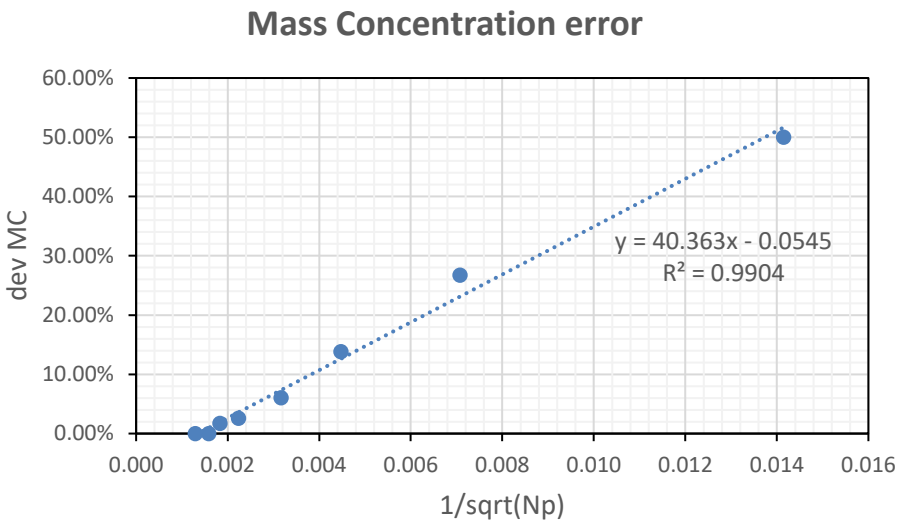

Figure 2.7. Evolution of the MC error with increasing number of computational droplets (Nozzle9C)

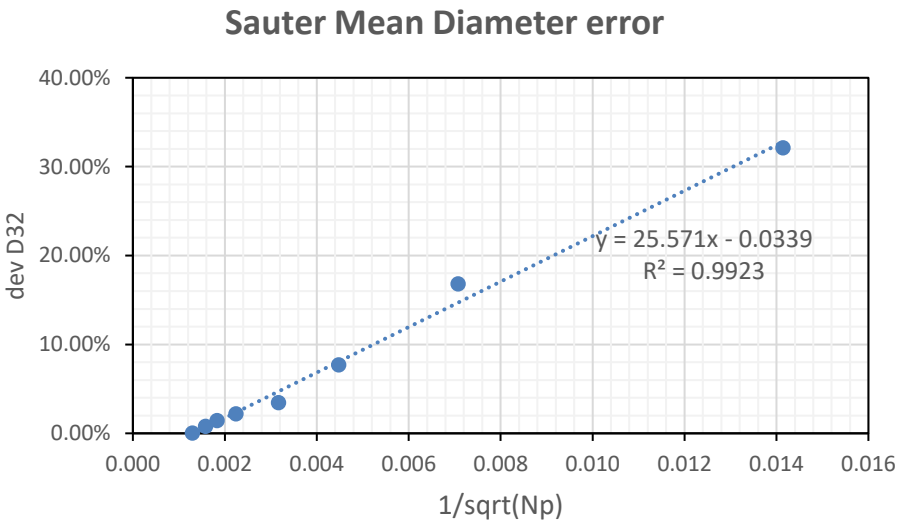

Figure 2.8. Evolution of the D32 error with increasing number of computational droplets (Nozzle9C)

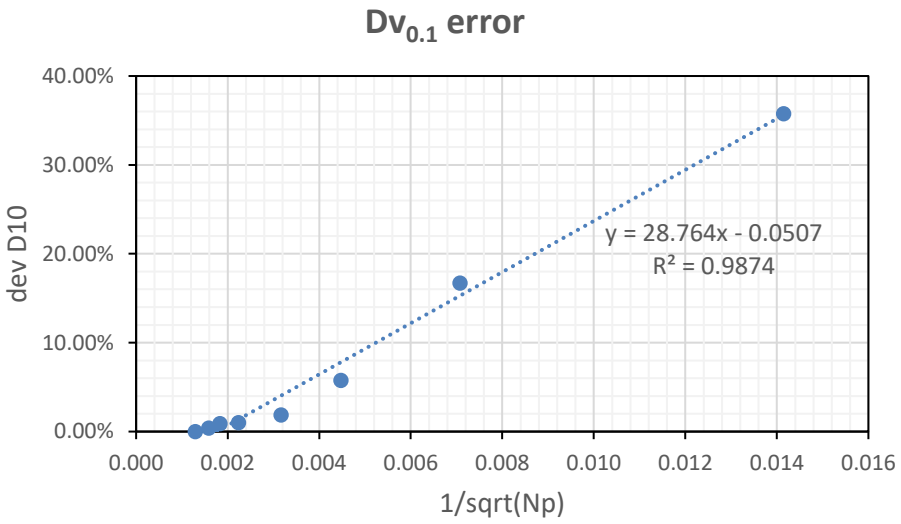

Figure 2.9. Evolution of the D10 error with increasing number of computational droplets (Nozzle9C)

In case of the PF error, the evolution of the error is given by the Eq. 2-3,

$$dev\ PF = 35.57 \times \frac{1}{\sqrt{N_p}} - 0.0577 \qquad \text{Eq. 2-3}$$

By equating $devPF$ to zero and solving the equation for N_p, we find the critical number of computational droplets $N_{p,cr}$, which in this case equals to $N_{p,cr} = 4.1 \times 10^5 s^{-1}$. We follow this procedure seventy-two times (18 nozzles times 4 meshes) and the final results, in terms of $N_{p,cr}$, are presented in section 3.3. The seventy-two individual method B models are presented in Appendix D. At this point we need to mention that Method B is very sensitive to the number of data (simulations) that is used to derive the fitting curve or line. Even one extra simulation is enough to drastically change the output. Therefore, the reader should be aware of the fact that the presented output is due to a particular set of simulations that was used to represent the behavior of the error.

III. The global statistical analysis (Method C)

The third approach, which was applied to find the appropriate number of computational droplets that is necessary to eliminate the statistical error, is similar in principal to the second one (error proportionality). The difference lies in the fact that we are not analyzing the simulation results nozzle by nozzle. We use, instead, the results in total (all nozzles, all meshes, all output variables), in order to find one global model that is able to describe the behavior of the error for the whole range of diameters at any given grid size and, as a result, to predict the number of droplets for a certain level of error. On account of this, we use the multivariable linear regression technique. The analysis was carried out through the SPSS statistics software package and the final output is presented in section 3.4.

The multivariable linear regression analysis requires a series of assumptions, among which the linear relationship between the dependent variable $1/\sqrt{N_p}$ and the independent variable ($devPF$), is considered to be the key element of applying the method. Other assumptions that should not be violated such as the multivariate normality, the multicollinearity, the auto-correlation, are all checked in SPSS, through a correlation coefficient and ANOVA analysis, and allow us to accept the model or not. The appropriateness and the fit of the model is achieved by evaluating the coefficient of determination R^2 and the significance of the model coefficients (P-values). The whole report of the analysis, as it was produced by the SPSS, is available in Appendix E.

The global statistical analysis ended up with the following model (Eq. 2-4), which predicts the quantity $1/\sqrt{N_p}$ as a function of the $Dv_{0.5}$ (μm), the cell size (cm), the error PF (%), the error MC (%), the error D32 (%) and the error D10 (%). Solving then for N_p one can calculate the required number of droplets (Eq. 2-5).

$$\begin{aligned}\frac{1}{sqrt(N_p)} = {} & 7.43 \times 10^{-4} + 4.63 \times 10^{-6} \times DV_{0.5} \\ & - 5.95 \times 10^{-5} \times cell - 1.6 \times 10^{-4} \times devPF \\ & + 2.71 \times 10^{-3} \times devMC \\ & - 3.18 \times 10^{-3} \times devD32 \\ & + 2.61 \times 10^{-2} \times devD10\end{aligned} \qquad \text{Eq. 2-4}$$

$$\begin{aligned}N_p = {} & (7.43 \times 10^{-4} + 4.63 \times 10^{-6} \times DV_{0.5} \\ & - 5.95 \times 10^{-5} \times cell - 1.6 \times 10^{-4} \times devPF \\ & + 2.71 \times 10^{-3} \times devMC \\ & - 3.18 \times 10^{-3} \times devD32 \\ & + 2.61 \times 10^{-2} \times devD10)^{-2}\end{aligned} \qquad \text{Eq. 2-5}$$

The equation above is very handy, because it makes it possible to calculate, for any given diameter (35 – 1000μm) and cell size (1.25 – 10cm) within the range of this study, the necessary number of particles, depending on the accuracy level that has been defined. And, in fact, it can give us a very good estimation of the number of particles needed, since the model explains 60.6% of the variation of the dependent variable, which means that 60.6% of the variance in the dependent variable $1/\sqrt{N_p}$ can be attributed to the movement in the independent variables (mean diameter, cell size, errors). This is considered as statistically significant. The remaining 39.4% is attributed to other factors. It is also noteworthy that the independent variables do not have the same significance. According to the analysis, the most important independent variable is the D10 diameter (standardized coefficient 0.645), taking dev PF the second place (standardized coefficient 0.399). Section 3.4 presents the $N_{p,cr}$. results for the whole range of diameters and meshes. The global statistical analysis has the same disadvantage as that of method B, since it also very prone to the sample that was analyzed.

2.7 Uncertainties Linked with the Analysis Methodology

We mentioned in the previous sections some shortcomings that affect the robustness of each method individually. Apart from that, there are also uncertainties concerning, not only the analysis methodology, but also the general set up of the experimental methodology that we followed, in order to perform the numerical experiments, and it is worth devoting some lines to them.

First, the selection of the water mist nozzles, in terms of their technical specifications, as devices that can produce the desired diameter range is of paramount importance. The main principle of the nozzle selection strategy, governed by the thesis objective to study the relationship between the number of computational and the mean diameters, was to find reliable data, so that we can describe a set of nozzles that produces water droplets, having a very broad range of mean diameters. Reliable data means that the produced drop diameter is physically possible, as a result of the nozzle specifications. This is, without any doubt, decisive for the validity of the results of the present research. However, the set of nozzles is not only diversified in terms of the mean diameter parameter, but also with regard to other physical parameters that describe a nozzle, such as the initial velocity and the spray angle. And even though the initial velocity appears to have little effect on the simulations result, this is not the case for the spray angle [5][38]. The effect of the initial velocity and the spray on the number of computational droplets has not been studied during this work and, therefore, this is considered as a source of uncertainty induced in our research methodology.

The second topic that needs to be further investigated concerns the level of error that is inserted in the numerical simulations, because of a PDPA device and, more concretely, due to the effect of a PDPA device on the local measurements of the prescribed quantities. We explained (section 2.4) that a PDPA is a sphere that samples a number of the particles that are introduced in the computational domain and computes averaged results of quantities in regard to the water droplet properties. The size of the sphere is user defined and it's the filter that determines the sample of the droplet, upon which the prescribed quantities are calculated. In order to understand the significance of the sample technique, try to answer the following question. Which one of the following polls would you trust more, a poll made with a sample of 100 persons, 1000 persons or one with 10000 persons? In a similar to the metaphor way, we can ask whether or not 100 droplets are adequate enough to describe the properties of the total number of droplets that are produced by the nozzle. In the present work, this error is the same for all simulations, since the same device has been used in all cases. Nevertheless, in case of a nozzle characterization numerical experiment, this kind of uncertainty needs to be quantified.

Last source of uncertainty, but not least, since it is the main source of error of the present work, it is the definition of the deviation (error) itself, as a quantification of the error that is originated by the limited number of computational droplets. Based on the definition of the error between the experiments and the numerical simulations, we formulated a

mathematically similar expression for the number of particles error, supposing that there is an error free simulation, because the statistical error converges. This error free simulation, according to our methodology is assumed to be the simulation with the higher number of droplets for each set of simulations. But is it actually like that? How much sensitive are the results to the error free simulation and how much different would they be the results, if we had decided for a different error free simulation. For the vast majority of the experiments we are confident that the error free simulation is well defined. However, in case of the small diameter nozzles, the computational resources and the simulation time limited somehow our ability to reach the actual error free simulation. Estimating the error free simulation is a difficult task, which always brings in a certain level of bias, which was acknowledged in this work and attracted our full attention.

3. Results

3.1 Introduction

This chapter contains the presentation of the final results, as they emerged from the analysis methodologies that explained in the previous chapter. The simulation results are presented in terms of $N_{p,cr}$-diameter graphs, showing the relationship between the mean diameter of the water droplets that are produced by the nozzles and the number of computational droplets that eradicates the statistical error (critical number of computational droplets per second $N_{p,cr}$), as it was estimated by each of the three methods (A, B and C) that have been followed. This relationship, which signifies the advancement of the $N_{p,cr}$ as the mean diameter progressively increases from 35 μm to 1000 μm, is also described by a model, which best fits the resulting graph. Finally, the three methodologies are combined together, in order to end up with a model that describes the combined total behavior of the critical number of computational droplets ($N_{p,cr}$) against the mean diameter. The simulation results presented in this section have been derived from the local measurements of the PDPA device placed at 1.0 m distance away from the nozzle. The rest two devices, placed at 0.8 m and 1.2 m, confirm the simulation results of the former device (1.0 m) and therefore will not be presented.

3.2 Method A Results

Table 3-1 presents the estimation of the critical number of computational particles $N_{p,cr}$ according to the Method A, whereas Figure 3.1 illustrates graphically the relationship between the $N_{p,cr}$ and the $Dv_{0.5}$. In addition, Figure 3.1 includes the curve (trendline) that best fits the resulted $N_{p,cr}$ estimation, along with its mathematical expression and the coefficient of determination R^2. In all four cases, the trendline that best describes the relationship between the $N_{p,cr}$ and the mean diameter $Dv_{0.5}$ of the nozzles complies with the power law.

The Method A results are all plotted in a common graph, in order to extract one model that describes the $N_{p,cr}$, solely as a function of the mean diameter $Dv_{0.5}$. The result is presented on Figure 3.2, while Table 3-2 assembles all Method A $N_{p,cr}$ prediction models. The suggested combined model has a coefficient of determination 85.99%, which makes us feel confident to predict the critical number of particles, by using just one independent variable, namely the mean diameter $Dv_{0.5}$ of the water mist nozzle.

Nozzle	$Dv_{0.5}$ (µm)	Mesh			
		C	M	F	VF
Nozzle 1	35	2.820.000	2.000.000	2.000.000	1.200.000
Nozzle 2	50	2.400.000	1.600.000	800.000	800.000
Nozzle 3	70	1.700.000	1.600.000	1.200.000	1.000.000
Nozzle 4	80	1.200.000	800.000	1.000.000	900.000
Nozzle 5	100	1.000.000	1.000.000	1.200.000	800.000
Nozzle 6	125	800.000	800.000	800.000	500.000
Nozzle 7	150	800.000	600.000	600.000	500.000
Nozzle 8	200	700.000	400.000	400.000	200.000
Nozzle 9	250	400.000	200.000	200.000	200.000
Nozzle 10	300	500.000	200.000	200.000	200.000
Nozzle 11	350	300.000	150.000	50.000	100.000
Nozzle 12	400	100.000	300.000	50.000	100.000
Nozzle 13	500	100.000	100.000	100.000	100.000
Nozzle 14	600	100.000	1.200.000	50.000	200.000
Nozzle 15	700	100.000	100.000	20.000	50.000
Nozzle 16	800	200.000	100.000	75.000	50.000
Nozzle 17	900	100.000	1.000.000	400.000	50.000
Nozzle 18	1000	50.000	600.000	50.000	50.000

Table 3-1. Estimation of the $N_{p,cr}$ (s^{-1}) (Method A)

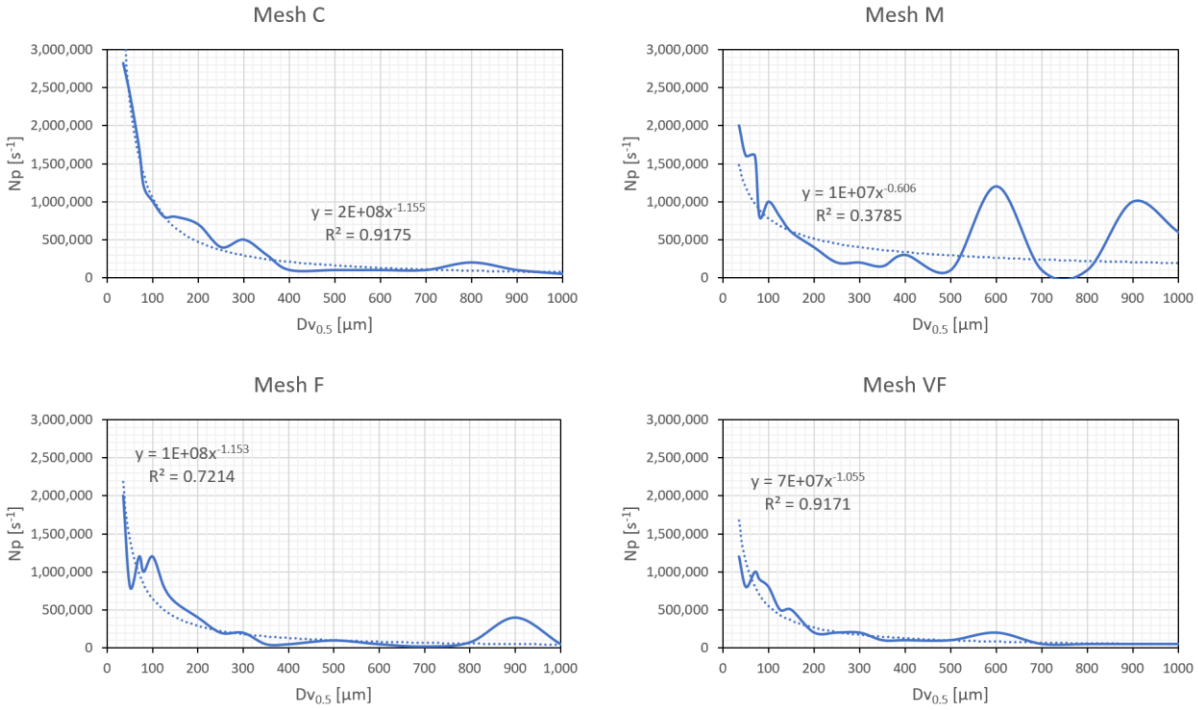

Figure 3.1. Evolution of the $N_{p,cr}$ within the diameter (35-1000µm) and mesh (C, M, F and VF) range (Method A)

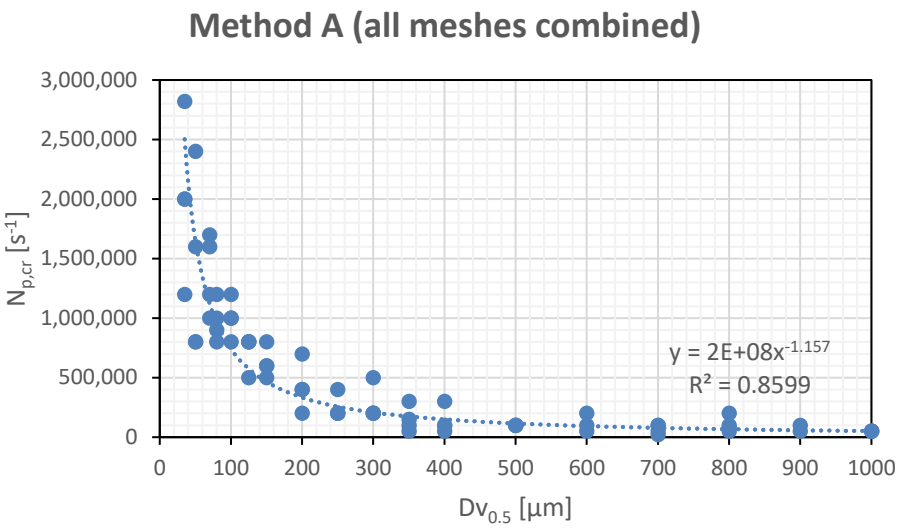

Figure 3.2. Method A combined total solution

	Prediction Model	R^2
C	$N_{p,cr} = 2 \times 10^8 \times Dv_{0.5}{}^{-1.155}$	91.75%
M	$N_{p,cr} = 10^7 \times Dv_{0.5}{}^{-0.606}$	37.85%
F	$N_{p,cr} = 10^8 \times Dv_{0.5}{}^{-1.153}$	72.14%
VF	$N_{p,cr} = 7 \times 10^7 \times Dv_{0.5}{}^{-1.055}$	91.71%
Combined Model A	$N_{p,cr} = 2 \times 10^8 \times Dv_{0.5}{}^{-1.157}$	85.99%
$N_{p,cr}$ (s^{-1}) $Dv_{0.5}$ (µm)		

Table 3-2. Summary table of the $N_{p,cr}$ prediction models (Method A)

3.3 Method B Results

Similar to Method A, Table 3-3 presents the estimation of the critical number of computational particles $N_{p,cr}$, as it was predicted by Method B described in section 2.6, while Figure 3.3 is the graphical representation, including the prediction models with the corresponding determination coefficients R^2. The total Method B solution was further elaborated by combining the four mesh-individual solution in a common scatter graph (Figure 3.4). Table 3-4 provides an overview of the $N_{p,cr}$ prediction models for each of the four meshes separately, as well as the total combined Method B prediction model.

Nozzle	$Dv_{0.5}$ (µm)	Mesh			
		C	M	F	VF
Nozzle 1	35	2.820.000	2.120.000	2.660.000	2.4300.00
Nozzle 2	50	2.260.000	2.040.000	1.730.000	1.980.000
Nozzle 3	70	2.270.000	2.980.000	2.190.000	2.470.000
Nozzle 4	80	1.450.000	1.670.000	1.820.000	1.900.000
Nozzle 5	100	1.250.000	1.820.000	2.120.000	1.960.000
Nozzle 6	125	1.520.000	1.430.000	1.780.000	1.130.000
Nozzle 7	150	1.340.000	960.000	1.100.000	1.160.000
Nozzle 8	200	670.000	490.000	610.000	310.000
Nozzle 9	250	410.000	740.000	800.000	350.000
Nozzle 10	300	650.000	260.000	380.000	290.000
Nozzle 11	350	710.000	270.000	100.000	150.000
Nozzle 12	400	250.000	360.000	150.000	140.000
Nozzle 13	500	170.000	180.000	250.000	160.000
Nozzle 14	600	120.000	1.660.000	110.000	310.000
Nozzle 15	700	210.000	140.000	50.000	140.000
Nozzle 16	800	270.000	80.000	130.000	50.000
Nozzle 17	900	260.000	40.000	630.000	240.000
Nozzle 18	1000	10.000	620.000	150.000	110.000

Table 3-3. Estimation of the $N_{p,cr}$ (s^{-1}) (Method B)

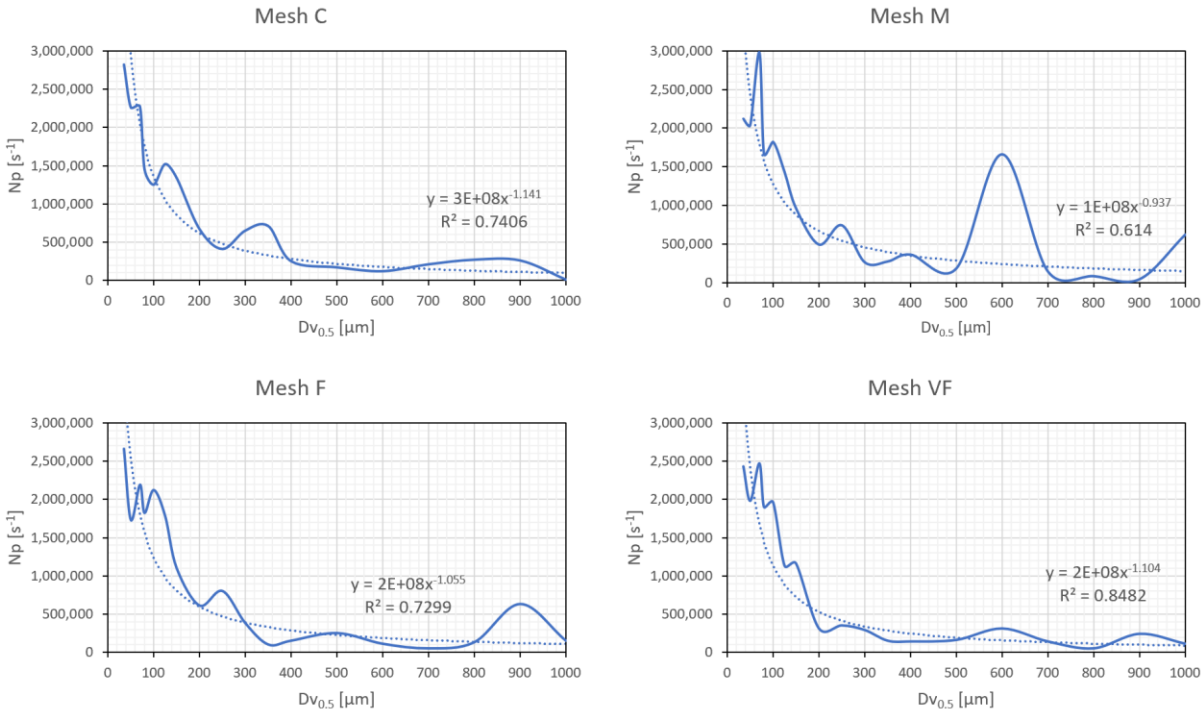

Figure 3.3. Evolution of the $N_{p,cr}$ within the diameter (35-1000µm) and mesh (C, M, F and VF) range (Method B)

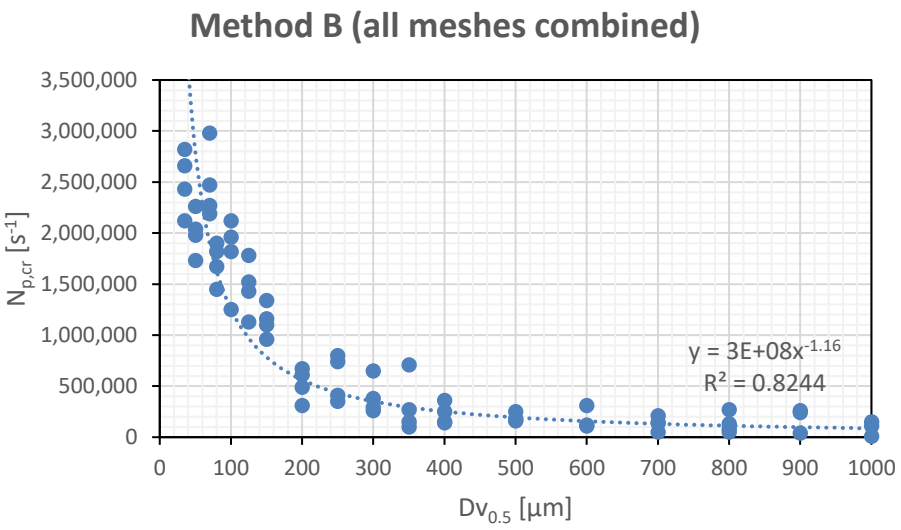

Figure 3.4. Method B combined total solution

	Prediction Model	R^2
C	$N_{p,cr} = 3 \times 10^8 \times Dv_{0.5}{}^{-1.141}$	74.06%
M	$N_{p,cr} = 10^8 \times Dv_{0.5}{}^{-0.937}$	61.4%
F	$N_{p,cr} = 2 \times 10^8 \times Dv_{0.5}{}^{-1.055}$	72.99%
VF	$N_{p,cr} = 2 \times 10^8 \times Dv_{0.5}{}^{-1.104}$	84.82%
Combined Model B	$N_{p,cr} = 3 \times 10^8 \times Dv_{0.5}{}^{-1.16}$	82.44%
$N_{p,cr}$ (s^{-1}) $Dv_{0.5}$ (µm)		

Table 3-4. Summary table of the $N_{p,cr}$ prediction models (Method B)

3.4 Method C Results

In a similar to methods A and B manner, the relevant information, with regard to Method C, are supplied by the following Table 3-5, Figure 3.5, Figure 3.6 and Table 3-6 respectively. As it was also mentioned in section 2.6, the estimation of the $N_{p.cr}$ was accomplished according to the Eq. 2-5, by defining the correspondent $Dv_{0.5}$ (µm) and the cell size (cm), and equating, at the same time, all quantity errors to zero.

Nozzle	$Dv_{0.5}$ (µm)	Mesh			
		C	M	F	VF
Nozzle 1	35	8.374.823	2.558.658	1.708.877	1.434.692
Nozzle 2	50	5.807.345	2.072.805	1.436.376	1.222.889
Nozzle 3	70	3.882.397	1.614.016	1.163.860	1.006.352
Nozzle 4	80	3.260.666	1.439.752	1.055.809	919.043
Nozzle 5	100	2.393.717	1.166.323	880.397	775.351
Nozzle 6	125	1.722.075	921.636	716.419	638.613
Nozzle 7	150	1.298.031	746.588	594.326	535.099
Nozzle 8	200	812.937	518.530	428.013	391.395
Nozzle 9	250	556.517	380.995	322.867	298.669
Nozzle 10	300	404.736	291.719	252.194	235.378
Nozzle 11	350	307.534	230.506	202.420	190.264
Nozzle 12	400	241.565	186.718	166.049	156.979
Nozzle 13	500	160.336	129.673	117.540	112.103
Nozzle 14	600	114.124	95.274	87.555	84.042
Nozzle 15	700	85.351	72.947	67.735	65.336
Nozzle 16	800	66.232	57.638	53.955	52.245
Nozzle 17	900	52.885	46.688	43.990	42.728
Nozzle 18	1000	43.201	38.586	36.551	35.593

Table 3-5. Estimation of the $N_{p,cr}$ (s^{-1}) (Method C)

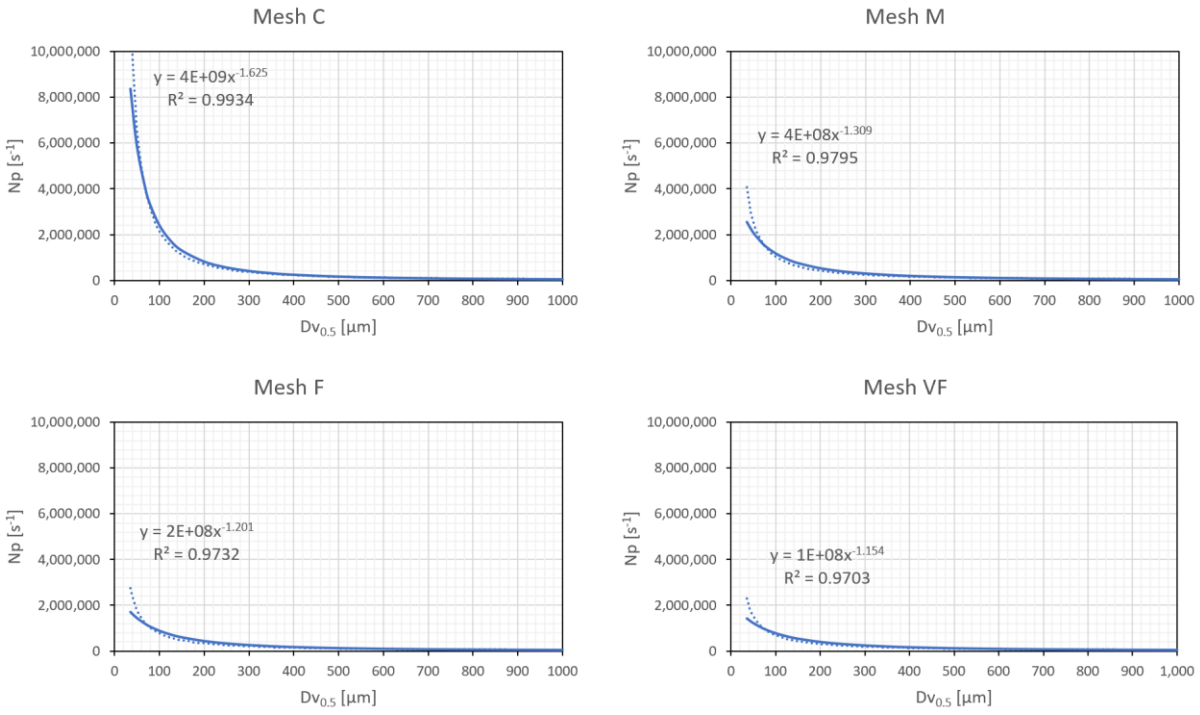

Figure 3.5. Evolution of the $N_{p,cr}$ within the diameter (35-1000µm) and mesh (C, M, F and VF) range (Method C)

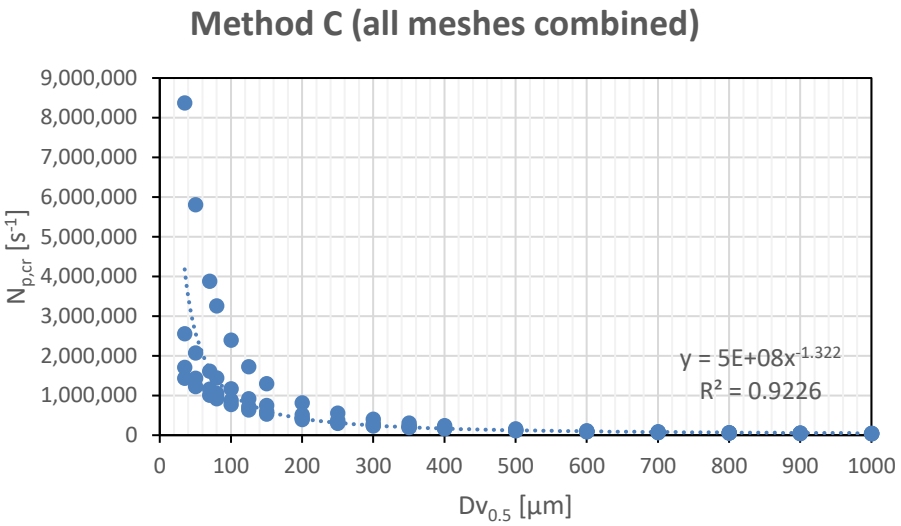

Figure 3.6. Method C combined total solution

	Prediction Model	R^2
C	$N_{p,cr} = 4 \times 10^9 \times Dv_{0.5}{}^{-1.625}$	99.34%
M	$N_{p,cr} = 4 \times 10^8 \times Dv_{0.5}{}^{-1.309}$	97.95%
F	$N_{p,cr} = 2 \times 10^8 \times Dv_{0.5}{}^{-1.201}$	97.32%
VF	$N_{p,cr} = 10^8 \times Dv_{0.5}{}^{-1.154}$	97.03%
Combined Model C	$N_{p,cr} = 5 \times 10^8 \times Dv_{0.5}{}^{-1.322}$	92.26%
$N_{p,cr}$ (s^{-1}) $Dv_{0.5}$ (µm)		

Table 3-6. Summary table of the $N_{p,cr}$ prediction models (Method C)

3.5 The "Averaged" Model

Each of the Methods A, B and C ended up with a single model, able to predict the critical number of computational droplets ($N_{p.cr}$), as a function of the mean diameter $Dv_{0.5}$, regardless of the mesh size of the numerical simulations. Due to the similarities of the predictions of the three individual models and, in order to have one model instead of three, we came up with the idea of ending up with one single model, able to predict the $N_{p.cr}$ for the whole range of dimeters and cell sizes, as a function solely of the $Dv_{0.5}$. The term "averaged" refers to the average over the four cell size simulation campaigns and denotes the decoupling of the cell size variable from the prediction of the $N_{p.cr}$, which replaces the three-model solution by one. For this reason, we merge the Method A, B and C solutions to one, in the way we performed the analysis for the mesh individual models, and we get the scatter diagram in Figure 3.7.

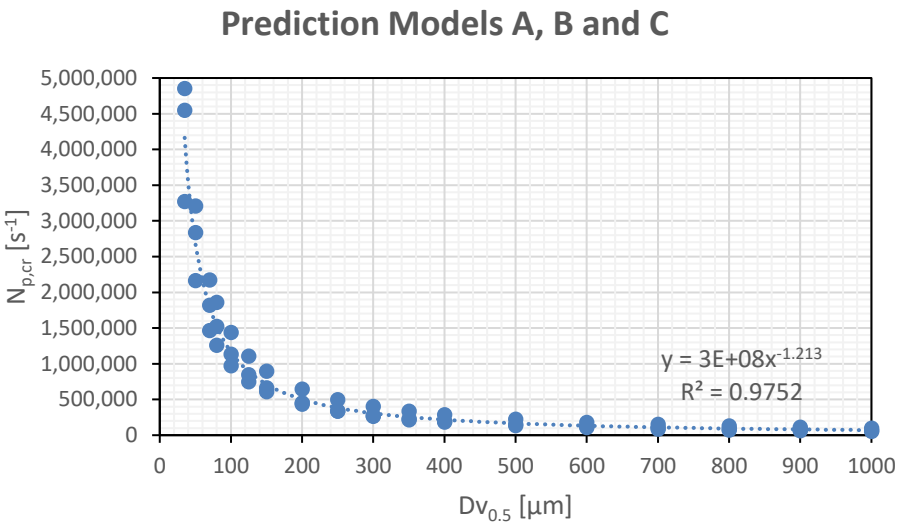

Figure 3.7. Common representation of the three individual solutions (Method A, B and C)

As a result, the combined output can be predicted by one single model, with an exceptionally coefficient of determination 97.52%. The universal model is described mathematically by Eq. 3-1

$$N_{p,cr} = 3 \times 10^{8} \times {Dv_{0.5}}^{-1.213} \qquad \text{Eq. 3-1}$$

and the universal behavior of the $N_{p.cr}$ in terms of the $Dv_{0.5}$ is depicted in Figure 3.8.

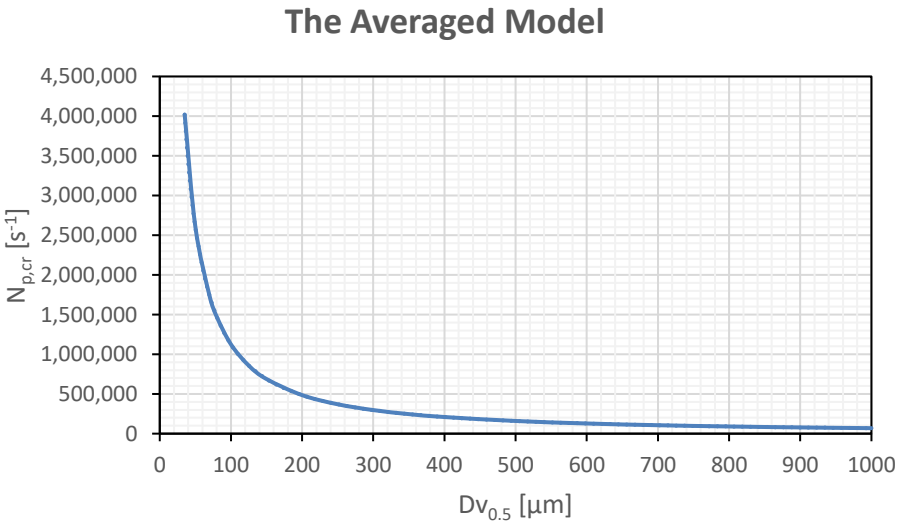

Figure 3.8. The determination of the Np,cr according to the averaged solution

4. Discussion

4.1 Introduction

This chapter contains comments with regard to the main findings of the experimental research methodology that was presented, in order to study the accuracy level of the water mist numerical simulations, in comparison with the number of computational particles per second (N_p) that needs to be defined to represent the water spray produced by the water mist nozzles. Following the theory assumption that the limited number of computational droplets constitutes a source of error and that there is a proportionality between the quantity $1/\sqrt{N_p}$ and the error, we designed and conducted a series of numerical experiments, aiming at understanding the nature of the error and providing, in this way, guidance to the future modelers, concerning the number of particles that are appropriate to get simulations with an affordable statistical error.

The number of particles that is proposed by our experimental methodology means in no case that it is the appropriate number to get correct simulation results. It is, according to our research, the number that eliminates the statistical error induced in the simulation by the limited particles. The numerical modelling contains a large number of simplifications, assumptions and numerical methods, each of which brings in place a certain error that questions the accuracy of the simulations. The present work helps to bring under control the error generated by one simplification, the confined number of computational particles. The validation of the simulation results is a different process and it is always the modeler's responsibility to perform it.

4.1 The Assessment of the Analysis Methodologies

The result analysis is consisted of three different methodologies (A, B and C), each of which predicts the critical number of computational particles ($N_{p,cr}$).The graphical analysis (Method A) is founded on the statistical convergence of the output variables. The intention was to find the number of particles, upon which there is no significant variation of the resulted quantities. Method A uses the total number of simulations that were performed for the experimental analysis, which comes up to 990 simulations. Moreover, the estimation of the critical number of droplets was brought off by taking into consideration the simulation results of all four output quantities, namely the PF, MC, D32 and D10. The study was performed nozzle by nozzle, mesh by mesh.

Method B uses the simulation output indirectly and focuses on the evolution of the error, as it is defined in section 2.5, trying to predict where the PF error faints. The PF error was chosen due to its higher significance in real life applications, compared to the remaining output quantities. For the majority of the experiments we can assume a linear relationship between the $1/\sqrt{N_p}$ and the error and, therefore, a linear model can adequately predict the enhancement of the error as the number of droplets increases. But as it will be seen in the

following section 4.2, this relationship is not always linear. In order to improve the efficacy of the model, we had to exclude values that disturb the linearity of the model, as we also did in case of outlying values. As a result, the number of simulations that were used for the analysis came up to 487. Similar to Method A, the analysis was carried out nozzle by nozzle, mesh by mesh.

Method C applies the same principle as that of Method B, except for that the determination of the critical number of droplets is not studied nozzle by nozzle and mesh by mesh and that the PF error is not the only determinant of the prediction model. The results of the 487 simulations that studied in Method B, are in this case analyzed together and result in a model that predicts the number of particles as a function of six independent variables, namely the $Dv_{0.5}$, the cell size, and the four errors (devPF, devMC, devD32, devD10).

Even though all three methodologies differ, in terms of the theory that lies behind or the implementation technique, they all captured the same picture, concerning the behavior of the $N_{p,cr}$ as a function of the $Dv_{0.5}$. Table 4-1 and, especially, Figure 4.1 are both constitute an evidence.

Nozzle	***$Dv_{0.5}$ (μm)***	***Model A***	***dev A***	***Model B***	***dev B***	***Model C***	***dev C***	***Averaged Model***
Nozzle 1	35	3.269.966	18.65%	4.852.911	20.74%	4.546.865	13.12%	4.019.451
Nozzle 2	50	2.164.321	17.01%	3.208.603	23.04%	2.837.472	8.81%	2.607.778
Nozzle 3	70	1.466.397	15.43%	2.171.738	25.25%	1.818.655	4.89%	1.733.873
Nozzle 4	80	1.256.478	14.79%	1.860.102	26.14%	1.524.351	3.37%	1.474.596
Nozzle 5	100	970.577	13.72%	1.435.890	27.64%	1.134.932	0.89%	1.124.919
Nozzle 6	125	749.730	12.64%	1.108.423	29.16%	844.997	1.53%	858.162
Nozzle 7	150	607.145	11.74%	897.130	30.42%	664.014	3.47%	687.896
Nozzle 8	200	435.250	10.31%	642.579	32.42%	453.950	6.45%	485.257
Nozzle 9	250	336.212	9.18%	496.033	34.00%	337.982	8.70%	370.186
Nozzle 10	300	272.271	8.25%	401.477	35.30%	265.592	10.50%	296.738
Nozzle 11	350	227.795	7.45%	335.739	36.41%	216.627	11.99%	246.131
Nozzle 12	400	195.185	6.76%	287.562	37.38%	181.571	13.26%	209.326
Nozzle 13	500	150.772	5.58%	221.981	39.01%	135.186	15.34%	159.687
Nozzle 14	600	122.098	4.61%	179.666	40.36%	106.232	17.01%	128.004
Nozzle 15	700	102.153	3.79%	150.248	41.51%	86.646	18.39%	106.174
Nozzle 16	800	87.530	3.06%	128.688	42.52%	72.625	19.57%	90.297
Nozzle 17	900	76.379	2.42%	112.254	43.41%	62.153	20.60%	78.275
Nozzle 18	1000	67.613	1.85%	99.339	44.21%	54.072	21.50%	68.884

Table 4-1. Np,cr prediction, according to the three models (A, B and C) and the averaged solution.

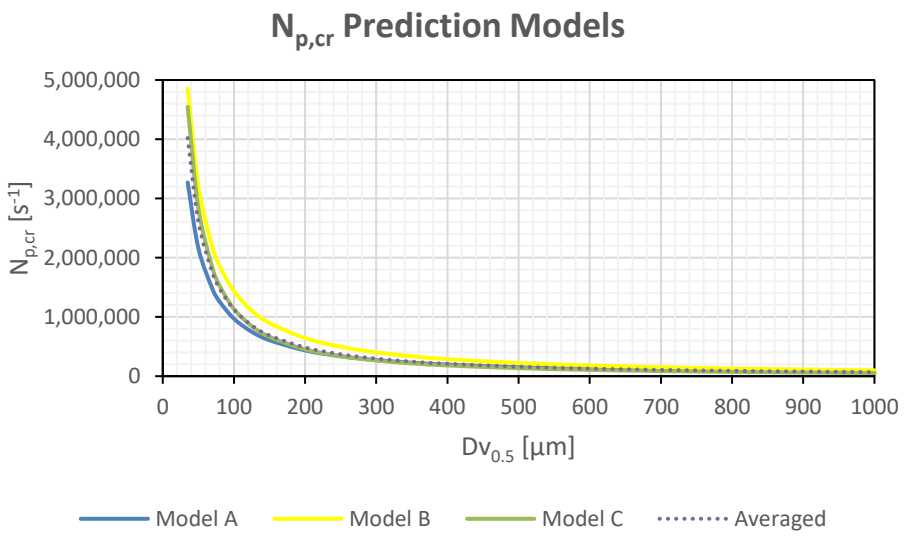

Figure 4.1. The four prediction models of the critical number of computational particles $N_{p,cr}$ (A, B, C and Averaged)

Although there are countable differences in absolute values among the model predictions, it should not be underestimated that they all indicate that the critical number of computational particles as a function of the mean diameter obeys the power law, and they all require the same level of $N_{p,cr}$, for a certain mean diameter. This can be deduced by looking the values of Table 4-1, and especially the columns with the deviation calculations, which denote the distance between the three solutions (A, B and C) and the averaged one. The differences between the models are due to the previously described nature of the models. Method A is a coarse prediction method, which accepts also a tolerance of ±3% fluctuating values, whereas method B and C use the linear regression method, predicting the $N_{p,cr}$, by studying the PF error and all errors respectively. Model A uses a total of 990 simulations, whereas the other two models almost half of them. Nevertheless, the differences between the models are small and are becoming less, as the mean diameter gets higher.

There is no verdict, concerning the best applied method. Each model is a suggestion of a methodology that can be applied in order to estimate the $N_{p,cr}$. There is no doubt that there are plenty of others. The reader is free to compare and decide over the method that is more appropriate and precise. As for the averaged model, it doesn't overrule the methodologies that were applied for its extraction. Quite the opposite, since the underlying methodologies are more precise over what they study. The averaged model intends to provide a simple and fast way to predict the $N_{p,cr}$, with a decent discount in accuracy, indicating by that the homogeneity of its behavior.

4.2 The Analysis of the N_p Statistical Error

The error that originates from the limited number of computational particles N_p is not universal in nature. Although there is always a proportionality between the error and the number of computational droplets, the type of the proportionality is not always the same.

The nozzle by nozzle study allowed us to characterize the nature of the N_p statistical error, and, therefore, to distinguish two main types of relation between the error and the quantity $1/\sqrt{N_p}$, the linear and the logarithmic respectively. This analysis is crucial for the determination of the model that can predict the $N_{p,cr}$.

I. Linear relation

The linear proportionality is the most typical relation between the error and the quantity $1/\sqrt{N_p}$. Figure 2.6 - Figure 2.9, as well as the following Figure 4.2, are indicative of that relation. The linear proportionality forms the basis of the analysis methodologies B and C.

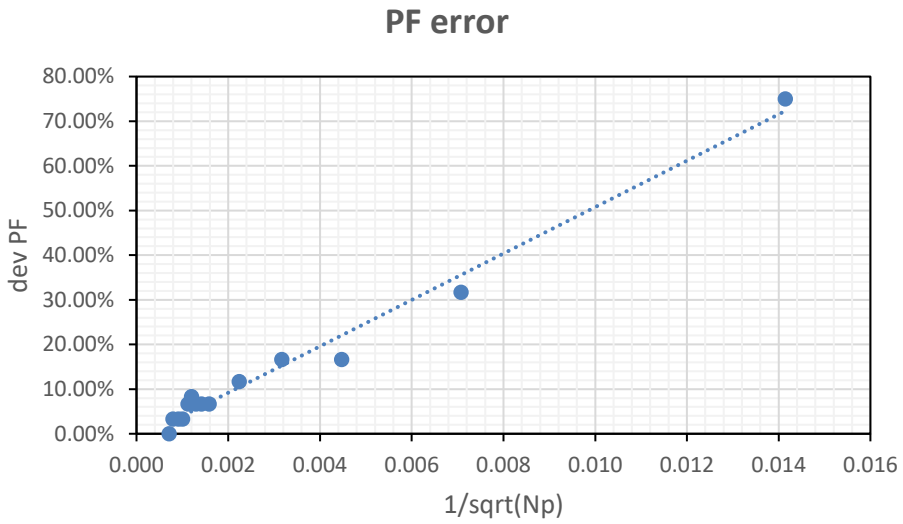

Figure 4.2 Typical representation of the linear proportionality between the error and the 1/sqrt(N_p) (Nozzle 8M)

II. Logarithmic relation

Except for the linear proportionality, it has been observed a logarithmic proportionality. This trend is very common especially for the nozzles with mean diameters ranging between 35 and 150 μm. Figure 4.3 is indicative of the logarithmic relationship.

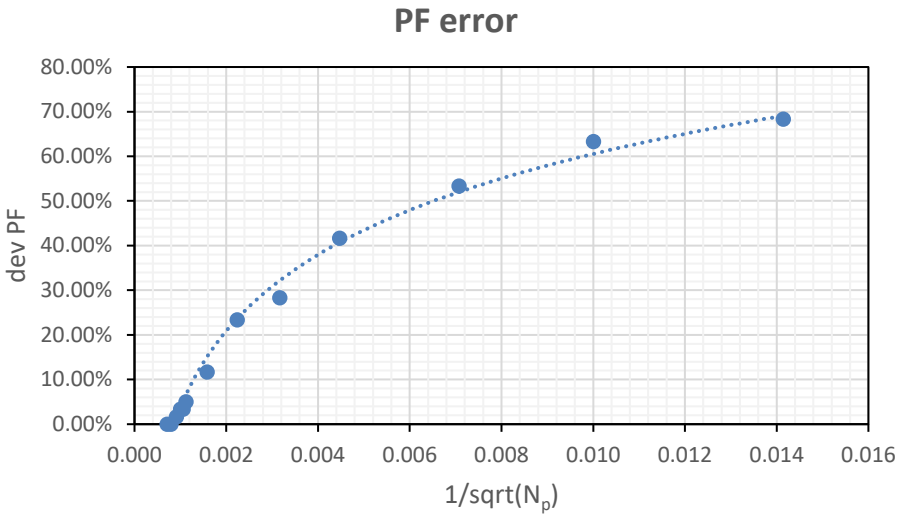

Figure 4.3. Typical representation of the logarithmic proportionality between the error and the 1/sqrt(N_p) (Nozzle 4VF)

The logarithmic relation, by its nature, denotes that there is a low rate of change of the error, as the number of computational droplets starts to increase, until it reaches a number of droplets, where the rate of change becomes faster. It is like there is an initial plateau, where the increase of the number of computational particles causes no effect on the simulation results. According to our study, for the case where the nature of the error is logarithmic, the low rate of error change ranges between $N_p = 5 \times 10^3 s^{-1}$ and $N_p = 10^5 s^{-1}$. The logarithmic nature of the error is in accordance with the findings of sensitivity studies in literature, since it explains why there is no significant variation of the results, whenever the increase of the number of particles was not enough to overrun the plateau with the low rate of error change. Such studies can be found in [5], [8] and [38]. The conclusion drawn was that the injected particles has no strong effect in the simulation results. Beji et al. [31] found this plateau where there was no change of the error and bounded it until $N_p = 5 \times 10^4 s^{-1}$ for the particular nozzle he studied.

4.3 The Relation between N_p and the Mean Nozzle Diameter $Dv_{0.5}$

The objective of the thesis is to provide guidance on the appropriate N_p that provide an acceptable accuracy level, by finding the relationship, if any, between the number of computational droplets and the mean drop diameter. The present work answers clearly and firmly that there is, indeed, a relation between them, and verifies that this relation has s power law expression. This is one of the main finding of the thesis.

The water mist nozzles were chosen, in order to create the desired diameter range. The volume median diameter $Dv_{0.5}$ was the only nozzle characterization parameter that was selected on purpose. Regarding the remaining physical parameters (e.g. initial velocity, spray angle) it wasn't meant to form a specific range. These parameters vary in an irregular manner and, more importantly, they influence the results. Even though this particular selection strategy was very likely to jeopardize the thesis objective, by hiding the exact relation

between the critical number of the computational particles and the mean drop diameter, this relation was observed, which indicated that it is clear and strong. As for the power law compliance, our certainty has its origins to the fact that we applied three different methodologies, all of which ended up to the same conclusion.

The study of the relation between the mean diameter and the critical number of particles allowed us to draw some further conclusions. It is without any doubt that each drop diameter requires a different critical number of computational particles. The small diameters (35-200 μm) demand significantly higher numbers of computational droplets, when compared with the higher diameters. According to Table 4-1 and the averaged solution in particular, it can be observed that a statistical error free simulation for a water mist nozzle with $Dv_{0.5} = 35\mu m$ needs more than $N_p = 4 \times 10^6 s^{-1}$, whereas a nozzle with $Dv_{0.5} = 1mm$ needs less than $N_p = 7 \times 10^4 s^{-1}$. The difference is chaotic. As the diameter increases, the critical number of computational particles $(N_{p,cr})$ decreases. However, there was no nozzle in the particular diameter range that required as many computational droplets as the default value in FDS $(N_p = 5 \times 10^3 s^{-1})$. Even the largest dimeters require ten to fifteen times more particles than the default N_p. Our initial assumption that the $N_p = 5 \times 10^3 s^{-1}$might be enough for nozzles with droplet diameters 500 μm and above has been proved incorrect.

Despite the fact that the $N_{p,cr}$ decreases with increasing the diameter, the rate of change is not the same for the whole diameter range. Bringing back in mind Figure 4.1, which exhibits the four model solutions (A, B, C and averaged), it is possible to distinguish two diameter regions, a lower one, ranging from 35 to 400 μm, and, an upper one, from 400 μm to 1000 μm. Starting with the first region, it can be easily observed that the curves that describe the relation between the diameter and the $N_{p,cr}$ are sharp, having steep slopes, while, on the contrary, the curves in the second diameter region are smooth and, practically, not inclined at all. Copying the numbers from Table 4-1, a diameter increase in the lower region from 50 μm to 150μm drops the $N_{p,cr}$ from $N_p = 2.6 \times 10^6 s^{-1}$ to less than $N_p = 7 \times 10^5 s^{-1}$. A similar increase in the upper region from 600 to 700 μm requires $N_p = 1.5 \times 10^4 s^{-1}$ less. This is a strong indication of homogeneity for the nozzles that belong to the upper diameter region. It is easier to predict the $N_{p,cr}$ for the higher diameter-nozzles and it is much harder for the small ones. All the action is taking place in the small diameters, which makes us believe that the number of computational droplets, as a simulation parameter, has higher significance, when simulating nozzles of low diameter droplets, indicating, at the same time, the necessity of studying the parameter N_p for simulating water mist nozzle.

4.4 The Relation between the Actual Number of Droplets and the Computational Number of Droplets

The introduction section 1.1.4 describes the process to calculate the actual number of droplets that is produced by a certain nozzle (Eq. 1-9 - Eq. 1-10), as well as the number of real droplets that is represented by one single computational droplet in FDS. The number of

actual and the representative droplets was calculated, and the results are presented below, in order to be compared with the $N_{p,cr}$, as it is predicted by the averaged model (the comparison can be made with the other three models as well). The computational process was accomplished in MATLAB. The results are presented in the following Table 4-2, while Figure 4.4 and Figure 4.5 present the development of the actual water droplets and the number of droplets that are represented by one particle in FDS respectively. Both charts confirm the solutions acquired by the prediction models, since it can be noticed the same power law relation between the number of droplets and the mean diameter, except for some irregularities, which are caused due to the combination of volumetric flow rate, the spray angle and the mean diameter. For example, the exceptionally high number of particles for Nozzle 6 can be partially explained as a result of the narrow spray pattern and the high flow rate. The initial assumption that we had of the existence of a constant representative number of droplets per each nozzle is not valid. The representative number of droplets follows the trend of the actual number of droplets.

Nozzle	***$Dv_{0.5}$ (μm)***	***$N_{p,cr,averaged}$ (s^{-1})***	***N_{actual}***	***n_{rep}***
Nozzle 1	35	4.019.451	316.160.000	78,66
Nozzle 2	50	2.607.778	303.640.000	116,44
Nozzle 3	70	1.733.873	94.847.000	54,70
Nozzle 4	80	1.474.596	70.600.000	47,88
Nozzle 5	100	1.124.919	54.221.000	48,20
Nozzle 6	125	858.162	263.730.000	307,32
Nozzle 7	150	687.895	11.6210.000	168,94
Nozzle 8	200	485.257	20.559.000	42,37
Nozzle 9	250	370.186	8.675.300	23,43
Nozzle 10	300	296.738	8.702.100	29,33
Nozzle 11	350	246.131	2.740.000	11,13
Nozzle 12	400	209.325	1.270.800	6,07
Nozzle 13	500	159.687	212.880	1,33
Nozzle 14	600	128.004	1.506.100	11,77
Nozzle 15	700	106.173	158.080	1,49
Nozzle 16	800	90.296	211.800	2,35
Nozzle 17	900	78.275	446.260	5,70
Nozzle 18	1000	68.884	497.020	7,22

Table 4-2. The actual number of water droplets that are produced by the nozzles and the representative number of droplets in FDS

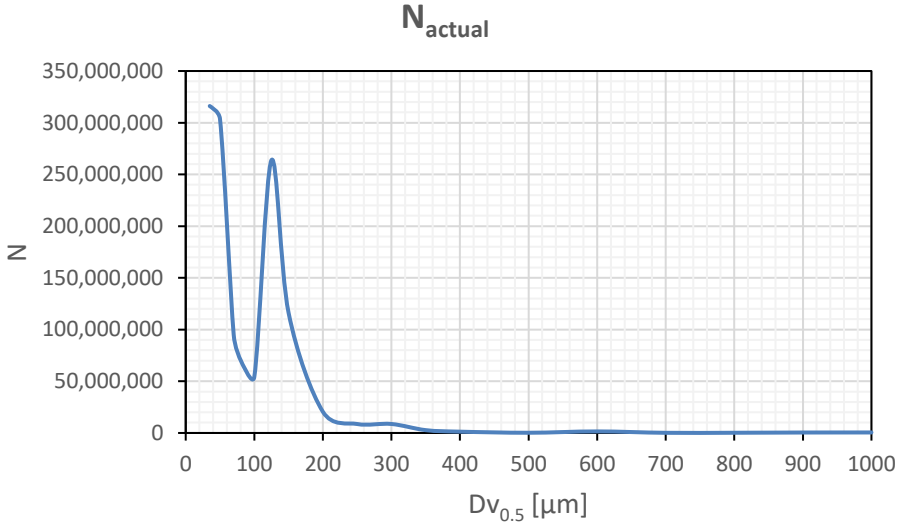

Figure 4.4. The actual number of computational droplets for each nozzle tested

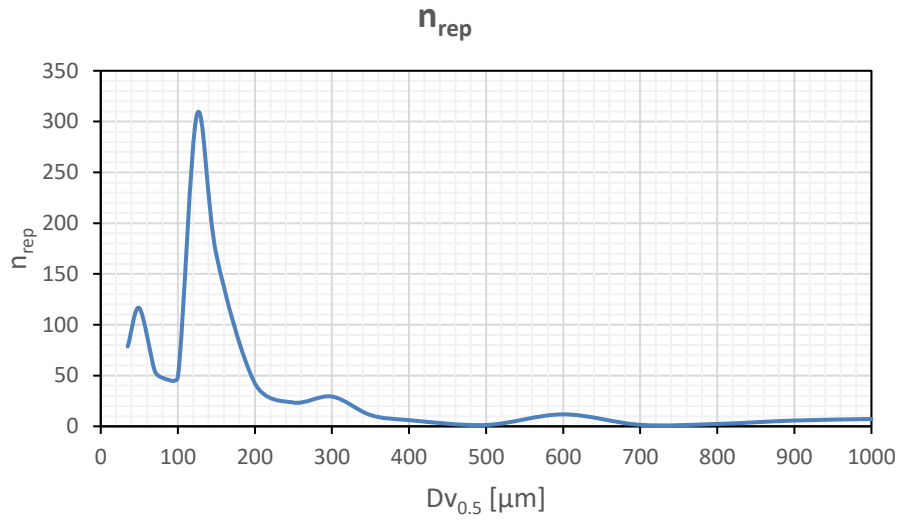

Figure 4.5. The number of real droplets that are represented by one computational particle in FDS (universal model)

4.5 The Relation between N_p and the Computational Mesh

The computational mesh was one of the major parameters that were studied during this work, aiming at finding the connection between the $N_{p,cr}$ and the size of the cells. The experimental methodology indicated that the computational mesh is one of the parameters that affect the number of computational droplets that are appropriate for an acceptable accuracy. In general, as the computational becomes finer, the $N_{p,cr}$ becomes even lower. The Method C prediction results are indicative of the relationship between the $N_{p,cr}$ and the computational mesh (Figure 4.6).

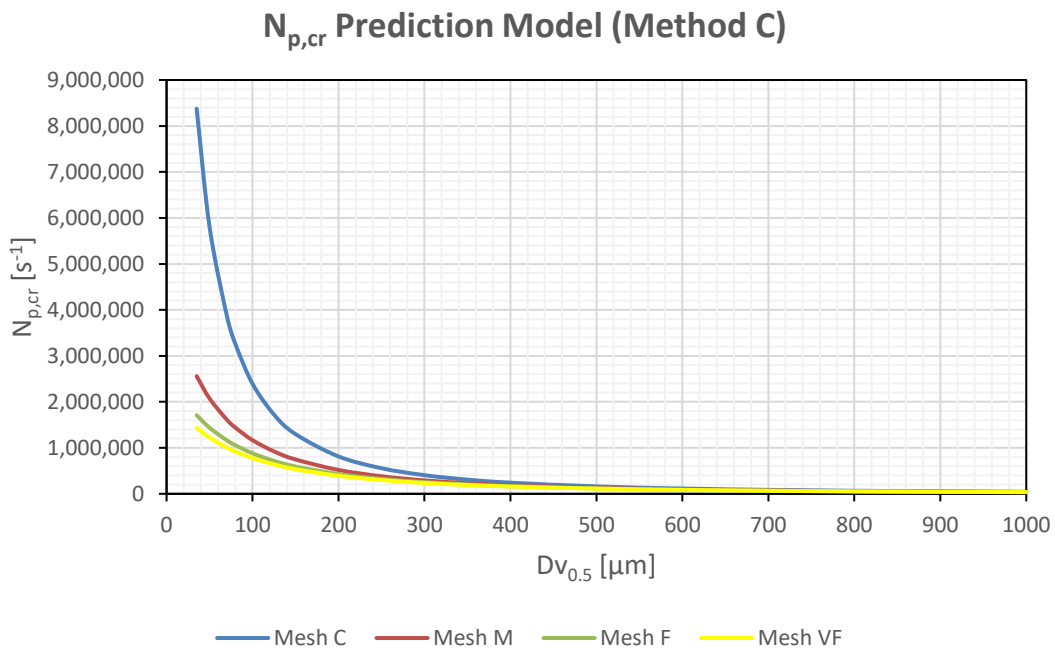

Figure 4.6. The relationship between the $N_{p,cr}$ and the computational meshes (Model C)

However, as the mean diameter gets higher, the differences in the $N_{p,cr}$ among the four meshes becomes smaller and smaller. Even in the smaller nozzle diameters, the differences in the $N_{p,cr}$, in terms of absolute values, are quite small, at least for the three out of the four meshes (M, F and VF). This observation explains the transition from the four different prediction models, each of which corresponding to one mesh, to one combined model.

4.6 The Effect of the N_p on the Simulations Computational Time

The influence of the N_p on the computational time (CPU) is indisputable. The computational time of each simulation was recorded and presented in graphs, in order to describe the type of the relationship between the computational particles and the increase of the computational cost. This was made feasible by running the total number of simulations on the same computer (HPC Ugent). Our research indicated two types of connection between the computational time (CPU) and the number of computational particles. In the vast majorities of the simulations there is a linear relation between the N_p and the CPU time. Figure 4.7 is a typical representation of the aforementioned relation. The CPU time was made non-dimensional, by dividing the computational time of each recorded simulation by the minimum computational time that was obtained by the simulation with the default number of computational droplets. This finding is in complete agreement with the research in [31].

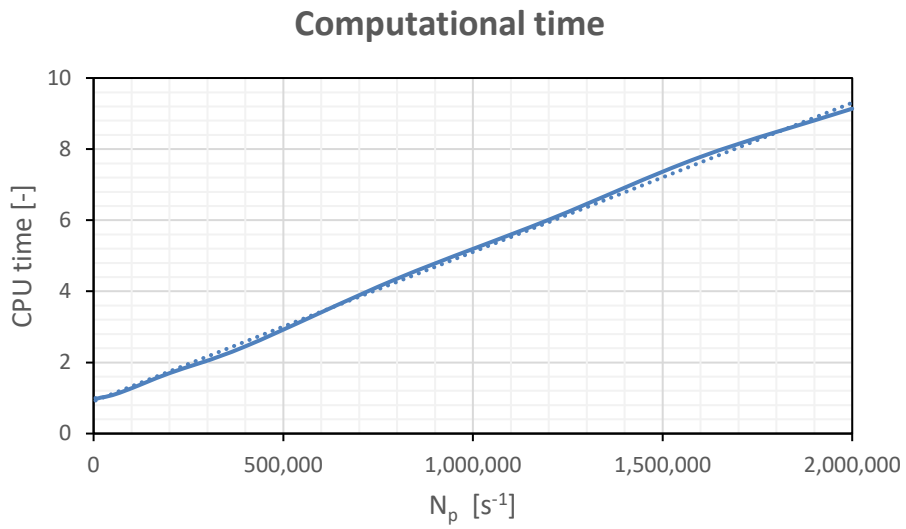

Figure 4.7. The linear growth of the CPU time as a function of the N_p (Nozzle 12F)

There are, however, cases, where the computational time follows an exponential trend. There is a simulation with a number of computational droplets, above which the computational time increases exponentially with the number of particles. This is the case in simulating the Nozzle 3F (Figure 4.8). The computational time increases linearly until the level of $N_p = 1.2 \times 10^6 s^{-1}$. When the N_p exceeds that number, then the increase in CPU time is exponential.

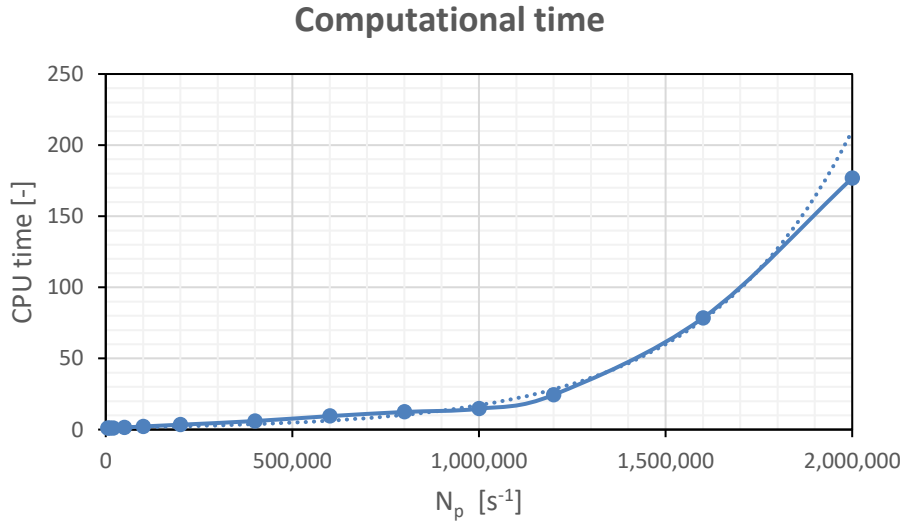

Figure 4.8. The exponential growth of the CPU time as a function of the Np (Nozzle 3F)

Finally, regarding the computational time, it has been noticed that there is a region, usually between $N_p = 5 \times 10^3 s^{-1}$ and $N_p = 2 \times 10^5 s^{-1}$, where the computational time either is reduced or stays untouched as the number of particles increases. Such a case is described in Table 4-3. The CPU time starts to increase above $N_p = 2 \times 10^5 s^{-1}$. Until there the CPU time decreases as the N_p gets higher.

N_p (s^{-1})	5.000	10.000	20.000	50.000	100.000	200.000	400.000	800.000
T (min)	205	195	186.7	208.3	168.3	205	288.3	456.7

Table 4-3. The CPU time as a function of the Np (Nozzle 4VF)

5. Conclusions

5.1 General Conclusions

The past decades the water mist fire suppression systems are increasingly being used in a wide variety of applications, connected to the protection of a broad range of properties and structures. The effectiveness of such systems, as well as their comparative advantages explain their expanding popularity. However, the performance and, more importantly, the success of water mist systems, with regard to the fire protection goal that has been set, is crucially dependent on the characteristics of the sprays that is produced by the water mist nozzles, and, especially on the size of the water droplets that are discharged by the water mist nozzle head. The water mist fire suppression mechanisms are, therefore, determined by the size of the water droplets. The application of such systems in particular is a challenging task, whose certification approval requires individual verification through experimental testing, and it is not subjected to regulations or standards.

The experimental testing, in spite of being undeniably necessary and useful, requires exceptionally high resources in time, effort and money, which, in a way, discourages the application of water mist systems. This issue can be surpassed by the use of numerical modeling through CFD packages. The ever-growing advances in numerical modelling offer a valuable tool, which supports the experimental testing for design purposes, and allow for exploring and studying a wide variety of fire scenarios at a reduced cost. The numerical modelling, however, has its own vulnerability, which is the accuracy. The numerical simulations include a number of assumptions, simplifications and models, all of which decrease the accuracy of the results and constitute a source of error.

Most CFD packages simulate the water sprays as Lagrangian particles. One water mist nozzle head produces in reality millions of water droplets. Simulating all these water droplets is prohibited, due to the bounded computational power. The Lagrangian approach allows water spray simulations with a limited number of water droplets, each of which represents a number of rear droplets. The water droplets are inserted in the computational domain as liquid particles (N_p) having predefined properties. The number of particles is limited because it is computationally expensive. As it was explained before, this is a source of error (statistical error), which affects the accuracy of the water spray simulations.

The present Master thesis deals with the accuracy of the numerical simulations of water sprays, by studying the statistical error that stems from the limited N_p. A series of numerical experiments (simulations) were conducted with FDS, for a wide variety of water mist nozzles that produce different water sprays, with mean diameters ranging from 35 to 1000 μm. The objective was to provide guidance to the future users, concerning the appropriate of computational particles ($N_{p,cr}$) that are necessary to offer an acceptable accuracy, as a function of the mean diameter $Dv_{0.5}$ and the resolution of the computational mesh (cell size). This was achieved by defining first the statistical error and studying its nature and, hereupon,

by setting up three distinct methods (prediction models) that enable us to estimate and predict the $N_{p,cr}$. As a final step the three individual methods were combined together, which gave us the possibility to suggest one averaged model that predicts the $N_{p,cr}$ solely as a function of the $Dv_{0.5}$, keeping out of the equation the computational mesh.

This work, not only provides simple engineering correlations (models) to calculate the $N_{p,cr}$, but also characterizes as linear or logarithmic the type of the relation between the statistical error and the quantity$1/\sqrt{N_p}$ (nature of the statistical error), affirms that there is a relation between the $DV_{0.5}$ and the $N_{p,cr}$, which obeys the power law, highlights that the default FDS N_p parameter ($N_p = 5 \times 10^3 s^{-1}$) is not enough to adequately represent the water spray for the whole range of diameters (35 -1000 μm) and indicates a homogeneous behavior of the $N_{p,cr}$ for water mist nozzles above 400 μm. The conclusions underline the importance and necessity of studying the N_p parameter for the small diameters in particular. Furthermore, it is well established by our research that the cell size does affect the $N_{p,cr}$. This connection is stronger in the lower region of diameters and faints out when the drop diameters become larger. The computational time increases linearly or exponentially, as the number of particles gets higher. Finally, it has been derived that the number of computational particles, as a function of the $Dv_{0.5}$, follows the trend of the number of actual particles, as a function of the $Dv_{0.5}$. The representative number of particles is not constant for the studied diameter range.

5.2 Future Work

The conclusions of the present thesis indicate the significance of the study of the number of the computational particles, as a parameter of the numerical simulations of water sprays. The results of this work have a certain validity range, which is the range of diameters that have been studied, as well as the range of computational meshes. It seems that is worth trying to predict the number of computational particles, because it strongly affects the accuracy of the simulations.

It is therefore recommended, not only to expand the validity range (diameters, cell sizes) of the study of the number of computational particles N_p, but also to improve the accuracy of the prediction models, by adding more simulations (data), which will increase the sample that constitutes the basis for the extraction of the prediction models. Besides, it is crucial to include in the future works, the study of the effect of other nozzle modelling parameters that contribute to the numerical accuracy, such as the initial velocity and the spray angle, so that to verify in which extent determine the $N_{p,cr}$. The study of these parameters was not performed during this thesis.

6. Acknowledgements

This thesis was done during the last semester of the International Master in Fire Safety Engineering (IMFSE). I would like to thank the IMFSE management board for the admission and the scientific stuff in the three full partner universities, namely in Ghent University, Lund University and the University of Edinburg for this unexpected two-year journey. I would like to refer to the following people in particular, without whom the present project would not have been possible.

I would like to thank my promoter Prof. Bart Merci for the teaching, the endless support, and, above all, the understanding, during those two years and the master thesis in particular.

I would like to express my deep gratitude to my promoter and supervisor dr. Tarek Beji for giving me the opportunity to work with him, for the guidance, the aid and the encouragement that so generously offered to me.

Special thanks to the members of the HPC Team and especially to Kenneth for their support in using the High-Performance Computer. My sincere thanks also to the PhD student Junyi Li, for helping me to run the first simulations and for his notes.

I would like also to thank Mr. Jean-Paul Vandevoorde from the Spraying Systems Co. Belgium for trusting me the company's documentation.

Finally, I would like to acknowledge my personal friend, colleague and scientist, dr. Konstantinos Georgiadis for his contribution to this project, through the fruitful discussions and the useful insights, for the unconditional support, the inspiration and the shared visions.

7. References

[1] L. Beda and C. Szikra, “Effect of the Flow of Large Water Droplets on the Water Mist Sprays,” *YBL J. Built Environ.*, vol. 2, no. 2, pp. 27–37, Dec. 2014.

[2] Zhigang Liu and A. K. Kim, “A Review of Water Mist Fire Suppression Systems--Fundamental Studies,” *J. Fire Prot. Eng.*, vol. 10, no. 3, pp. 32–50, Jan. 1999.

[3] X. Zhou, S. P. D’Aniello, and H. Z. Yu, “Spray characterization measurements of a pendent fire sprinkler,” *Fire Saf. J.*, vol. 54, pp. 36–48, 2012.

[4] S. C. Kim and H. S. Ryou, “An experimental and numerical study on fire suppression using a water mist in an enclosure,” *Build. Environ.*, vol. 38, no. 11, pp. 1309–1316, Nov. 2003.

[5] T. Sikanen, J. Vaari, S. Hostikka, and A. Paajanen, “Modeling and Simulation of High Pressure Water Mist Systems,” *Fire Technol.*, vol. 50, no. 3, pp. 483–504, May 2014.

[6] A. Jenft, A. Collin, P. Boulet, G. Pianet, A. Breton, and A. Muller, “Experimental and numerical study of pool fire suppression using water mist,” *Fire Saf. J.*, vol. 67, pp. 1–12, Jul. 2014.

[7] National Fire Protection Association, *NFPA 750 Standard on Water Mist Fire Protection Systems 2000 Edition*, 2000 Editi. 2000.

[8] B. P. Husted, “Experimental measurements of water mist systems and implications for modelling in CFD Doctoral Thesis,” Lund Univeristy, 2007.

[9] P. E. Santangelo, “Characterization of high-pressure water-mist sprays: Experimental analysis of droplet size and dispersion,” *Exp. Therm. Fluid Sci.*, vol. 34, no. 8, pp. 1353–1366, Nov. 2010.

[10] H. M. I. Mahmud, K. A. M. Moinuddin, and G. R. Thorpe, “Experimental and numerical study of high-pressure water-mist nozzle sprays,” *Fire Saf. J.*, vol. 81, pp. 109–117, Apr. 2016.

[11] T. M. Jayaweera and H.-Z. Yu, “Scaling of fire cooling by water mist under low drop Reynolds number conditions,” *Fire Saf. J.*, vol. 43, no. 1, pp. 63–70, Jan. 2008.

[12] Z. Liu, A. K. Kim, D. Carpenter, J. M. Kanabus-Kaminska, and P.-L. Yen, “Extinguishment of Cooking Oil Fires by Water Mist Fire Suppression Systems,” *Fire Technol.*, vol. 40, no. 4, pp. 309–333, Oct. 2004.

[13] H. M. I. Mahmud, Moinuddin K. A. M., and G. R. Torphe, “Characterization of a water-mist spray : Numerical modelling and experimental validation,” in *18th Australasian Fluid Mechanics Conference*, 2012, no. 3-7 December.

[14] B. Ditch and H. Yu, “Water Mist Spray Characterization and Its Proper Application for Numerical Simulations,” *Fire Saf. Sci.*, vol. 9, pp. 541–552, 2008.

[15] L. Yinshui, J. Zhuo, W. Dan, and L. Xiaohui, “Experimental research on the water mist

fire suppression performance in an enclosed space by changing the characteristics of nozzles," *Exp. Therm. Fluid Sci.*, vol. 52, pp. 174–181, Jan. 2014.

[16] P. E. Santangelo, P. Tartarini, A. W. Marshall, and M. Bettati, "On the Characterization of Sprays Produced By Water-Mist Injectors," in *International Water Mist Conference 2009*, 2009, no. 23-24 September, pp. 1–8.

[17] Y.-M. Ferng and C.-H. Liu, "Numerically investigating fire suppression mechanisms for the water mist with various droplet sizes through FDS code," *Nucl. Eng. Des.*, vol. 241, no. 8, pp. 3142–3148, Aug. 2011.

[18] M. F. AbdRabbo and A. M. Ayoub, "Study the Properties of Water Mist Droplet by Using FDS," *J. Civ. Environ. Eng.*, vol. 6, no. 3, 2016.

[19] E. A. Kolstad and B. P. Husted, "Effect Of Water Mist And Ventilation on Engine Room Fire," in *Conference Paper*, 2013, no. June.

[20] S. Takieddin, "A Numerical Investigation of Spray-Plume Interactions," 2016.

[21] A. Jenft, P. Boulet, A. Collin, G. Pianet, A. Breton, and A. Muller, "Can we predict fire extinction by water mist with FDS?," in *21eme Congres Francais de Mecanique*, 2013, pp. 1–6.

[22] K. C. Adiga, R. F. Hatcher, R. S. Sheinson, F. W. Williams, and S. Ayers, "A computational and experimental study of ultra fine water mist as a total flooding agent," *Fire Saf. J.*, vol. 42, no. 2, pp. 150–160, Mar. 2007.

[23] A. Arrowsmith, "Atomization and Sprays," *Chem. Eng. Sci.*, vol. 45, no. 5, p. 1435, 1990.

[24] K. McGrattan, S. Hostikka, J. Floyd, R. Mcdermott, C. Weinschenk, and K. Overholt, "Sixth Edition Fire Dynamics Simulator User ' s Guide," *NIST Spec. Publ.*, vol. 1019, 2010.

[25] D. Sheppard, "Spray Characteristics of Fire Sprinklers, Doctoral Thesis prepared for the Building and Fire Research Laboratory of the National Institue of Standards and Technology," Northwestern Univeristy, 2002.

[26] M. J. Hurley *et al.*, Eds., *SFPE Handbook of Fire Protection Engineering*, Fifth Edit. New York, NY: Springer New York, 2016.

[27] G. Heskestad, "Scaling the interaction of water sprays and flames," *Fire Saf. J.*, vol. 37, no. 6, pp. 535–548, Sep. 2002.

[28] G. Tanner and K. F. Knasiak, "Spray Characterization of Typical Fire Suppression Nozzles," in *Third International Water Mist Conference*, 2003, no. 22-24 September.

[29] K. McGrattan, A. Hamins, and D. Stroup, "Sprinkler , Smoke & Heat Vent , Draft Curtain Interaction - Large Scale Experiments and Model Development.," 1998.

[30] K. B. McGrattan, S. Hostikka, R. McDermott, J. Floyd, and M. Vanella, "Fire Dynamics Simulator Technical Reference Guide Volume 1 : Mathematical Model," *NIST Spec. Publ. 1018-1 Sixth Ed.*, vol. 1, 2019.

[31] T. Beji, S. E. Zadeh, G. Maragkos, and B. Merci, “Influence of the particle injection rate, droplet size distribution and volume flux angular distribution on the results and computational time of water spray CFD simulations,” *Fire Saf. J.*, vol. 91, no. January, pp. 586–595, Jul. 2017.

[32] K. McGrattan, S. Hostikka, R. McDermott, J. Floyd, and M. Vanella, “Fire Dynamics Simulator User’s Guide,” 2019.

[33] T. Beji, S. Ebrahimzadeh, G. Maragkos, and B. Merci, “Numerical modelling of the interaction between water sprays and hot air jets - Part II: Two-phase flow simulations,” *Fire Saf. J.*, vol. 96, pp. 143–152, Mar. 2018.

[34] R. Garg, C. Narayanan, D. Lakehal, and S. Subramaniam, “Accurate numerical estimation of interphase momentum transfer in Lagrangian–Eulerian simulations of dispersed two-phase flows,” *Int. J. Multiph. Flow*, vol. 33, no. 12, pp. 1337–1364, Dec. 2007.

[35] P. Andersson, M. Arvidson, and G. Holmstedt, “Small Scale Experiments and Theoretical Aspects of Flame Extinguishment with Water Mist,” Lund Univeristy, 1996.

[36] J. Ho and H. Yang, “Effects of Water Mist System on a Controlled Fire, Report 5498, IMFSE Master Thesis,” Lund University, 2015.

[37] Z. Tang, Z. Fang, J. Sun, T. Beji, and B. Merci, “Computational fluid dynamics simulations of the impact of a water spray on a fire-induced smoke layer inside a hood,” *J. Fire Sci.*, vol. 36, no. 5, pp. 380–405, Sep. 2018.

[38] M. Bourque and Thomas Svirksy, “Computational Modeling of Fire Sprinkler Spray Characteristics Using the Fire Dynamics Simulator, Bachelor of Science Thesis,” Worcester Polytechnic Institute, 2013.

8. Appendices

8.1 Appendix A

The figure below presents the mean diameter $DV_{0.5}$ chart that was provided by Spraying Systems CO. for their full product range.

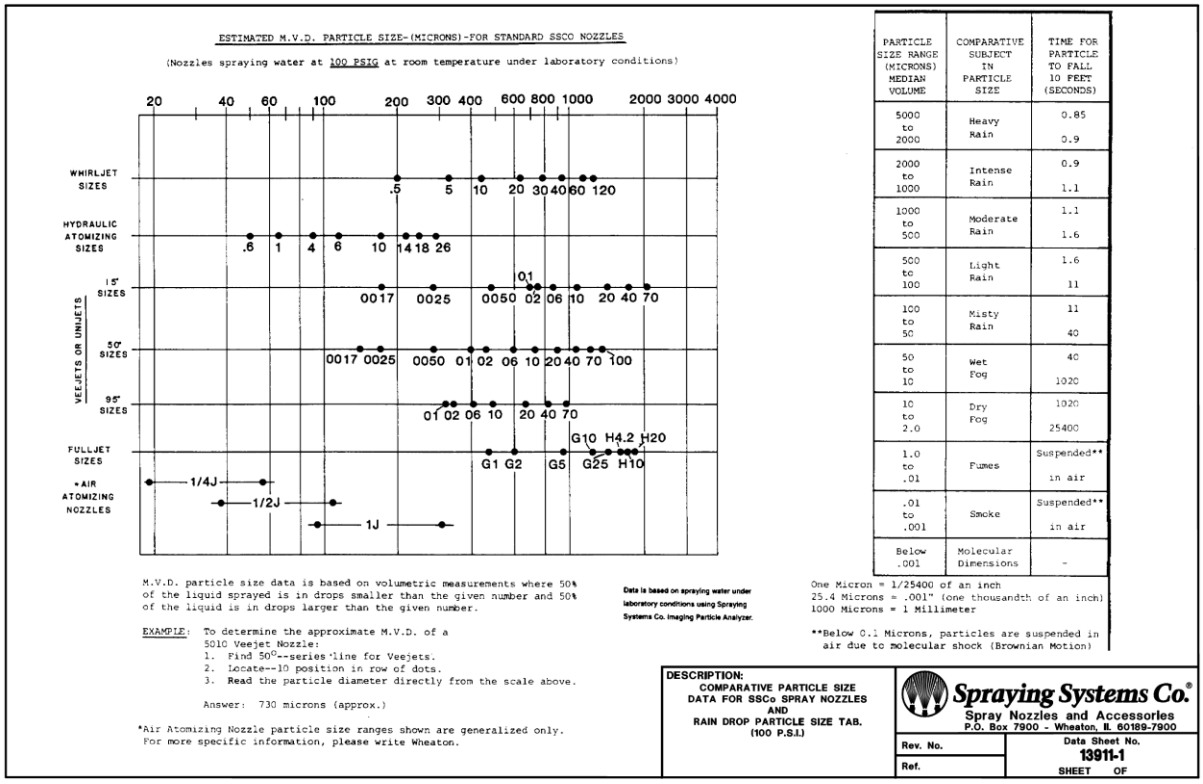

PARTICLE SIZE RANGE (MICRONS) MEDIAN VOLUME	COMPARATIVE SUBJECT IN PARTICLE SIZE	TIME FOR PARTICLE TO FALL 10 FEET (SECONDS)
5000 to 2000	Heavy Rain	0.85 to 0.9
2000 to 1000	Intense Rain	0.9 to 1.1
1000 to 500	Moderate Rain	1.1 to 1.6
500 to 100	Light Rain	1.6 to 11
100 to 50	Misty Rain	11 to 40
50 to 10	Wet Fog	40 to 1020
10 to 2.0	Dry Fog	1020 to 25400
1.0 to .01	Fumes	Suspended** in air
.01 to .001	Smoke	Suspended** in air
Below .001	Molecular Dimensions	-

8.2 Appendix B

Below is the FDS code (Nozzle 1VF), as it was used to perform the numerical experiments. The mean dimeter, the mesh and the number of computational droplets are the parameters that differentiate the simulations and they can be seen in bold.

&HEAD CHID='VFine_5000', TITLE='Nozzle1' /
&MESH ID='MESH', IJK=80,80,120, XB=-0.5,0.5,-0.5,0.5,0.0,1.5 /
&RADI RADIATION=.FALSE. /
&TIME T_END=10. /
&VENT MB='XMIN',SURF_ID='OPEN'/
&VENT MB='XMAX',SURF_ID='OPEN'/
&VENT MB='YMIN',SURF_ID='OPEN'/
&VENT MB='YMAX',SURF_ID='OPEN'/
&VENT MB='ZMIN',SURF_ID='OPEN'/
&SPEC ID='WATER VAPOR'/
&PART ID='waterdrops', SPEC_ID='WATER VAPOR'**, DIAMETER=35. /**
&PROP ID ='mist_system',
PART_ID ='waterdrops',
SPRAY_ANGLE = 0.,38.,
FLOW_RATE = 0.15,

```
    PARTICLE_VELOCITY    = 74.,
    PARTICLES_PER_SECOND = 5000. /
&DEVC XYZ=0.0,0.0,1.4, PROP_ID='mist_system', ID='nozzle', QUANTITY='TIME', SETPOINT=0. /
&PROP ID='pdpa_flux', PART_ID='waterdrops', QUANTITY='PARTICLE FLUX Z', PDPA_RADIUS=0.01,
PDPA_START=2., PDPA_END=10. /
&DEVC XYZ= 0.0,0.0,0.6, QUANTITY='PDPA', PROP_ID='pdpa_flux',ID='PF1' /
&DEVC XYZ= 0.0,0.0,0.4, QUANTITY='PDPA', PROP_ID='pdpa_flux',ID='PF2' /
&DEVC XYZ= 0.0,0.0,0.2, QUANTITY='PDPA', PROP_ID='pdpa_flux',ID='PF3' /
&PROP ID='pdpa_mass_conc', PART_ID='waterdrops', QUANTITY='MASS CONCENTRATION',
PDPA_RADIUS =0.01, PDPA_START=2., PDPA_END=10. /
&DEVC XYZ= 0.0,0.0,0.6, QUANTITY='PDPA', PROP_ID='pdpa_mass_conc',ID='MC1' /
&DEVC XYZ= 0.0,0.0,0.4, QUANTITY='PDPA', PROP_ID='pdpa_mass_conc',ID='MC2' /
&DEVC XYZ= 0.0,0.0,0.2, QUANTITY='PDPA', PROP_ID='pdpa_mass_conc',ID='MC3' /
&PROP ID='pdpa_d32'
    PART_ID              = 'waterdrops'
    PDPA_RADIUS          = 0.01
    PDPA_START           = 2.
    PDPA_END             = 10.
    PDPA_M               = 3
    PDPA_N               = 2/
&DEVC XYZ= 0.0,0.0,0.6, QUANTITY='PDPA', PROP_ID='pdpa_d32', ID='SMD1' /
&DEVC XYZ= 0.0,0.0,0.4, QUANTITY='PDPA', PROP_ID='pdpa_d32', ID='SMD2' /
&DEVC XYZ= 0.0,0.0,0.2, QUANTITY='PDPA', PROP_ID='pdpa_d32', ID='SMD3' /
&PROP ID='pdpa_d10'
    PART_ID              = 'waterdrops'
    PDPA_RADIUS          = 0.01
    PDPA_START           = 2.
    PDPA_END             = 10.
    PDPA_M               = 1
    PDPA_N               = 0/
&DEVC XYZ= 0.0,0.0,0.6, QUANTITY='PDPA', PROP_ID='pdpa_d10', ID='D10_1' /
&DEVC XYZ= 0.0,0.0,0.4, QUANTITY='PDPA', PROP_ID='pdpa_d10', ID='D10_2' /
&DEVC XYZ= 0.0,0.0,0.2, QUANTITY='PDPA', PROP_ID='pdpa_d10', ID='D10_3' /
&TAIL /
```

8.3 Appendix C

The following table presents the simulation results post processed

	$Dv_{0.5}$	Cell	Np	PF	devPF	MC	devMC	D32	devD32	D10	devD10	T (min)
1	35	10	5000	0.21	0.64	0.09	0.65	28.00	0.09	19.00	0.16	0.10
2	35	10	10000	0.38	0.36	0.17	0.35	24.30	0.05	17.00	0.25	0.20
3	35	10	20000	0.44	0.25	0.19	0.27	23.90	0.07	16.80	0.26	0.30
4	35	10	50000	0.59	0.00	0.26	0.00	23.40	0.09	18.20	0.20	0.80
5	35	10	100000	0.82	0.39	0.36	0.38	21.90	0.14	17.70	0.22	1.60
6	35	10	200000	0.86	0.46	0.38	0.46	21.70	0.15	17.60	0.22	3.40
7	35	10	400000	0.87	0.47	0.38	0.46	21.30	0.17	16.10	0.29	6.60
8	35	10	800000	0.77	0.31	0.34	0.31	22.40	0.13	15.70	0.31	13.50
9	35	10	1200000	0.69	0.17	0.30	0.15	25.60	0.00	21.00	0.07	23.60

10	35	10	1600000	0.65	0.10	0.29	0.12	25.80	0.01	23.10	0.02	41.60
11	35	10	2000000	0.62	0.05	0.27	0.04	25.70	0.00	23.00	0.01	397.80
12	35	10	2400000	0.59	0.00	0.26	0.00	25.60	0.00	22.70	0.00	1580.00
13	35	5	5000	0.18	0.76	0.07	0.70	27.40	0.27	18.30	0.11	0.60
14	35	5	10000	0.24	0.68	0.08	0.65	25.30	0.18	17.70	0.07	0.70
15	35	5	20000	0.29	0.61	0.10	0.57	24.10	0.12	16.30	0.01	1.30
16	35	5	50000	0.46	0.39	0.15	0.35	22.70	0.06	16.00	0.03	2.30
17	35	5	100000	0.45	0.40	0.14	0.39	22.80	0.06	16.10	0.02	5.20
18	35	5	200000	0.52	0.31	0.16	0.30	22.10	0.03	15.80	0.04	8.90
19	35	5	400000	0.67	0.11	0.21	0.09	21.20	0.01	15.50	0.06	19.00
20	35	5	600000	0.75	0.00	0.23	0.00	20.70	0.04	15.30	0.07	52.30
21	35	5	800000	0.73	0.03	0.22	0.04	21.00	0.02	15.70	0.05	35.30
22	35	5	1000000	0.70	0.07	0.21	0.09	21.40	0.00	16.10	0.02	91.70
23	35	5	1200000	0.77	0.03	0.24	0.04	21.00	0.02	15.80	0.04	56.80
24	35	5	1400000	0.75	0.00	0.23	0.00	21.10	0.02	15.80	0.04	132.00
25	35	5	1600000	0.72	0.04	0.22	0.04	21.40	0.00	16.00	0.03	81.00
26	35	5	1800000	0.72	0.04	0.22	0.04	21.50	0.00	16.30	0.01	83.10
27	35	5	2000000	0.77	0.03	0.23	0.00	21.30	0.01	16.60	0.01	225.00
28	35	5	2400000	0.73	0.03	0.23	0.00	21.50	0.00	16.40	0.01	677.50
29	35	5	2800000	0.75	0.00	0.23	0.00	21.50	0.00	16.50	0.00	1533.30
30	35	2.5	5000	0.07	0.88	0.03	0.79	30.10	0.37	18.50	0.17	12.60
31	35	2.5	10000	0.10	0.82	0.04	0.71	31.00	0.41	19.20	0.22	10.80
32	35	2.5	20000	0.15	0.73	0.05	0.64	28.00	0.27	18.20	0.15	11.40
33	35	2.5	50000	0.21	0.63	0.06	0.57	26.20	0.19	16.80	0.06	14.90
34	35	2.5	100000	0.28	0.50	0.08	0.43	25.00	0.14	16.60	0.05	21.90
35	35	2.5	200000	0.28	0.50	0.08	0.43	25.10	0.14	16.50	0.04	37.30
36	35	2.5	400000	0.38	0.32	0.10	0.29	24.00	0.09	16.40	0.04	65.80
37	35	2.5	800000	0.42	0.25	0.11	0.21	23.30	0.06	16.10	0.02	126.70
38	35	2.5	900000	0.46	0.18	0.12	0.14	23.10	0.05	16.00	0.01	141.70
39	35	2.5	1000000	0.49	0.13	0.12	0.14	22.80	0.04	15.80	0.00	154.20
40	35	2.5	1200000	0.49	0.13	0.13	0.07	22.60	0.03	15.70	0.01	172.50
41	35	2.5	1600000	0.46	0.18	0.12	0.14	23.30	0.06	16.30	0.03	229.20
42	35	2.5	2000000	0.55	0.02	0.14	0.00	21.90	0.00	15.70	0.01	650.00
43	35	2.5	2400000	0.56	0.00	0.14	0.00	22.00	0.00	15.80	0.00	4680.00
44	35	1.25	5000	0.06	0.78	0.02	0.67	31.70	0.19	18.70	0.09	305.00
45	35	1.25	10000	0.09	0.67	0.03	0.50	30.90	0.16	19.20	0.12	245.00
46	35	1.25	20000	0.10	0.63	0.03	0.50	29.80	0.12	19.10	0.12	248.30
47	35	1.25	50000	0.11	0.59	0.04	0.33	30.30	0.14	18.70	0.09	200.00
48	35	1.25	100000	0.15	0.44	0.04	0.33	29.40	0.11	18.70	0.09	243.30
49	35	1.25	200000	0.18	0.33	0.05	0.17	28.80	0.08	18.20	0.06	240.00
50	35	1.25	400000	0.19	0.30	0.05	0.17	28.50	0.07	17.90	0.05	338.30
51	35	1.25	800000	0.25	0.07	0.06	0.00	27.70	0.04	17.50	0.02	516.70
52	35	1.25	900000	0.24	0.11	0.06	0.00	27.80	0.05	17.60	0.03	551.70
53	35	1.25	1000000	0.25	0.07	0.06	0.00	27.20	0.02	17.20	0.01	571.70
54	35	1.25	1100000	0.24	0.11	0.06	0.00	27.60	0.04	17.40	0.02	596.70
55	35	1.25	1200000	0.27	0.00	0.06	0.00	27.10	0.02	17.30	0.01	748.30

56	35	1.25	1600000	0.27	0.00	0.06	0.00	26.80	0.01	16.90	0.01	950.00
57	35	1.25	2000000	0.27	0.00	0.06	0.00	26.60	0.00	17.10	0.00	1365.00
58	50	10	5000	0.99	0.84	0.31	0.84	45.20	0.24	29.20	0.04	0.30
59	50	10	10000	1.35	0.78	0.42	0.78	42.60	0.17	27.20	0.03	0.40
60	50	10	20000	1.69	0.73	0.53	0.73	43.40	0.19	28.90	0.03	0.70
61	50	10	50000	3.14	0.49	0.98	0.49	38.90	0.07	27.60	0.02	1.80
62	50	10	100000	5.18	0.16	1.62	0.16	36.00	0.01	26.40	0.06	4.00
63	50	10	200000	6.01	0.03	1.88	0.03	35.40	0.03	25.60	0.09	9.20
64	50	10	400000	6.91	0.12	2.16	0.11	34.70	0.05	25.00	0.11	18.80
65	50	10	800000	7.74	0.25	2.43	0.25	34.60	0.05	25.90	0.08	34.30
66	50	10	900000	7.86	0.27	2.46	0.27	34.80	0.04	27.10	0.04	15.00
67	50	10	1000000	8.18	0.32	2.56	0.32	34.60	0.05	27.40	0.02	17.20
68	50	10	1100000	8.18	0.32	2.56	0.32	34.80	0.04	27.80	0.01	25.00
69	50	10	1200000	8.29	0.34	2.60	0.34	34.60	0.05	27.90	0.01	63.30
70	50	10	1600000	8.34	0.35	2.62	0.35	34.50	0.05	27.70	0.01	74.00
71	50	10	2000000	8.47	0.37	2.66	0.37	34.50	0.05	27.50	0.02	108.00
72	50	10	2400000	6.20	0.00	1.95	0.01	36.80	0.01	28.70	0.02	220.00
73	50	10	2800000	6.19	0.00	1.94	0.00	36.40	0.00	28.10	0.00	278.30
74	50	5	5000	1.25	0.87	0.25	0.87	40.90	0.33	26.90	0.17	0.70
75	50	5	10000	1.87	0.81	0.37	0.81	39.90	0.30	27.20	0.18	0.70
76	50	5	20000	2.64	0.73	0.52	0.73	38.00	0.23	26.20	0.14	0.90
77	50	5	50000	4.10	0.59	0.80	0.59	35.50	0.15	24.90	0.08	1.40
78	50	5	100000	5.31	0.47	1.03	0.47	33.70	0.09	23.90	0.04	2.80
79	50	5	200000	6.78	0.32	1.33	0.32	32.50	0.06	23.40	0.02	6.90
80	50	5	400000	8.69	0.13	1.70	0.13	31.10	0.01	22.70	0.01	11.30
81	50	5	800000	9.33	0.06	1.84	0.06	30.60	0.01	22.60	0.02	22.80
82	50	5	1000000	9.47	0.05	1.86	0.05	30.50	0.01	22.60	0.02	41.20
83	50	5	1200000	9.49	0.05	1.86	0.05	30.60	0.01	22.60	0.02	58.00
84	50	5	1400000	9.44	0.05	1.86	0.05	30.60	0.01	22.70	0.01	28.30
85	50	5	1600000	9.82	0.01	1.93	0.01	30.70	0.00	22.90	0.00	30.80
86	50	5	2000000	9.87	0.01	1.94	0.01	30.80	0.00	23.10	0.00	33.80
87	50	5	2400000	9.94	0.00	1.95	0.00	30.80	0.00	23.00	0.00	41.20
88	50	2.5	5000	1.84	0.62	0.28	0.62	42.20	0.25	29.00	0.21	17.70
89	50	2.5	10000	2.55	0.47	0.37	0.49	39.50	0.17	27.00	0.13	18.30
90	50	2.5	20000	3.34	0.30	0.47	0.36	36.80	0.09	25.80	0.08	14.90
91	50	2.5	50000	4.06	0.15	0.56	0.23	34.60	0.03	24.60	0.03	23.50
92	50	2.5	100000	4.72	0.01	0.63	0.14	33.10	0.02	23.70	0.01	18.00
93	50	2.5	200000	5.18	0.08	0.68	0.07	32.30	0.04	23.30	0.03	24.90
94	50	2.5	300000	5.20	0.09	0.70	0.04	32.20	0.04	23.10	0.03	33.50
95	50	2.5	400000	5.21	0.09	0.70	0.04	32.30	0.04	23.20	0.03	41.90
96	50	2.5	800000	4.79	0.00	0.71	0.03	33.70	0.00	24.10	0.01	75.10
97	50	2.5	1000000	4.83	0.01	0.72	0.01	33.50	0.01	23.80	0.00	89.20
98	50	2.5	1600000	4.75	0.01	0.74	0.01	34.30	0.02	24.30	0.02	132.50
99	50	2.5	2000000	4.79	0.00	0.73	0.00	33.70	0.00	23.90	0.00	164.20
100	50	1.25	5000	0.88	0.71	0.14	0.59	44.80	0.19	29.20	0.15	413.30
101	50	1.25	10000	1.03	0.66	0.15	0.56	44.20	0.17	29.20	0.15	370.00

102	50	1.25	20000	1.35	0.55	0.19	0.44	43.20	0.15	28.70	0.13	346.70
103	50	1.25	50000	1.67	0.45	0.22	0.35	41.60	0.10	27.90	0.09	291.70
104	50	1.25	100000	2.01	0.33	0.25	0.26	40.30	0.07	27.10	0.06	355.00
105	50	1.25	200000	2.34	0.23	0.28	0.18	39.70	0.05	26.80	0.05	311.70
106	50	1.25	400000	2.67	0.12	0.31	0.09	38.60	0.02	25.90	0.02	426.70
107	50	1.25	600000	2.88	0.05	0.33	0.03	38.20	0.01	25.80	0.01	455.00
108	50	1.25	800000	3.05	0.01	0.34	0.00	37.40	0.01	25.10	0.02	486.70
109	50	1.25	1000000	2.81	0.07	0.32	0.06	38.30	0.02	25.90	0.02	518.30
110	50	1.25	1200000	2.95	0.02	0.33	0.03	37.80	0.00	25.20	0.01	670.00
111	50	1.25	1600000	3.16	0.05	0.35	0.03	37.30	0.01	25.00	0.02	685.00
112	50	1.25	2000000	3.02	0.00	0.34	0.00	37.70	0.00	25.50	0.00	866.70
113	70	10	5000	10.92	0.85	0.88	0.87	70.70	0.61	48.80	0.49	0.20
114	70	10	10000	12.44	0.83	1.03	0.85	65.80	0.50	45.00	0.38	0.20
115	70	10	20000	16.88	0.77	1.43	0.79	60.40	0.37	41.90	0.28	0.20
116	70	10	50000	22.78	0.69	1.95	0.71	57.40	0.30	40.70	0.24	0.40
117	70	10	100000	35.20	0.53	3.07	0.54	52.10	0.18	37.30	0.14	0.80
118	70	10	200000	35.57	0.52	3.10	0.53	53.20	0.21	38.70	0.18	1.80
119	70	10	400000	50.57	0.32	4.48	0.33	48.50	0.10	35.80	0.09	4.20
120	70	10	800000	60.86	0.18	5.41	0.19	46.50	0.06	34.60	0.06	8.90
121	70	10	1200000	71.98	0.03	6.42	0.04	44.30	0.01	33.00	0.01	13.90
124	70	10	1600000	68.32	0.08	6.09	0.09	45.30	0.03	34.10	0.04	18.90
125	70	10	1700000	73.44	0.02	6.56	0.02	44.20	0.00	33.00	0.01	20.00
126	70	10	1800000	73.08	0.02	6.53	0.02	44.10	0.00	32.80	0.00	24.80
127	70	10	2000000	75.37	0.01	6.74	0.01	43.80	0.00	32.60	0.00	26.60
128	70	10	2400000	74.56	0.00	6.66	0.00	44.00	0.00	32.70	0.00	31.40
129	70	5	5000	16.32	0.77	0.77	0.79	65.30	0.59	44.70	0.47	2.30
130	70	5	10000	19.91	0.72	0.96	0.74	61.80	0.51	43.20	0.42	2.10
131	70	5	20000	24.62	0.66	1.20	0.67	57.30	0.40	39.10	0.28	2.10
132	70	5	50000	35.93	0.50	1.78	0.51	50.90	0.24	35.90	0.18	2.30
133	70	5	100000	44.28	0.39	2.21	0.40	47.70	0.16	34.00	0.11	2.90
134	70	5	200000	52.73	0.27	2.66	0.28	45.10	0.10	32.50	0.07	4.40
135	70	5	400000	64.08	0.11	3.25	0.11	42.50	0.04	31.10	0.02	8.00
136	70	5	800000	64.62	0.10	3.28	0.11	42.40	0.03	30.90	0.01	16.90
137	70	5	1000000	65.35	0.09	3.32	0.10	42.30	0.03	30.90	0.01	26.80
138	70	5	1200000	67.55	0.06	3.43	0.07	41.90	0.02	30.70	0.01	30.40
139	70	5	1400000	67.73	0.06	3.44	0.06	41.90	0.02	30.70	0.01	39.00
140	70	5	1600000	71.14	0.01	3.62	0.01	41.10	0.00	30.50	0.00	42.10
141	70	5	2000000	73.94	0.02	3.76	0.02	41.40	0.01	30.70	0.01	42.10
142	70	5	2400000	68.68	0.05	3.49	0.05	41.60	0.01	30.60	0.00	52.50
143	70	5	2800000	72.18	0.00	3.67	0.00	41.00	0.00	30.50	0.00	60.40
144	70	2.5	5000	30.56	0.32	0.95	0.30	57.40	0.35	39.00	0.34	62.00
145	70	2.5	10000	34.45	0.23	1.06	0.22	54.00	0.27	37.40	0.28	56.00
146	70	2.5	20000	36.36	0.19	1.13	0.17	51.50	0.21	36.10	0.24	49.80
147	70	2.5	50000	36.14	0.19	1.13	0.17	49.40	0.16	34.80	0.19	45.20
148	70	2.5	100000	37.93	0.15	1.18	0.13	47.20	0.11	32.90	0.13	44.10
149	70	2.5	200000	39.58	0.12	1.23	0.10	45.50	0.07	31.60	0.08	47.60

150	70	2.5	400000	41.67	0.07	1.28	0.06	44.10	0.04	30.50	0.04	56.20
151	70	2.5	500000	42.35	0.05	1.30	0.04	43.80	0.03	30.30	0.04	66.30
152	70	2.5	600000	42.56	0.05	1.30	0.04	43.70	0.03	30.20	0.03	83.00
153	70	2.5	700000	43.22	0.03	1.32	0.03	43.40	0.02	30.00	0.03	67.30
154	70	2.5	800000	43.35	0.03	1.32	0.03	43.20	0.02	29.80	0.02	73.30
155	70	2.5	1200000	44.01	0.02	1.34	0.01	42.90	0.01	29.60	0.01	91.70
156	70	2.5	1600000	44.35	0.01	1.34	0.01	42.70	0.00	29.40	0.01	110.80
157	70	2.5	2000000	44.77	0.00	1.36	0.00	42.50	0.00	29.30	0.00	159.80
158	70	2.5	2400000	44.78	0.00	1.36	0.00	42.50	0.00	29.20	0.00	168.30
159	70	1.25	20000	35.68	0.27	0.89	0.26	53.10	0.17	38.30	0.16	1025.00
160	70	1.25	50000	40.89	0.17	1.01	0.16	50.20	0.11	36.60	0.11	910.00
161	70	1.25	100000	42.67	0.13	1.07	0.11	48.70	0.07	35.50	0.07	1121.70
162	70	1.25	200000	44.28	0.10	1.11	0.07	47.70	0.05	34.80	0.05	846.70
163	70	1.25	400000	45.46	0.07	1.14	0.05	47.10	0.04	34.40	0.04	866.70
164	70	1.25	800000	47.03	0.04	1.16	0.03	46.30	0.02	33.80	0.02	898.30
165	70	1.25	900000	47.46	0.03	1.18	0.02	46.30	0.02	33.90	0.02	923.30
166	70	1.25	1000000	47.73	0.03	1.18	0.02	46.10	0.02	33.60	0.02	943.30
167	70	1.25	1100000	47.52	0.03	1.17	0.03	46.10	0.02	33.70	0.02	948.30
168	70	1.25	1200000	47.76	0.03	1.18	0.02	46.00	0.01	33.60	0.02	1115.00
169	70	1.25	1600000	48.16	0.02	1.18	0.02	45.80	0.01	33.40	0.01	1213.30
170	70	1.25	2000000	49.09	0.00	1.20	0.00	45.40	0.00	33.10	0.00	1080.00
171	70	1.25	2400000	49.12	0.00	1.20	0.00	45.40	0.00	33.10	0.00	1038.30
172	80	10	5000	0.42	0.50	0.17	0.50	50.50	0.17	37.20	0.27	0.10
173	80	10	10000	0.64	0.24	0.26	0.24	45.40	0.06	33.00	0.13	0.10
174	80	10	20000	0.60	0.29	0.24	0.29	43.80	0.02	32.40	0.11	0.20
175	80	10	50000	0.74	0.12	0.30	0.12	41.80	0.03	30.50	0.04	0.70
176	80	10	100000	0.88	0.05	0.36	0.06	40.20	0.07	28.60	0.02	1.50
177	80	10	200000	0.92	0.10	0.37	0.09	40.10	0.07	29.10	0.00	2.90
178	80	10	400000	0.94	0.12	0.38	0.12	40.80	0.05	29.40	0.01	5.80
179	80	10	600000	0.91	0.08	0.37	0.09	41.40	0.04	29.70	0.02	8.90
180	80	10	800000	0.91	0.08	0.37	0.09	41.90	0.03	32.10	0.10	11.70
181	80	10	1000000	0.90	0.07	0.37	0.09	41.90	0.03	31.80	0.09	15.00
182	80	10	1200000	0.88	0.05	0.36	0.06	42.20	0.02	30.90	0.06	18.00
183	80	10	1400000	0.88	0.05	0.36	0.06	42.30	0.02	30.80	0.05	22.90
184	80	10	1600000	0.86	0.02	0.35	0.03	42.50	0.01	30.10	0.03	29.40
185	80	10	2000000	0.84	0.00	0.34	0.00	43.00	0.00	29.20	0.00	145.00
186	80	5	5000	0.33	0.59	0.11	0.52	49.00	0.27	35.10	0.23	0.70
187	80	5	10000	0.32	0.60	0.10	0.57	47.00	0.22	34.30	0.20	1.00
188	80	5	20000	0.45	0.44	0.14	0.39	45.70	0.19	33.30	0.17	1.20
189	80	5	50000	0.53	0.35	0.16	0.30	42.80	0.11	31.60	0.11	3.00
190	80	5	100000	0.62	0.23	0.18	0.22	41.30	0.07	30.80	0.08	6.00
191	80	5	200000	0.69	0.15	0.20	0.13	39.50	0.03	29.20	0.02	10.80
192	80	5	400000	0.75	0.07	0.22	0.04	39.00	0.01	28.70	0.01	18.40
193	80	5	600000	0.77	0.05	0.22	0.04	38.90	0.01	28.70	0.01	27.10
194	80	5	800000	0.80	0.01	0.23	0.00	38.40	0.00	28.20	0.01	36.70
195	80	5	1000000	0.79	0.02	0.23	0.00	38.40	0.00	28.60	0.00	44.20

196	80	5	1200000	0.79	0.02	0.23	0.00	38.40	0.00	28.50	0.00	62.10
197	80	5	1400000	0.81	0.00	0.23	0.00	38.50	0.00	28.60	0.00	61.30
198	80	5	1600000	0.81	0.00	0.23	0.00	38.40	0.00	28.60	0.00	75.80
199	80	5	2000000	0.81	0.00	0.23	0.00	38.50	0.00	28.50	0.00	591.70
200	80	2.5	5000	0.21	0.70	0.07	0.59	59.00	0.34	40.20	0.26	10.70
201	80	2.5	10000	0.28	0.61	0.09	0.47	60.10	0.36	40.80	0.28	14.00
202	80	2.5	20000	0.31	0.56	0.09	0.47	52.90	0.20	37.20	0.17	12.70
203	80	2.5	50000	0.41	0.42	0.11	0.35	51.30	0.16	35.40	0.11	20.70
204	80	2.5	100000	0.50	0.30	0.13	0.24	47.50	0.08	33.20	0.04	20.00
205	80	2.5	200000	0.57	0.20	0.14	0.18	45.10	0.02	31.90	0.00	34.20
206	80	2.5	400000	0.64	0.10	0.15	0.12	43.30	0.02	30.90	0.03	66.20
207	80	2.5	800000	0.67	0.06	0.16	0.06	42.60	0.03	30.40	0.05	119.20
208	80	2.5	900000	0.69	0.03	0.16	0.06	42.30	0.04	30.50	0.04	132.50
209	80	2.5	1000000	0.70	0.01	0.17	0.00	43.70	0.01	31.50	0.01	150.80
210	80	2.5	1200000	0.69	0.03	0.17	0.00	43.80	0.01	31.50	0.01	180.80
211	80	2.5	1400000	0.71	0.00	0.17	0.00	42.80	0.03	30.40	0.05	208.30
212	80	2.5	1600000	0.71	0.00	0.18	0.06	43.70	0.01	31.80	0.00	321.70
213	80	2.5	2000000	0.71	0.00	0.17	0.00	44.10	0.00	31.90	0.00	821.70
214	80	1.25	5000	0.19	0.68	0.06	0.50	60.50	0.26	42.00	0.24	205.00
215	80	1.25	10000	0.22	0.63	0.07	0.42	59.70	0.24	40.20	0.19	195.00
216	80	1.25	20000	0.28	0.53	0.08	0.33	61.10	0.27	41.50	0.23	186.70
217	80	1.25	50000	0.35	0.42	0.09	0.25	57.20	0.19	39.70	0.17	208.30
218	80	1.25	100000	0.43	0.28	0.10	0.17	54.30	0.13	37.80	0.12	168.30
219	80	1.25	200000	0.46	0.23	0.10	0.17	52.90	0.10	36.90	0.09	205.00
220	80	1.25	400000	0.53	0.12	0.11	0.08	51.10	0.06	35.80	0.06	288.30
221	80	1.25	800000	0.57	0.05	0.11	0.08	49.60	0.03	34.60	0.02	456.70
222	80	1.25	900000	0.58	0.03	0.11	0.08	49.10	0.02	34.20	0.01	493.30
223	80	1.25	1000000	0.58	0.03	0.12	0.00	49.00	0.02	34.20	0.01	518.30
224	80	1.25	1200000	0.59	0.02	0.12	0.00	48.50	0.01	33.90	0.00	593.30
225	80	1.25	1600000	0.60	0.00	0.12	0.00	48.30	0.00	33.80	0.00	873.30
226	80	1.25	2000000	0.60	0.00	0.12	0.00	48.10	0.00	33.80	0.00	1350.00
227	100	10	5000	0.45	0.50	0.16	0.50	55.70	0.15	41.70	0.26	0.10
228	100	10	10000	0.63	0.30	0.23	0.28	54.60	0.13	38.90	0.17	0.10
229	100	10	20000	0.60	0.33	0.21	0.34	52.50	0.09	38.30	0.15	0.30
230	100	10	50000	0.79	0.12	0.28	0.13	48.30	0.00	35.20	0.06	0.70
231	100	10	100000	0.84	0.07	0.30	0.06	47.20	0.02	35.20	0.06	1.50
232	100	10	200000	0.94	0.04	0.34	0.06	46.80	0.03	33.80	0.02	3.40
233	100	10	400000	0.95	0.06	0.34	0.06	47.10	0.02	34.10	0.03	5.80
234	100	10	800000	0.92	0.02	0.33	0.03	47.40	0.02	35.00	0.05	11.00
235	100	10	1200000	0.91	0.01	0.32	0.00	48.20	0.00	33.60	0.01	19.30
236	100	10	1400000	0.90	0.00	0.32	0.00	48.10	0.00	33.80	0.02	19.60
237	100	10	1600000	0.90	0.00	0.32	0.00	48.20	0.00	33.40	0.01	24.10
238	100	10	2000000	0.90	0.00	0.32	0.00	48.30	0.00	33.20	0.00	121.10
239	100	5	5000	0.36	0.54	0.11	0.42	56.20	0.27	42.80	0.30	1.10
240	100	5	10000	0.33	0.58	0.09	0.53	58.20	0.31	41.60	0.26	0.70
241	100	5	20000	0.46	0.41	0.12	0.37	53.70	0.21	40.10	0.22	0.90

242	100	5	50000	0.48	0.38	0.12	0.37	51.90	0.17	38.90	0.18	2.60
243	100	5	100000	0.59	0.24	0.15	0.21	48.90	0.10	36.10	0.09	4.10
244	100	5	200000	0.64	0.18	0.16	0.16	46.90	0.06	35.10	0.06	8.50
245	100	5	400000	0.64	0.18	0.16	0.16	47.00	0.06	35.20	0.07	18.70
246	100	5	600000	0.69	0.12	0.17	0.11	46.40	0.05	34.40	0.04	24.60
247	100	5	800000	0.73	0.06	0.18	0.05	45.30	0.02	33.70	0.02	37.20
248	100	5	1000000	0.76	0.03	0.19	0.00	44.30	0.00	32.40	0.02	41.20
249	100	5	1200000	0.78	0.00	0.19	0.00	44.30	0.00	32.70	0.01	48.80
250	100	5	1400000	0.76	0.03	0.19	0.00	44.70	0.01	33.20	0.01	66.70
251	100	5	1600000	0.75	0.04	0.19	0.00	45.00	0.01	33.40	0.01	69.60
252	100	5	2000000	0.77	0.01	0.19	0.00	44.60	0.00	33.20	0.01	173.80
253	100	5	2400000	0.78	0.00	0.19	0.00	44.40	0.00	33.00	0.00	741.70
254	100	2.5	5000	0.26	0.62	0.07	0.50	65.10	0.32	49.10	0.37	15.80
255	100	2.5	10000	0.32	0.54	0.08	0.43	67.50	0.37	47.90	0.34	10.80
256	100	2.5	20000	0.37	0.46	0.09	0.36	61.90	0.26	45.00	0.26	14.80
257	100	2.5	50000	0.48	0.30	0.11	0.21	58.40	0.19	41.20	0.15	14.40
258	100	2.5	100000	0.53	0.23	0.11	0.21	53.80	0.09	38.80	0.08	19.80
259	100	2.5	200000	0.59	0.14	0.12	0.14	53.00	0.08	38.10	0.06	34.70
260	100	2.5	400000	0.62	0.10	0.13	0.07	50.10	0.02	36.50	0.02	68.60
261	100	2.5	600000	0.62	0.10	0.12	0.14	48.50	0.01	34.70	0.03	88.30
262	100	2.5	800000	0.65	0.06	0.13	0.07	49.20	0.00	35.40	0.01	115.80
263	100	2.5	1000000	0.64	0.07	0.13	0.07	48.10	0.02	34.50	0.04	142.50
264	100	2.5	1200000	0.68	0.01	0.14	0.00	48.60	0.01	35.10	0.02	162.50
265	100	2.5	1400000	0.69	0.00	0.14	0.00	48.80	0.01	35.40	0.01	190.80
266	100	2.5	1600000	0.67	0.03	0.14	0.00	48.50	0.01	35.00	0.02	224.20
267	100	2.5	2000000	0.69	0.00	0.14	0.00	49.20	0.00	35.80	0.00	490.80
268	100	1.25	5000	0.18	0.70	0.05	0.50	72.80	0.35	47.20	0.22	286.70
269	100	1.25	10000	0.27	0.56	0.07	0.30	66.90	0.24	49.50	0.28	221.70
270	100	1.25	20000	0.32	0.48	0.08	0.20	68.80	0.28	49.30	0.27	185.00
271	100	1.25	50000	0.40	0.34	0.08	0.20	63.90	0.19	46.30	0.19	163.70
272	100	1.25	100000	0.46	0.25	0.09	0.10	61.30	0.14	44.50	0.15	178.30
273	100	1.25	200000	0.50	0.18	0.09	0.10	59.20	0.10	43.00	0.11	215.00
274	100	1.25	400000	0.55	0.10	0.10	0.00	56.90	0.06	41.20	0.06	288.30
275	100	1.25	600000	0.58	0.05	0.10	0.00	55.70	0.03	40.30	0.04	366.70
276	100	1.25	800000	0.60	0.02	0.10	0.00	55.20	0.02	39.90	0.03	438.30
277	100	1.25	1000000	0.59	0.03	0.10	0.00	55.20	0.02	39.90	0.03	558.30
278	100	1.25	1200000	0.61	0.00	0.10	0.00	54.50	0.01	39.20	0.01	671.70
279	100	1.25	1600000	0.62	0.02	0.10	0.00	54.40	0.01	39.50	0.02	720.00
280	100	1.25	2000000	0.61	0.00	0.10	0.00	53.90	0.00	38.80	0.00	1228.30
281	125	10	5000	20.80	0.66	1.57	0.72	99.50	0.57	71.70	0.47	0.10
282	125	10	10000	22.02	0.64	1.79	0.68	88.00	0.39	62.30	0.28	0.20
283	125	10	20000	27.88	0.55	2.31	0.59	83.70	0.32	62.40	0.28	0.20
284	125	10	50000	35.34	0.43	3.04	0.46	76.20	0.21	56.10	0.15	0.40
285	125	10	100000	42.77	0.31	3.81	0.33	71.00	0.12	53.50	0.10	0.60
286	125	10	200000	51.29	0.17	4.62	0.19	67.20	0.06	51.00	0.05	1.40
287	125	10	400000	56.13	0.09	5.11	0.10	64.90	0.03	49.70	0.02	3.30

288	125	10	600000	59.34	0.04	5.40	0.05	64.20	0.02	49.20	0.01	6.30
289	125	10	800000	60.15	0.03	5.49	0.03	63.80	0.01	49.10	0.01	7.10
290	125	10	1200000	61.09	0.01	5.58	0.02	63.30	0.00	48.80	0.00	11.20
291	125	10	1600000	57.86	0.07	5.26	0.07	62.20	0.02	47.90	0.02	15.30
292	125	10	2000000	61.90	0.00	5.67	0.00	63.20	0.00	48.80	0.00	19.00
293	125	5	5000	24.81	0.40	1.17	0.45	93.10	0.42	69.60	0.50	1.80
294	125	5	10000	25.58	0.38	1.21	0.43	89.80	0.37	63.90	0.38	1.70
295	125	5	20000	28.18	0.32	1.38	0.35	81.60	0.25	58.30	0.26	1.70
296	125	5	50000	32.29	0.22	1.60	0.25	76.00	0.16	54.20	0.17	2.00
297	125	5	100000	38.45	0.07	1.95	0.08	69.10	0.06	49.20	0.06	3.20
298	125	5	200000	36.71	0.11	1.86	0.12	69.90	0.07	49.30	0.06	3.70
299	125	5	400000	38.81	0.06	1.98	0.07	67.20	0.03	47.50	0.02	7.50
300	125	5	600000	39.23	0.05	2.00	0.06	67.20	0.03	47.50	0.02	11.20
301	125	5	800000	41.58	0.01	2.13	0.00	65.80	0.01	47.10	0.02	16.60
302	125	5	1000000	41.90	0.01	2.15	0.01	65.80	0.01	47.20	0.02	18.80
303	125	5	1200000	39.52	0.04	2.02	0.05	66.60	0.02	47.20	0.02	22.80
304	125	5	1400000	38.21	0.08	1.94	0.08	68.00	0.04	47.70	0.03	27.00
305	125	5	1600000	40.16	0.03	2.05	0.03	66.40	0.02	46.80	0.01	32.10
306	125	5	2000000	41.32	0.00	2.12	0.00	65.40	0.00	46.40	0.00	38.30
307	125	2.5	5000	34.41	0.06	1.08	0.06	88.10	0.24	61.50	0.34	46.90
308	125	2.5	10000	33.44	0.03	1.07	0.05	82.40	0.16	56.90	0.24	41.50
309	125	2.5	20000	33.69	0.04	1.08	0.06	78.60	0.10	54.10	0.18	38.10
310	125	2.5	50000	31.97	0.01	1.03	0.01	75.30	0.06	51.00	0.11	36.60
311	125	2.5	100000	32.88	0.02	1.05	0.03	73.20	0.03	48.90	0.06	38.20
312	125	2.5	200000	32.31	0.00	1.03	0.01	72.40	0.02	47.90	0.04	45.10
313	125	2.5	400000	32.10	0.01	1.02	0.00	72.10	0.01	47.10	0.02	47.80
314	125	2.5	600000	32.91	0.02	1.06	0.04	71.00	0.00	47.00	0.02	61.30
315	125	2.5	700000	32.83	0.02	1.05	0.03	71.20	0.00	46.90	0.02	64.30
316	125	2.5	800000	31.37	0.03	0.99	0.03	72.40	0.02	46.60	0.01	66.30
317	125	2.5	1200000	31.23	0.03	0.98	0.04	72.40	0.02	46.40	0.01	85.80
318	125	2.5	1600000	31.17	0.04	0.98	0.04	72.20	0.01	46.10	0.00	102.50
319	125	2.5	1800000	31.71	0.02	1.00	0.02	71.80	0.01	46.30	0.01	115.00
320	125	2.5	2000000	32.33	0.00	1.02	0.00	71.20	0.00	46.00	0.00	115.80
322	125	1.25	10000	30.95	0.06	0.81	0.02	87.50	0.21	61.90	0.27	820.00
323	125	1.25	20000	30.37	0.08	0.82	0.01	83.70	0.16	59.60	0.22	750.00
324	125	1.25	50000	31.78	0.04	0.85	0.02	79.00	0.10	55.90	0.14	891.70
325	125	1.25	100000	32.11	0.03	0.85	0.02	76.50	0.06	53.50	0.09	666.70
326	125	1.25	200000	32.47	0.01	0.86	0.04	74.70	0.04	51.90	0.06	770.00
327	125	1.25	400000	32.75	0.01	0.85	0.02	73.60	0.02	50.90	0.04	665.00
328	125	1.25	500000	32.88	0.00	0.85	0.02	73.40	0.02	50.70	0.04	695.00
329	125	1.25	600000	32.84	0.00	0.85	0.02	73.10	0.01	50.30	0.03	803.30
330	125	1.25	800000	32.99	0.00	0.85	0.02	72.80	0.01	50.00	0.02	733.30
331	125	1.25	1200000	33.01	0.00	0.84	0.01	72.40	0.00	49.30	0.01	795.00
332	125	1.25	1600000	33.00	0.00	0.83	0.00	72.10	0.00	48.90	0.00	830.00
333	125	1.25	2000000	32.95	0.00	0.83	0.00	72.10	0.00	48.90	0.00	890.00
334	150	10	5000	8.40	0.67	0.93	0.70	96.50	0.44	72.70	0.39	0.10

335	150	10	10000	11.82	0.54	1.26	0.59	94.40	0.41	69.70	0.33	0.10
336	150	10	20000	13.17	0.49	1.44	0.54	87.90	0.31	65.50	0.25	0.20
337	150	10	50000	16.72	0.35	1.93	0.38	79.70	0.19	60.30	0.15	0.30
338	150	10	100000	20.24	0.22	2.38	0.23	73.50	0.10	56.00	0.07	0.60
339	150	10	200000	22.08	0.14	2.62	0.15	70.20	0.05	54.20	0.03	1.60
340	150	10	400000	24.29	0.06	2.90	0.06	68.50	0.02	53.00	0.01	3.30
341	150	10	500000	24.61	0.05	2.95	0.05	68.00	0.01	52.90	0.01	4.30
342	150	10	600000	25.21	0.02	3.01	0.03	67.90	0.01	52.80	0.01	5.50
343	150	10	800000	25.59	0.01	3.07	0.01	67.70	0.01	52.70	0.01	7.40
344	150	10	1000000	25.89	0.00	3.11	0.00	67.60	0.01	52.70	0.01	13.70
345	150	10	1200000	26.15	0.01	3.14	0.01	67.50	0.01	52.70	0.01	11.40
346	150	10	1400000	26.12	0.01	3.14	0.01	67.50	0.01	52.60	0.00	13.60
347	150	10	1600000	26.11	0.01	3.13	0.01	67.30	0.00	52.60	0.00	15.40
348	150	10	2000000	25.79	0.00	3.10	0.00	67.00	0.00	52.40	0.00	19.10
349	150	5	5000	9.90	0.38	0.62	0.42	99.40	0.41	73.70	0.49	1.30
350	150	5	10000	12.02	0.24	0.77	0.28	90.80	0.29	64.30	0.30	1.30
351	150	5	20000	12.65	0.20	0.82	0.23	83.30	0.18	58.20	0.18	1.30
352	150	5	50000	13.77	0.13	0.91	0.15	77.20	0.10	54.00	0.09	1.60
353	150	5	100000	14.77	0.07	0.99	0.07	73.40	0.04	51.80	0.05	2.30
354	150	5	200000	15.12	0.05	1.02	0.05	72.40	0.03	51.10	0.03	3.70
355	150	5	400000	15.99	0.01	1.08	0.01	70.60	0.00	49.70	0.00	7.70
356	150	5	600000	16.36	0.03	1.11	0.04	70.10	0.00	49.40	0.00	14.10
357	150	5	800000	16.44	0.04	1.11	0.04	69.90	0.01	49.30	0.00	15.20
358	150	5	1000000	16.40	0.04	1.11	0.04	69.80	0.01	49.10	0.01	18.30
359	150	5	1200000	16.33	0.03	1.10	0.03	69.60	0.01	49.10	0.01	23.50
360	150	5	1400000	16.62	0.05	1.13	0.06	69.60	0.01	49.70	0.00	27.00
361	150	5	1600000	15.72	0.01	1.06	0.01	71.30	0.01	49.80	0.01	33.30
362	150	5	2000000	15.84	0.00	1.07	0.00	70.30	0.00	49.50	0.00	40.40
363	150	2.5	5000	12.63	0.05	0.56	0.02	95.60	0.27	66.90	0.38	32.80
364	150	2.5	10000	12.25	0.08	0.53	0.07	91.70	0.22	62.70	0.29	29.40
365	150	2.5	20000	11.94	0.10	0.52	0.09	89.00	0.18	60.20	0.24	27.80
366	150	2.5	50000	11.27	0.15	0.48	0.16	86.10	0.14	56.00	0.15	27.60
367	150	2.5	100000	11.96	0.10	0.51	0.11	82.90	0.10	53.60	0.11	28.80
368	150	2.5	200000	11.80	0.11	0.50	0.12	81.50	0.08	51.80	0.07	33.50
369	150	2.5	400000	11.04	0.17	0.46	0.19	83.60	0.11	51.90	0.07	43.80
370	150	2.5	600000	12.93	0.02	0.55	0.04	76.90	0.02	49.30	0.02	60.40
371	150	2.5	800000	11.00	0.17	0.46	0.19	83.40	0.11	51.30	0.06	63.20
372	150	2.5	1000000	13.34	0.01	0.57	0.00	75.30	0.00	48.70	0.00	87.50
373	150	2.5	1200000	13.34	0.01	0.57	0.00	75.30	0.00	48.70	0.00	85.00
374	150	2.5	1400000	13.26	0.00	0.57	0.00	75.40	0.00	48.70	0.00	95.80
375	150	2.5	2000000	13.19	0.00	0.57	0.00	75.50	0.00	48.60	0.00	128.30
376	150	2.5	2400000	13.30	0.00	0.58	0.02	74.80	0.01	48.40	0.00	147.50
377	150	2.5	2800000	13.25	0.00	0.57	0.00	75.20	0.00	48.50	0.00	169.20
378	150	1.25	5000	10.00	0.19	0.39	0.09	103.70	0.28	72.40	0.35	613.30
379	150	1.25	10000	11.87	0.03	0.45	0.05	98.00	0.21	70.40	0.31	806.70
380	150	1.25	20000	11.66	0.05	0.45	0.05	94.30	0.17	67.10	0.25	531.70

381	150	1.25	50000	11.81	0.04	0.45	0.05	88.70	0.10	62.40	0.16	551.70
382	150	1.25	100000	12.10	0.02	0.45	0.05	85.30	0.06	59.60	0.11	503.30
383	150	1.25	200000	12.30	0.00	0.45	0.05	83.60	0.03	57.80	0.08	490.00
384	150	1.25	400000	12.39	0.01	0.44	0.02	82.40	0.02	56.20	0.05	521.70
385	150	1.25	500000	12.34	0.00	0.44	0.02	82.10	0.02	55.80	0.04	636.70
386	150	1.25	600000	12.36	0.01	0.43	0.00	81.70	0.01	55.50	0.03	780.00
387	150	1.25	800000	12.33	0.00	0.43	0.00	81.50	0.01	54.70	0.02	571.70
388	150	1.25	1200000	12.34	0.00	0.43	0.00	81.10	0.00	54.30	0.01	631.70
389	150	1.25	1600000	12.30	0.00	0.43	0.00	81.10	0.00	54.00	0.01	693.30
390	150	1.25	2000000	12.29	0.00	0.43	0.00	80.80	0.00	53.70	0.00	748.30
391	200	10	5000	0.36	0.53	0.07	0.61	104.70	0.38	72.10	0.33	0.10
392	200	10	10000	0.39	0.49	0.09	0.50	86.50	0.14	65.20	0.21	0.10
393	200	10	20000	0.53	0.30	0.12	0.33	89.50	0.18	62.50	0.16	0.20
394	200	10	50000	0.66	0.13	0.14	0.22	83.80	0.11	60.60	0.12	0.40
395	200	10	100000	0.71	0.07	0.16	0.11	81.50	0.08	58.50	0.08	0.90
396	200	10	200000	0.68	0.11	0.16	0.11	77.50	0.03	56.60	0.05	1.70
397	200	10	400000	0.75	0.01	0.17	0.06	78.50	0.04	56.60	0.05	3.90
398	200	10	500000	0.73	0.04	0.16	0.11	78.40	0.04	55.70	0.03	4.80
399	200	10	600000	0.73	0.04	0.16	0.11	77.50	0.03	55.30	0.02	5.90
400	200	10	700000	0.77	0.01	0.18	0.00	77.60	0.03	55.20	0.02	6.80
401	200	10	800000	0.77	0.01	0.18	0.00	77.70	0.03	55.20	0.02	7.70
402	200	10	1200000	0.76	0.00	0.17	0.06	76.10	0.01	54.10	0.00	11.80
403	200	10	1600000	0.76	0.00	0.18	0.00	76.10	0.01	54.20	0.00	16.10
404	200	10	2000000	0.70	0.08	0.16	0.11	79.60	0.05	57.50	0.06	20.20
405	200	10	2400000	0.76	0.00	0.18	0.00	75.60	0.00	54.10	0.00	33.50
406	200	5	5000	0.15	0.75	0.03	0.67	78.60	0.05	64.60	0.26	0.60
407	200	5	10000	0.37	0.38	0.06	0.33	98.70	0.31	71.60	0.40	0.70
408	200	5	20000	0.41	0.32	0.06	0.33	92.60	0.23	65.00	0.27	0.90
409	200	5	50000	0.50	0.17	0.07	0.22	90.60	0.20	62.40	0.22	1.40
410	200	5	100000	0.50	0.17	0.07	0.22	84.70	0.13	57.20	0.12	2.60
411	200	5	200000	0.53	0.12	0.08	0.11	80.30	0.07	54.40	0.06	5.10
412	200	5	400000	0.56	0.07	0.08	0.11	80.70	0.07	54.70	0.07	10.50
413	200	5	500000	0.56	0.07	0.08	0.11	79.00	0.05	53.40	0.05	14.20
414	200	5	600000	0.56	0.07	0.08	0.11	79.70	0.06	53.80	0.05	15.90
415	200	5	700000	0.55	0.08	0.08	0.11	77.20	0.03	51.80	0.01	25.20
416	200	5	800000	0.56	0.07	0.08	0.11	78.00	0.04	52.80	0.03	21.20
417	200	5	1000000	0.58	0.03	0.09	0.00	76.80	0.02	52.50	0.03	28.80
418	200	5	1200000	0.58	0.03	0.09	0.00	76.70	0.02	52.10	0.02	31.20
419	200	5	1600000	0.58	0.03	0.09	0.00	76.30	0.01	51.40	0.01	42.10
420	200	5	2000000	0.60	0.00	0.09	0.00	75.20	0.00	51.10	0.00	51.30
421	200	2.5	5000	0.34	0.19	0.05	0.00	103.20	0.11	78.40	0.32	18.00
422	200	2.5	10000	0.36	0.14	0.05	0.00	99.80	0.07	73.70	0.24	12.90
423	200	2.5	20000	0.41	0.02	0.05	0.00	98.30	0.05	71.00	0.20	16.00
424	200	2.5	50000	0.44	0.05	0.05	0.00	95.10	0.02	67.10	0.13	14.10
425	200	2.5	100000	0.43	0.02	0.05	0.00	92.80	0.01	64.30	0.09	16.60
426	200	2.5	200000	0.43	0.02	0.05	0.00	91.00	0.02	61.50	0.04	23.50

427	200	2.5	400000	0.41	0.02	0.05	0.00	92.30	0.01	60.10	0.02	39.80
428	200	2.5	500000	0.43	0.02	0.05	0.00	90.40	0.03	56.90	0.04	46.30
429	200	2.5	600000	0.42	0.00	0.05	0.00	92.40	0.01	60.10	0.02	54.30
430	200	2.5	700000	0.43	0.02	0.05	0.00	91.70	0.02	57.80	0.02	90.80
431	200	2.5	800000	0.42	0.00	0.05	0.00	93.50	0.00	62.30	0.05	72.70
432	200	2.5	1000000	0.42	0.00	0.05	0.00	91.70	0.02	59.50	0.01	85.80
433	200	2.5	1200000	0.42	0.00	0.05	0.00	91.80	0.02	56.70	0.04	102.50
434	200	2.5	1600000	0.42	0.00	0.05	0.00	91.00	0.02	56.10	0.05	132.50
435	200	2.5	2000000	0.42	0.00	0.05	0.00	93.30	0.00	59.20	0.00	161.70
436	200	1.25	5000	0.33	0.27	0.04	0.00	111.60	0.21	77.10	0.28	300.00
437	200	1.25	10000	0.33	0.27	0.04	0.00	103.30	0.12	78.10	0.30	255.00
438	200	1.25	20000	0.38	0.16	0.05	0.25	101.80	0.10	76.00	0.26	206.70
439	200	1.25	50000	0.43	0.04	0.05	0.25	100.60	0.09	72.70	0.21	193.30
440	200	1.25	100000	0.46	0.02	0.05	0.25	96.40	0.05	68.40	0.14	196.70
441	200	1.25	200000	0.45	0.00	0.05	0.25	94.80	0.03	66.60	0.11	245.00
442	200	1.25	400000	0.45	0.00	0.04	0.00	93.90	0.02	64.20	0.07	251.70
443	200	1.25	500000	0.46	0.02	0.04	0.00	92.80	0.01	63.30	0.05	353.30
444	200	1.25	600000	0.46	0.02	0.04	0.00	92.10	0.00	62.70	0.04	293.30
445	200	1.25	700000	0.46	0.02	0.04	0.00	92.30	0.00	62.40	0.04	311.70
446	200	1.25	800000	0.46	0.02	0.04	0.00	92.10	0.00	62.00	0.03	326.70
447	200	1.25	1000000	0.45	0.00	0.04	0.00	91.80	0.00	61.30	0.02	365.00
448	200	1.25	1200000	0.46	0.02	0.04	0.00	92.10	0.00	61.10	0.02	410.00
449	200	1.25	1600000	0.45	0.00	0.04	0.00	92.00	0.00	60.30	0.00	505.00
450	200	1.25	2000000	0.45	0.00	0.04	0.00	92.20	0.00	60.10	0.00	585.00
451	250	10	5000	3.06	0.45	0.58	0.51	139.10	0.32	108.20	0.36	0.10
452	250	10	10000	4.84	0.14	0.84	0.29	140.60	0.34	104.30	0.31	0.10
453	250	10	20000	4.25	0.24	0.85	0.29	123.00	0.17	93.00	0.17	0.10
454	250	10	50000	4.86	0.13	1.00	0.16	113.40	0.08	84.30	0.06	0.30
455	250	10	100000	5.22	0.07	1.09	0.08	108.90	0.04	81.20	0.02	1.00
456	250	10	200000	5.41	0.04	1.13	0.05	107.60	0.02	80.50	0.01	1.60
457	250	10	250000	5.38	0.04	1.13	0.05	106.80	0.02	80.20	0.01	2.10
458	250	10	300000	5.39	0.04	1.14	0.04	106.80	0.02	80.40	0.01	2.10
459	250	10	400000	5.45	0.03	1.16	0.03	106.10	0.01	80.00	0.01	3.10
460	250	10	600000	5.45	0.03	1.16	0.03	105.30	0.00	79.70	0.00	4.90
461	250	10	800000	5.52	0.02	1.18	0.01	105.30	0.00	79.70	0.00	6.20
462	250	10	1000000	5.53	0.01	1.18	0.01	105.20	0.00	79.50	0.00	7.70
463	250	10	1200000	5.53	0.01	1.18	0.01	105.10	0.00	79.50	0.00	9.50
464	250	10	1600000	5.54	0.01	1.18	0.01	105.00	0.00	79.50	0.00	12.40
465	250	10	2000000	5.61	0.00	1.19	0.00	105.20	0.00	79.50	0.00	15.50
466	250	5	5000	3.56	0.15	0.41	0.20	140.10	0.27	99.10	0.31	1.60
467	250	5	10000	3.55	0.15	0.41	0.20	130.20	0.18	91.10	0.21	0.70
468	250	5	20000	3.64	0.13	0.43	0.16	121.20	0.10	83.30	0.10	0.70
469	250	5	50000	3.71	0.11	0.44	0.14	116.60	0.06	79.30	0.05	1.30
470	250	5	100000	3.73	0.11	0.45	0.12	112.60	0.02	77.20	0.02	1.60
471	250	5	200000	4.21	0.01	0.51	0.00	111.30	0.01	76.00	0.01	3.10
472	250	5	400000	4.06	0.03	0.49	0.04	110.40	0.00	75.70	0.00	7.60

473	250	5	600000	4.14	0.01	0.50	0.02	110.50	0.01	75.70	0.00	9.10
474	250	5	800000	4.22	0.01	0.51	0.00	109.90	0.00	75.40	0.00	12.70
475	250	5	1000000	4.23	0.01	0.51	0.00	109.90	0.00	75.40	0.00	15.70
476	250	5	1200000	4.20	0.00	0.51	0.00	110.30	0.00	75.50	0.00	18.60
477	250	5	1400000	4.15	0.01	0.50	0.02	110.40	0.00	75.50	0.00	29.00
478	250	5	1600000	4.14	0.01	0.50	0.02	110.50	0.01	75.60	0.00	25.20
479	250	5	2000000	4.18	0.00	0.51	0.00	109.90	0.00	75.40	0.00	31.40
480	250	2.5	5000	3.42	0.02	0.27	0.08	143.20	0.09	94.80	0.20	13.30
481	250	2.5	10000	3.34	0.00	0.26	0.04	136.60	0.04	88.20	0.12	12.90
482	250	2.5	20000	3.47	0.04	0.27	0.08	135.60	0.03	85.80	0.08	13.00
483	250	2.5	50000	3.31	0.01	0.25	0.00	133.70	0.02	83.10	0.05	15.20
484	250	2.5	100000	3.39	0.01	0.26	0.04	132.90	0.01	81.50	0.03	15.10
485	250	2.5	200000	3.31	0.01	0.25	0.00	132.90	0.01	80.70	0.02	20.60
486	250	2.5	400000	3.28	0.02	0.25	0.00	134.50	0.02	80.80	0.02	30.90
487	250	2.5	600000	3.33	0.00	0.25	0.00	133.80	0.02	80.20	0.01	44.50
488	250	2.5	800000	3.35	0.00	0.25	0.00	133.90	0.02	80.30	0.02	50.10
489	250	2.5	1200000	3.38	0.01	0.25	0.00	130.90	0.01	79.40	0.00	62.40
490	250	2.5	1600000	3.20	0.04	0.24	0.04	135.60	0.03	80.60	0.02	71.50
491	250	2.5	2000000	3.27	0.02	0.25	0.00	133.50	0.01	79.70	0.01	102.50
492	250	2.5	2400000	3.17	0.05	0.24	0.04	135.50	0.03	80.50	0.02	198.30
493	250	2.5	2800000	3.34	0.00	0.25	0.00	131.70	0.00	79.10	0.00	240.00
494	250	1.25	5000	3.54	0.06	0.24	0.14	151.30	0.12	106.00	0.24	311.70
495	250	1.25	10000	3.40	0.02	0.24	0.14	144.70	0.07	101.70	0.19	291.70
496	250	1.25	20000	3.39	0.01	0.23	0.10	143.60	0.06	97.60	0.14	283.30
497	250	1.25	50000	3.28	0.02	0.22	0.05	140.00	0.03	94.20	0.10	281.70
498	250	1.25	100000	3.26	0.02	0.22	0.05	138.70	0.02	91.30	0.07	301.70
499	250	1.25	200000	3.31	0.01	0.21	0.00	137.30	0.01	89.80	0.05	335.00
500	250	1.25	250000	3.31	0.01	0.21	0.00	138.10	0.02	89.90	0.05	243.30
501	250	1.25	300000	3.31	0.01	0.21	0.00	137.40	0.01	89.10	0.04	245.00
502	250	1.25	350000	3.30	0.01	0.21	0.00	137.90	0.02	89.40	0.05	473.30
503	250	1.25	400000	3.33	0.00	0.21	0.00	137.50	0.01	88.60	0.04	435.00
504	250	1.25	600000	3.35	0.00	0.21	0.00	136.30	0.01	87.30	0.02	298.30
505	250	1.25	800000	3.35	0.00	0.21	0.00	135.90	0.00	86.80	0.02	453.30
506	250	1.25	1000000	3.36	0.01	0.21	0.00	135.60	0.00	86.00	0.01	315.00
507	250	1.25	1200000	3.34	0.00	0.21	0.00	135.90	0.00	86.10	0.01	336.70
508	250	1.25	1400000	3.33	0.00	0.21	0.00	136.30	0.01	86.30	0.01	355.00
509	250	1.25	1600000	3.35	0.00	0.21	0.00	135.80	0.00	85.80	0.00	373.30
510	250	1.25	2000000	3.34	0.00	0.21	0.00	135.60	0.00	85.50	0.00	430.00
511	300	10	5000	0.41	0.00	0.06	0.25	145.50	0.34	95.00	0.28	0.10
512	300	10	10000	0.47	0.15	0.07	0.13	134.40	0.24	94.40	0.27	0.10
513	300	10	20000	0.42	0.02	0.07	0.13	135.30	0.25	91.60	0.23	0.10
514	300	10	50000	0.29	0.29	0.05	0.38	115.50	0.07	82.20	0.10	0.20
515	300	10	100000	0.46	0.12	0.08	0.00	120.10	0.11	77.60	0.04	0.60
516	300	10	200000	0.47	0.15	0.09	0.13	119.50	0.10	80.10	0.08	1.30
517	300	10	400000	0.48	0.17	0.09	0.13	117.20	0.08	76.70	0.03	2.80
518	300	10	500000	0.41	0.00	0.08	0.00	109.80	0.01	75.40	0.01	3.60

519	300	10	600000	0.39	0.05	0.08	0.00	109.70	0.01	76.40	0.03	4.90
520	300	10	800000	0.41	0.00	0.09	0.13	108.40	0.00	75.10	0.01	5.70
521	300	10	1000000	0.39	0.05	0.08	0.00	108.60	0.00	74.60	0.00	8.10
522	300	10	1200000	0.43	0.05	0.08	0.00	110.90	0.02	74.60	0.00	9.00
523	300	10	1600000	0.40	0.02	0.08	0.00	108.00	0.00	74.60	0.00	12.00
524	300	10	2000000	0.37	0.10	0.08	0.00	105.90	0.02	73.50	0.01	15.00
525	300	10	2400000	0.41	0.00	0.08	0.00	108.40	0.00	74.50	0.00	24.20
526	300	5	5000	0.36	0.05	0.03	0.25	152.10	0.19	93.10	0.33	0.60
527	300	5	10000	0.24	0.37	0.03	0.25	136.60	0.07	96.50	0.37	0.70
528	300	5	20000	0.34	0.11	0.04	0.00	145.80	0.14	90.70	0.29	0.70
529	300	5	50000	0.34	0.11	0.04	0.00	142.40	0.12	83.20	0.19	1.10
530	300	5	100000	0.39	0.03	0.04	0.00	142.30	0.12	80.70	0.15	1.90
531	300	5	200000	0.36	0.05	0.04	0.00	136.40	0.07	76.90	0.10	4.30
532	300	5	400000	0.35	0.08	0.04	0.00	127.30	0.00	74.70	0.06	7.70
533	300	5	600000	0.39	0.03	0.04	0.00	131.20	0.03	72.30	0.03	12.10
534	300	5	800000	0.38	0.00	0.04	0.00	130.40	0.02	73.10	0.04	16.80
535	300	5	1200000	0.37	0.03	0.04	0.00	128.30	0.01	71.50	0.02	24.90
536	300	5	1600000	0.38	0.00	0.04	0.00	128.10	0.01	70.60	0.01	33.10
537	300	5	2000000	0.38	0.00	0.04	0.00	127.40	0.00	70.20	0.00	41.50
538	300	2.5	5000	0.32	0.03	0.03	0.00	153.10	0.04	101.60	0.20	13.40
539	300	2.5	10000	0.35	0.06	0.03	0.00	156.90	0.02	103.40	0.22	12.10
540	300	2.5	20000	0.36	0.09	0.03	0.00	148.70	0.07	96.40	0.14	14.50
541	300	2.5	50000	0.34	0.03	0.03	0.00	147.80	0.07	89.10	0.05	12.40
542	300	2.5	100000	0.35	0.06	0.03	0.00	150.50	0.06	87.00	0.03	15.50
543	300	2.5	200000	0.34	0.03	0.03	0.00	153.80	0.04	85.70	0.01	19.80
544	300	2.5	300000	0.34	0.03	0.03	0.00	155.40	0.03	86.40	0.02	28.70
545	300	2.5	400000	0.33	0.00	0.03	0.00	155.10	0.03	84.20	0.01	29.80
546	300	2.5	600000	0.33	0.00	0.03	0.00	156.60	0.02	83.50	0.01	41.20
547	300	2.5	800000	0.33	0.00	0.03	0.00	159.80	0.00	85.10	0.00	51.90
548	300	2.5	1000000	0.33	0.00	0.03	0.00	161.60	0.01	84.50	0.00	60.70
549	300	2.5	1200000	0.33	0.00	0.03	0.00	160.00	0.00	83.20	0.02	72.80
550	300	2.5	1600000	0.34	0.03	0.03	0.00	161.20	0.01	83.60	0.01	93.30
551	300	2.5	2000000	0.33	0.00	0.03	0.00	159.60	0.00	84.70	0.00	116.70
552	300	1.25	5000	0.33	0.03	0.03	0.50	159.80	0.03	100.70	0.17	241.70
553	300	1.25	10000	0.38	0.12	0.04	1.00	152.00	0.02	104.00	0.21	206.70
554	300	1.25	20000	0.39	0.15	0.03	0.50	159.10	0.02	104.50	0.21	216.70
555	300	1.25	50000	0.39	0.15	0.03	0.50	153.70	0.01	97.40	0.13	178.30
556	300	1.25	100000	0.36	0.06	0.03	0.50	152.10	0.02	94.00	0.09	180.00
557	300	1.25	200000	0.34	0.00	0.02	0.00	150.10	0.04	90.80	0.05	190.00
558	300	1.25	300000	0.35	0.03	0.03	0.50	152.40	0.02	88.20	0.02	205.00
559	300	1.25	400000	0.34	0.00	0.02	0.00	153.50	0.01	87.30	0.01	220.00
560	300	1.25	800000	0.35	0.03	0.02	0.00	153.90	0.01	86.50	0.00	271.70
561	300	1.25	1200000	0.34	0.00	0.02	0.00	155.00	0.00	85.80	0.00	418.30
562	300	1.25	1600000	0.34	0.00	0.02	0.00	156.90	0.01	86.50	0.00	393.30
563	300	1.25	2000000	0.34	0.00	0.02	0.00	155.70	0.00	86.10	0.00	448.30
564	350	10	5000	1.69	0.15	0.33	0.27	173.10	0.30	135.20	0.39	0.10

565	350	10	10000	1.74	0.13	0.31	0.31	168.00	0.26	119.60	0.23	0.10
566	350	10	20000	1.76	0.12	0.34	0.24	150.80	0.13	107.20	0.10	0.10
567	350	10	50000	1.72	0.14	0.37	0.18	138.20	0.04	100.10	0.03	0.20
568	350	10	100000	1.86	0.07	0.40	0.11	136.00	0.02	97.60	0.00	0.50
569	350	10	200000	1.94	0.03	0.45	0.00	134.30	0.01	98.80	0.01	1.40
570	350	10	300000	1.97	0.01	0.44	0.02	134.80	0.01	98.30	0.01	2.00
571	350	10	400000	2.07	0.04	0.44	0.02	136.60	0.02	97.50	0.00	2.50
572	350	10	600000	2.00	0.01	0.43	0.04	134.40	0.01	96.80	0.01	4.30
573	350	10	800000	1.99	0.00	0.44	0.02	134.00	0.00	97.10	0.00	5.30
574	350	10	1000000	1.99	0.00	0.43	0.04	133.80	0.00	96.70	0.01	6.90
575	350	10	1200000	2.00	0.01	0.43	0.04	133.90	0.00	96.70	0.01	9.60
576	350	10	1600000	1.99	0.00	0.43	0.04	133.80	0.00	96.60	0.01	10.50
577	350	10	2000000	1.99	0.00	0.45	0.00	133.40	0.00	97.40	0.00	12.90
578	350	5	5000	1.66	0.16	0.18	0.18	190.00	0.20	124.80	0.30	0.50
579	350	5	10000	1.87	0.05	0.20	0.09	187.80	0.19	117.50	0.22	0.50
580	350	5	20000	1.81	0.08	0.20	0.09	178.20	0.13	112.50	0.17	0.70
581	350	5	50000	1.70	0.14	0.19	0.14	167.10	0.06	102.70	0.07	0.80
582	350	5	100000	1.86	0.06	0.21	0.05	161.20	0.02	97.70	0.01	1.40
583	350	5	200000	1.68	0.15	0.19	0.14	161.00	0.02	98.90	0.03	2.70
584	350	5	400000	1.72	0.13	0.20	0.09	159.40	0.01	98.60	0.02	5.90
585	350	5	500000	1.66	0.16	0.20	0.09	154.20	0.02	97.60	0.01	27.80
586	350	5	600000	2.00	0.02	0.22	0.00	158.20	0.00	96.60	0.00	8.70
587	350	5	800000	1.68	0.15	0.20	0.09	156.10	0.01	98.00	0.02	11.80
588	350	5	900000	1.92	0.03	0.22	0.00	159.40	0.01	96.80	0.01	0.00
589	350	5	1000000	1.89	0.04	0.22	0.00	157.70	0.00	96.80	0.01	14.80
590	350	5	1200000	1.97	0.00	0.22	0.00	158.00	0.00	96.50	0.00	16.90
591	350	5	1400000	1.89	0.04	0.22	0.00	157.50	0.00	96.70	0.00	20.40
592	350	5	1600000	1.92	0.03	0.22	0.00	157.70	0.00	96.60	0.00	22.70
593	350	5	2000000	1.97	0.00	0.22	0.00	157.90	0.00	96.30	0.00	27.90
594	350	2.5	5000	1.74	0.03	0.13	0.08	204.00	0.02	122.60	0.04	12.20
595	350	2.5	10000	1.81	0.07	0.14	0.17	201.80	0.03	119.90	0.02	9.40
596	350	2.5	20000	1.80	0.07	0.14	0.17	208.60	0.00	122.80	0.05	13.00
597	350	2.5	50000	1.65	0.02	0.12	0.00	206.10	0.01	119.90	0.02	10.30
598	350	2.5	100000	1.65	0.02	0.12	0.00	205.20	0.01	118.80	0.01	12.80
599	350	2.5	200000	1.72	0.02	0.13	0.08	206.90	0.01	119.00	0.01	18.60
600	350	2.5	400000	1.65	0.02	0.12	0.00	206.40	0.01	118.30	0.01	22.00
601	350	2.5	600000	1.69	0.00	0.13	0.08	205.40	0.01	116.00	0.01	34.10
602	350	2.5	800000	1.69	0.00	0.12	0.00	209.30	0.01	120.20	0.02	51.90
603	350	2.5	1000000	1.70	0.01	0.12	0.00	208.30	0.00	116.90	0.01	43.20
604	350	2.5	1200000	1.71	0.01	0.12	0.00	207.80	0.00	116.90	0.01	51.10
605	350	2.5	1400000	1.69	0.00	0.12	0.00	207.40	0.00	117.10	0.00	68.60
606	350	2.5	1600000	1.69	0.00	0.12	0.00	208.30	0.00	117.60	0.00	70.40
607	350	2.5	2000000	1.69	0.00	0.12	0.00	208.00	0.00	117.50	0.00	76.40
608	350	1.25	5000	1.87	0.06	0.13	0.18	205.40	0.02	135.20	0.19	195.00
609	350	1.25	10000	1.80	0.02	0.13	0.18	201.20	0.00	129.20	0.14	218.30
610	350	1.25	20000	1.86	0.05	0.13	0.18	201.20	0.00	124.80	0.10	186.70

611	350	1.25	50000	1.80	0.02	0.12	0.09	202.30	0.00	122.10	0.08	208.30
612	350	1.25	100000	1.75	0.01	0.12	0.09	200.70	0.01	119.10	0.05	176.70
613	350	1.25	200000	1.75	0.01	0.12	0.09	199.30	0.01	116.60	0.03	256.70
614	350	1.25	250000	1.75	0.01	0.11	0.00	200.80	0.01	116.80	0.03	195.00
615	350	1.25	300000	1.75	0.01	0.11	0.00	201.20	0.00	116.50	0.03	226.70
616	350	1.25	350000	1.77	0.00	0.11	0.00	201.20	0.00	116.20	0.03	225.00
617	350	1.25	400000	1.76	0.01	0.11	0.00	202.90	0.00	116.20	0.03	206.70
618	350	1.25	500000	1.76	0.01	0.11	0.00	201.10	0.00	115.10	0.02	251.70
619	350	1.25	600000	1.76	0.01	0.11	0.00	203.40	0.01	116.30	0.03	241.70
620	350	1.25	800000	1.78	0.01	0.11	0.00	200.60	0.01	113.50	0.00	263.30
621	350	1.25	1000000	1.77	0.00	0.11	0.00	200.90	0.01	112.90	0.00	303.30
622	350	1.25	1200000	1.77	0.00	0.11	0.00	201.50	0.00	113.50	0.00	403.30
623	350	1.25	1400000	1.77	0.00	0.11	0.00	200.20	0.01	112.60	0.01	293.30
624	350	1.25	1600000	1.77	0.00	0.11	0.00	200.30	0.01	112.70	0.01	366.70
625	350	1.25	2000000	1.77	0.00	0.11	0.00	202.10	0.00	113.30	0.00	343.30
626	400	10	5000	0.92	0.07	0.24	0.14	177.00	0.18	132.70	0.21	0.00
627	400	10	10000	0.92	0.07	0.23	0.18	170.80	0.13	125.20	0.14	0.00
628	400	10	20000	0.92	0.07	0.24	0.14	158.60	0.05	115.90	0.06	0.10
629	400	10	50000	0.88	0.11	0.26	0.07	152.40	0.01	111.70	0.02	0.40
630	400	10	100000	0.97	0.02	0.28	0.00	148.60	0.01	110.70	0.01	0.50
631	400	10	200000	0.99	0.00	0.28	0.00	151.00	0.00	110.30	0.01	1.60
632	400	10	400000	0.88	0.11	0.26	0.07	147.40	0.02	108.50	0.01	2.10
633	400	10	600000	1.00	0.01	0.28	0.00	149.70	0.01	109.60	0.00	3.30
634	400	10	800000	0.94	0.05	0.27	0.04	150.20	0.00	108.60	0.01	4.30
635	400	10	1200000	0.97	0.02	0.27	0.04	150.40	0.00	109.20	0.00	6.60
636	400	10	1600000	0.96	0.03	0.27	0.04	150.30	0.00	108.90	0.00	9.00
637	400	10	2000000	0.99	0.00	0.28	0.00	150.60	0.00	109.40	0.00	12.30
638	400	5	5000	1.06	0.21	0.13	0.24	202.30	0.12	125.40	0.19	0.30
639	400	5	10000	1.29	0.04	0.16	0.06	205.60	0.13	122.30	0.16	0.40
640	400	5	20000	1.38	0.03	0.17	0.00	194.00	0.07	113.40	0.08	0.40
641	400	5	50000	1.25	0.07	0.16	0.06	182.40	0.01	108.00	0.02	0.70
642	400	5	100000	1.12	0.16	0.15	0.12	180.80	0.00	107.70	0.02	1.20
643	400	5	200000	1.21	0.10	0.16	0.06	181.50	0.00	107.50	0.02	2.50
644	400	5	300000	1.34	0.00	0.17	0.00	182.90	0.01	105.10	0.00	4.70
645	400	5	400000	1.34	0.00	0.17	0.00	180.20	0.01	104.60	0.01	4.80
646	400	5	600000	1.34	0.00	0.17	0.00	180.30	0.00	104.60	0.01	7.40
647	400	5	800000	1.28	0.04	0.17	0.00	180.60	0.00	106.30	0.01	10.30
648	400	5	1200000	1.27	0.05	0.16	0.06	179.40	0.01	105.40	0.00	15.10
649	400	5	1600000	1.30	0.03	0.17	0.00	178.00	0.02	104.10	0.01	20.30
650	400	5	2000000	1.34	0.00	0.17	0.00	181.20	0.00	105.40	0.00	24.30
651	400	2.5	5000	1.24	0.11	0.12	0.20	230.60	0.03	137.70	0.11	7.30
652	400	2.5	10000	1.17	0.04	0.11	0.10	235.00	0.05	139.40	0.12	7.20
653	400	2.5	20000	1.21	0.08	0.11	0.10	238.40	0.06	137.30	0.10	7.40
654	400	2.5	50000	1.11	0.01	0.10	0.00	233.00	0.04	132.30	0.06	7.90
655	400	2.5	100000	1.11	0.01	0.10	0.00	235.50	0.05	136.00	0.09	9.30
656	400	2.5	200000	1.09	0.03	0.10	0.00	231.50	0.03	132.30	0.06	12.40

657	400	2.5	400000	1.11	0.01	0.10	0.00	231.40	0.03	130.90	0.05	17.90
658	400	2.5	800000	1.12	0.00	0.10	0.00	235.50	0.05	133.00	0.07	31.80
659	400	2.5	1200000	1.12	0.00	0.10	0.00	235.30	0.05	132.40	0.06	43.90
660	400	2.5	1600000	1.12	0.00	0.10	0.00	235.80	0.05	132.70	0.07	56.80
661	400	2.5	2000000	1.12	0.00	0.10	0.00	224.50	0.00	124.40	0.00	66.70
662	400	1.25	5000	1.24	0.08	0.10	0.11	238.10	0.03	151.70	0.19	141.20
663	400	1.25	10000	1.14	0.01	0.10	0.11	226.20	0.02	143.90	0.13	131.20
664	400	1.25	20000	1.20	0.04	0.10	0.11	231.40	0.00	140.80	0.10	129.50
665	400	1.25	50000	1.16	0.01	0.09	0.00	229.00	0.01	136.10	0.06	128.80
666	400	1.25	100000	1.14	0.01	0.09	0.00	228.60	0.01	133.30	0.04	130.70
667	400	1.25	150000	1.13	0.02	0.09	0.00	228.10	0.02	131.60	0.03	326.70
668	400	1.25	200000	1.14	0.01	0.09	0.00	229.20	0.01	131.50	0.03	139.80
669	400	1.25	400000	1.15	0.00	0.09	0.00	230.00	0.01	130.20	0.02	156.80
670	400	1.25	800000	1.16	0.01	0.09	0.00	231.20	0.00	128.80	0.01	191.70
671	400	1.25	1200000	1.16	0.01	0.09	0.00	232.10	0.00	128.30	0.00	226.70
672	400	1.25	1600000	1.16	0.01	0.09	0.00	231.70	0.00	127.80	0.00	381.70
673	400	1.25	2000000	1.15	0.00	0.09	0.00	231.80	0.00	127.90	0.00	286.70
674	500	10	5000	0.10	1.00	0.03	0.50	202.90	0.11	136.90	0.04	0.10
675	500	10	10000	0.09	0.80	0.03	0.50	195.00	0.07	133.60	0.02	0.30
676	500	10	20000	0.08	0.60	0.03	0.50	195.00	0.07	134.70	0.03	0.30
677	500	10	50000	0.07	0.40	0.03	0.50	184.60	0.01	131.30	0.00	0.90
678	500	10	100000	0.06	0.20	0.03	0.50	184.20	0.01	131.10	0.00	1.80
679	500	10	200000	0.06	0.20	0.03	0.50	185.40	0.01	132.30	0.01	4.00
680	500	10	300000	0.06	0.20	0.02	0.00	182.80	0.00	129.00	0.02	5.70
681	500	10	400000	0.05	0.00	0.02	0.00	182.70	0.00	130.20	0.01	7.90
682	500	10	800000	0.05	0.00	0.02	0.00	181.30	0.01	129.30	0.01	16.40
683	500	10	1000000	0.05	0.00	0.02	0.00	181.50	0.01	128.50	0.02	22.50
684	500	10	1200000	0.05	0.00	0.02	0.00	181.50	0.01	129.60	0.01	26.00
685	500	10	1400000	0.05	0.00	0.02	0.00	182.60	0.00	130.80	0.00	30.80
686	500	10	1600000	0.05	0.00	0.02	0.00	182.60	0.00	132.40	0.01	35.20
687	500	10	2000000	0.05	0.00	0.02	0.00	182.80	0.00	131.10	0.00	44.70
688	500	5	5000	0.10	1.00	0.03	0.50	202.90	0.11	136.90	0.04	0.10
689	500	5	10000	0.09	0.80	0.03	0.50	195.00	0.07	133.60	0.02	0.30
690	500	5	20000	0.08	0.60	0.03	0.50	195.00	0.07	134.70	0.03	0.30
691	500	5	50000	0.07	0.40	0.03	0.50	184.60	0.01	131.30	0.00	0.90
692	500	5	100000	0.06	0.20	0.03	0.50	184.20	0.01	131.10	0.00	1.80
693	500	5	200000	0.06	0.20	0.03	0.50	185.40	0.01	132.30	0.01	4.00
694	500	5	300000	0.06	0.20	0.02	0.00	182.80	0.00	129.00	0.02	5.70
695	500	5	400000	0.05	0.00	0.02	0.00	182.70	0.00	130.20	0.01	7.90
696	500	5	800000	0.05	0.00	0.02	0.00	181.30	0.01	129.30	0.01	16.40
697	500	5	1000000	0.05	0.00	0.02	0.00	181.50	0.01	128.50	0.02	22.50
698	500	5	1200000	0.05	0.00	0.02	0.00	181.50	0.01	129.60	0.01	26.00
699	500	5	1400000	0.05	0.00	0.02	0.00	182.60	0.00	130.80	0.00	30.80
700	500	5	1600000	0.05	0.00	0.02	0.00	182.60	0.00	132.40	0.01	35.20
701	500	5	2000000	0.05	0.00	0.02	0.00	182.80	0.00	131.10	0.00	44.70
702	500	3	5000	0.17	0.15	0.02	0.00	258.80	0.07	149.00	0.06	9.60

703	500	2.5	10000	0.18	0.10	0.02	0.00	262.90	0.05	148.80	0.06	8.70
704	500	2.5	20000	0.23	0.15	0.02	0.00	285.40	0.03	147.50	0.05	8.50
705	500	2.5	50000	0.19	0.05	0.02	0.00	271.10	0.02	141.70	0.01	11.10
706	500	2.5	100000	0.20	0.00	0.02	0.00	280.30	0.01	142.00	0.01	11.40
707	500	2.5	200000	0.20	0.00	0.02	0.00	275.10	0.01	138.10	0.01	16.00
708	500	2.5	400000	0.21	0.05	0.02	0.00	282.30	0.02	139.90	0.00	24.20
709	500	2.5	600000	0.20	0.00	0.02	0.00	278.80	0.01	138.20	0.01	33.50
710	500	2.5	800000	0.21	0.05	0.02	0.00	283.60	0.02	139.20	0.01	43.20
711	500	2.5	1000000	0.20	0.00	0.02	0.00	275.30	0.01	138.80	0.01	51.80
712	500	2.5	1200000	0.21	0.05	0.02	0.00	281.80	0.02	138.00	0.02	61.80
713	500	2.5	1400000	0.22	0.10	0.02	0.00	289.10	0.04	138.20	0.01	69.50
714	500	2.5	1600000	0.20	0.00	0.02	0.00	277.40	0.00	139.20	0.01	78.50
715	500	2.5	2000000	0.20	0.00	0.02	0.00	277.40	0.00	140.20	0.00	96.00
716	500	1.25	5000	0.18	0.05	0.02	1.00	267.20	0.03	166.50	0.14	104.00
717	500	1.25	10000	0.17	0.11	0.02	1.00	261.60	0.05	159.60	0.09	96.80
718	500	1.25	20000	0.19	0.00	0.02	1.00	280.10	0.01	159.20	0.09	76.00
719	500	1.25	50000	0.20	0.05	0.02	1.00	274.00	0.01	154.30	0.05	121.70
720	500	1.25	100000	0.19	0.00	0.01	0.00	274.00	0.01	152.50	0.04	88.70
721	500	1.25	150000	0.19	0.00	0.02	1.00	275.90	0.00	152.00	0.04	76.80
722	500	1.25	200000	0.19	0.00	0.01	0.00	274.80	0.01	150.50	0.03	110.00
723	500	1.25	400000	0.19	0.00	0.01	0.00	274.00	0.01	150.10	0.03	91.70
724	500	1.25	600000	0.19	0.00	0.01	0.00	277.20	0.00	148.40	0.01	106.80
725	500	1.25	800000	0.19	0.00	0.01	0.00	274.40	0.01	148.20	0.01	117.70
726	500	1.25	1000000	0.19	0.00	0.01	0.00	275.70	0.00	148.70	0.02	124.80
727	500	1.25	1200000	0.19	0.00	0.01	0.00	276.40	0.00	148.00	0.01	140.30
728	500	1.25	1400000	0.19	0.00	0.01	0.00	274.40	0.01	147.40	0.01	165.70
729	500	1.25	1600000	0.19	0.00	0.01	0.00	274.50	0.01	147.30	0.01	190.00
730	500	1.25	2000000	0.19	0.00	0.01	0.00	276.40	0.00	146.40	0.00	200.00
731	600	10	5000	0.35	1.06	0.03	0.50	255.40	0.29	152.30	0.20	0.00
732	600	10	10000	0.11	0.35	0.02	0.00	207.30	0.05	150.50	0.18	0.10
733	600	10	20000	0.32	0.88	0.03	0.50	255.90	0.29	159.60	0.26	0.10
734	600	10	50000	0.17	0.00	0.02	0.00	227.30	0.15	143.10	0.13	0.20
735	600	10	100000	0.14	0.18	0.02	0.00	201.20	0.02	133.10	0.05	0.40
736	600	10	200000	0.14	0.18	0.02	0.00	190.80	0.04	130.60	0.03	0.70
737	600	10	400000	0.22	0.29	0.03	0.50	215.00	0.08	132.20	0.04	1.70
738	600	10	600000	0.21	0.24	0.03	0.50	209.80	0.06	131.10	0.03	2.70
739	600	10	800000	0.17	0.00	0.02	0.00	199.70	0.01	130.00	0.02	3.40
740	600	10	1200000	0.16	0.06	0.02	0.00	196.70	0.01	128.60	0.01	5.60
741	600	10	1600000	0.16	0.06	0.02	0.00	193.90	0.02	126.50	0.00	7.60
742	600	10	2000000	0.17	0.00	0.02	0.00	198.20	0.00	127.10	0.00	9.30
743	600	5	5000	0.02	0.98	0.00	1.00	187.60	0.59	173.40	0.05	0.60
744	600	5	10000	0.43	0.53	0.02	0.50	333.50	0.27	193.50	0.17	0.60
745	600	5	20000	0.47	0.48	0.03	0.25	331.90	0.27	195.60	0.18	0.60
746	600	5	50000	0.58	0.36	0.03	0.25	402.00	0.12	182.60	0.10	0.80
747	600	5	100000	0.65	0.29	0.03	0.25	415.10	0.09	178.90	0.08	1.30
748	600	5	200000	0.51	0.44	0.03	0.25	370.90	0.19	169.60	0.02	2.40

749	600	5	400000	0.75	0.18	0.04	0.00	430.70	0.06	180.30	0.09	4.80
750	600	5	800000	0.60	0.34	0.03	0.25	386.00	0.16	156.10	0.06	9.70
751	600	5	900000	0.73	0.20	0.04	0.00	410.50	0.10	159.80	0.04	10.40
752	600	5	1000000	0.73	0.20	0.04	0.00	399.30	0.13	156.80	0.05	11.40
753	600	5	1100000	0.86	0.05	0.04	0.00	464.50	0.02	180.50	0.09	13.00
754	600	5	1200000	0.91	0.00	0.04	0.00	454.40	0.01	172.00	0.04	14.80
755	600	5	1600000	0.90	0.01	0.04	0.00	450.40	0.01	167.80	0.01	19.10
756	600	5	2000000	0.91	0.00	0.04	0.00	456.90	0.00	165.60	0.00	24.10
757	600	2.5	5000	0.53	0.15	0.02	0.33	423.60	0.02	207.80	0.06	11.70
758	600	2.5	10000	0.51	0.18	0.02	0.33	405.40	0.06	187.80	0.15	11.60
759	600	2.5	20000	0.66	0.06	0.03	0.00	398.00	0.07	210.70	0.04	10.70
760	600	2.5	50000	0.62	0.00	0.03	0.00	400.80	0.07	214.60	0.02	11.30
761	600	2.5	100000	0.56	0.10	0.03	0.00	393.90	0.08	216.10	0.02	11.80
762	600	2.5	200000	0.63	0.02	0.03	0.00	400.70	0.07	219.30	0.00	15.00
763	600	2.5	400000	0.62	0.00	0.03	0.00	414.20	0.04	217.50	0.01	21.80
764	600	2.5	800000	0.64	0.03	0.03	0.00	431.50	0.00	218.70	0.01	33.70
765	600	2.5	1200000	0.64	0.03	0.03	0.00	439.00	0.02	221.20	0.01	46.70
766	600	2.5	1600000	0.65	0.05	0.03	0.00	430.70	0.00	218.10	0.01	60.80
767	600	2.5	2000000	0.62	0.00	0.03	0.00	430.10	0.00	220.00	0.00	73.40
768	600	1.25	5000	0.67	0.08	0.03	0.00	394.10	0.08	217.70	0.00	211.70
769	600	1.25	10000	0.67	0.08	0.03	0.00	392.90	0.08	219.00	0.01	190.00
770	600	1.25	20000	0.66	0.06	0.03	0.00	405.50	0.05	214.20	0.01	176.70
771	600	1.25	50000	0.69	0.11	0.03	0.00	418.30	0.02	213.30	0.02	168.30
772	600	1.25	100000	0.64	0.03	0.03	0.00	417.70	0.02	214.10	0.01	170.00
773	600	1.25	200000	0.62	0.00	0.03	0.00	419.00	0.02	212.80	0.02	175.00
774	600	1.25	400000	0.61	0.02	0.03	0.00	424.60	0.01	214.50	0.01	190.00
775	600	1.25	800000	0.60	0.03	0.03	0.00	425.10	0.01	214.40	0.01	238.30
776	600	1.25	1200000	0.61	0.02	0.03	0.00	427.30	0.00	217.90	0.01	255.00
777	600	1.25	1600000	0.61	0.02	0.03	0.00	426.10	0.00	215.60	0.01	290.00
778	600	1.25	2000000	0.62	0.00	0.03	0.00	428.10	0.00	216.70	0.00	326.70
779	700	10	5000	0.45	21.50	0.04	3.00	375.80	0.83	212.90	0.30	0.00
780	700	10	10000	0.27	12.50	0.03	2.00	318.60	0.55	193.60	0.18	0.00
781	700	10	20000	0.26	12.00	0.03	2.00	320.30	0.56	193.50	0.18	0.00
782	700	10	50000	0.09	3.50	0.02	1.00	250.70	0.22	178.90	0.09	0.00
783	700	10	100000	0.03	0.50	0.01	0.00	218.70	0.06	168.70	0.03	0.00
784	700	10	200000	0.03	0.50	0.01	0.00	210.70	0.02	167.60	0.02	0.00
785	700	10	400000	0.03	0.50	0.01	0.00	209.10	0.02	167.10	0.02	0.00
786	700	10	600000	0.02	0.00	0.01	0.00	208.70	0.02	165.70	0.01	0.00
787	700	10	800000	0.02	0.00	0.01	0.00	206.20	0.00	164.10	0.00	0.00
788	700	10	1200000	0.02	0.00	0.01	0.00	205.80	0.00	163.80	0.00	0.00
789	700	10	1600000	0.02	0.00	0.01	0.00	205.70	0.00	163.80	0.00	0.00
790	700	10	2000000	0.02	0.00	0.01	0.00	205.60	0.00	163.80	0.00	0.00
791	700	5	5000	0.29	0.93	0.02	0.00	375.90	0.31	220.40	0.31	1.00
792	700	5	10000	0.24	0.60	0.02	0.00	343.80	0.20	212.90	0.27	1.20
793	700	5	20000	0.18	0.20	0.02	0.00	312.00	0.09	191.30	0.14	1.20
794	700	5	50000	0.16	0.07	0.02	0.00	296.80	0.04	176.40	0.05	2.60

795	700	5	100000	0.15	0.00	0.02	0.00	289.60	0.01	173.10	0.03	3.80
796	700	5	200000	0.15	0.00	0.02	0.00	288.40	0.01	172.90	0.03	5.70
797	700	5	400000	0.17	0.13	0.02	0.00	307.00	0.07	188.50	0.12	11.60
798	700	5	600000	0.15	0.00	0.02	0.00	286.80	0.00	168.40	0.00	24.80
799	700	5	800000	0.15	0.00	0.02	0.00	286.60	0.00	167.40	0.00	25.50
800	700	5	1000000	0.14	0.07	0.02	0.00	278.10	0.03	165.00	0.02	29.50
801	700	5	1200000	0.18	0.20	0.02	0.00	304.20	0.06	182.60	0.09	38.50
802	700	5	1400000	0.15	0.00	0.02	0.00	284.10	0.01	168.20	0.00	46.70
803	700	5	1600000	0.15	0.00	0.02	0.00	287.50	0.00	170.80	0.02	46.70
804	700	5	2000000	0.15	0.00	0.02	0.00	286.30	0.00	168.10	0.00	73.70
805	700	2.5	5000	0.39	0.13	0.02	0.33	456.00	0.07	238.20	0.03	10.40
806	700	2.5	10000	0.39	0.13	0.02	0.33	464.10	0.05	230.60	0.00	10.00
807	700	2.5	20000	0.45	0.00	0.03	0.00	491.00	0.00	228.70	0.01	10.10
808	700	2.5	50000	0.43	0.04	0.02	0.33	479.30	0.02	233.80	0.01	13.20
809	700	2.5	100000	0.49	0.09	0.03	0.00	516.60	0.05	234.20	0.01	12.30
810	700	2.5	200000	0.42	0.07	0.02	0.33	474.80	0.03	233.10	0.01	17.30
811	700	2.5	400000	0.52	0.16	0.03	0.00	519.00	0.06	235.00	0.02	34.00
812	700	2.5	600000	0.44	0.02	0.02	0.33	481.40	0.02	233.50	0.01	39.30
813	700	2.5	800000	0.46	0.02	0.03	0.00	501.30	0.02	233.30	0.01	42.30
814	700	2.5	1000000	0.44	0.02	0.02	0.33	486.90	0.01	232.00	0.01	46.30
815	700	2.5	1200000	0.48	0.07	0.03	0.00	509.90	0.04	232.50	0.01	55.70
816	700	2.5	1400000	0.45	0.00	0.03	0.00	493.10	0.00	232.30	0.01	68.80
817	700	2.5	1600000	0.43	0.04	0.02	0.33	477.40	0.03	232.90	0.01	69.30
818	700	2.5	2000000	0.49	0.09	0.03	0.00	513.10	0.05	233.90	0.01	91.80
819	700	2.5	2400000	0.42	0.07	0.02	0.33	471.40	0.04	234.50	0.02	116.20
820	700	2.5	2800000	0.45	0.00	0.03	0.00	493.70	0.01	233.00	0.01	115.30
821	700	2.5	3200000	0.51	0.13	0.03	0.00	516.90	0.05	234.70	0.02	155.80
822	700	2.5	3600000	0.45	0.00	0.03	0.00	490.70	0.00	229.20	0.01	146.50
823	700	2.5	4000000	0.45	0.00	0.03	0.00	490.70	0.00	230.80	0.00	162.20
824	700	1.25	5000	0.36	0.12	0.02	0.00	444.20	0.09	234.20	0.02	136.50
825	700	1.25	10000	0.43	0.05	0.02	0.00	464.10	0.05	256.60	0.08	97.80
826	700	1.25	20000	0.45	0.10	0.03	0.50	480.50	0.01	242.10	0.02	112.80
827	700	1.25	50000	0.41	0.00	0.02	0.00	474.80	0.02	240.90	0.01	86.00
828	700	1.25	100000	0.42	0.02	0.02	0.00	479.80	0.01	240.40	0.01	87.30
829	700	1.25	200000	0.40	0.02	0.02	0.00	475.60	0.02	237.70	0.00	92.30
830	700	1.25	400000	0.41	0.00	0.02	0.00	484.10	0.00	237.60	0.00	122.00
831	700	1.25	600000	0.41	0.00	0.02	0.00	483.10	0.01	236.40	0.01	127.80
832	700	1.25	800000	0.41	0.00	0.02	0.00	483.20	0.01	236.30	0.01	136.70
833	700	1.25	1000000	0.40	0.02	0.02	0.00	478.70	0.02	238.90	0.00	210.00
834	700	1.25	1200000	0.41	0.00	0.02	0.00	482.20	0.01	238.00	0.00	142.20
835	700	1.25	1400000	0.41	0.00	0.02	0.00	482.10	0.01	237.70	0.00	203.30
836	700	1.25	1600000	0.40	0.02	0.02	0.00	480.00	0.01	236.40	0.01	161.80
837	700	1.25	2000000	0.41	0.00	0.02	0.00	486.50	0.00	238.40	0.00	203.30
838	800	10	5000	2.87	142.50	0.13	12.00	855.40	3.12	224.90	0.30	0.00
839	800	10	10000	2.76	137.00	0.14	13.00	674.40	2.25	248.80	0.44	0.10
840	800	10	20000	3.84	191.00	0.18	17.00	763.30	2.67	262.90	0.52	0.10

841	800	10	50000	2.45	121.50	0.12	11.00	658.10	2.17	253.40	0.47	0.10
842	800	10	75000	1.76	87.00	0.10	9.00	531.00	1.56	254.60	0.48	0.20
843	800	10	100000	2.08	103.00	0.11	10.00	611.50	1.94	241.20	0.40	0.30
844	800	10	150000	2.03	100.50	0.11	10.00	572.80	1.76	244.40	0.42	0.40
845	800	10	200000	1.49	73.50	0.09	8.00	524.50	1.52	237.70	0.38	0.50
846	800	10	250000	1.56	77.00	0.09	8.00	507.40	1.44	241.80	0.40	0.50
847	800	10	300000	1.44	71.00	0.08	7.00	541.30	1.60	224.40	0.30	0.60
848	800	10	400000	1.06	52.00	0.06	5.00	471.30	1.27	217.00	0.26	1.20
849	800	10	600000	0.03	0.50	0.01	0.00	213.60	0.03	176.60	0.02	1.60
850	800	10	800000	0.03	0.50	0.01	0.00	212.00	0.02	175.30	0.02	1.70
851	800	10	1000000	0.03	0.50	0.01	0.00	212.30	0.02	176.20	0.02	2.30
852	800	10	1200000	0.03	0.50	0.01	0.00	211.40	0.02	174.00	0.01	2.80
853	800	10	1600000	0.02	0.00	0.01	0.00	207.40	0.00	172.70	0.00	3.60
854	800	10	2000000	0.02	0.00	0.01	0.00	207.80	0.00	172.50	0.00	5.40
855	800	5	5000	1.30	0.16	0.06	0.14	676.80	0.09	296.80	0.27	0.30
856	800	5	10000	1.37	0.12	0.06	0.14	669.20	0.07	282.00	0.20	0.50
857	800	5	20000	1.94	0.25	0.09	0.29	673.70	0.08	286.60	0.22	0.40
858	800	5	50000	1.58	0.02	0.07	0.00	645.30	0.04	272.60	0.16	0.50
859	800	5	100000	1.38	0.11	0.07	0.00	609.40	0.02	254.20	0.08	0.80
860	800	5	200000	1.38	0.11	0.07	0.00	631.70	0.01	267.30	0.14	1.70
861	800	5	400000	1.44	0.07	0.07	0.00	632.50	0.01	238.80	0.02	2.90
862	800	5	600000	1.52	0.02	0.07	0.00	600.90	0.04	235.80	0.01	5.00
863	800	5	800000	1.51	0.03	0.07	0.00	633.10	0.02	230.90	0.02	6.30
864	800	5	1200000	1.41	0.09	0.07	0.00	578.50	0.07	227.60	0.03	8.70
865	800	5	1400000	1.56	0.01	0.07	0.00	616.90	0.01	237.60	0.01	10.70
866	800	5	1600000	1.55	0.00	0.07	0.00	623.40	0.00	234.50	0.00	11.90
867	800	2.5	5000	0.90	0.03	0.04	0.00	542.40	0.05	316.20	0.03	7.50
868	800	2.5	10000	1.01	0.09	0.05	0.25	573.70	0.00	309.80	0.01	6.90
869	800	2.5	20000	0.92	0.01	0.04	0.00	548.20	0.04	306.80	0.00	8.30
870	800	2.5	50000	0.85	0.09	0.04	0.00	556.10	0.03	305.80	0.00	7.40
871	800	2.5	100000	0.80	0.14	0.04	0.00	538.60	0.06	306.40	0.00	8.20
872	800	2.5	200000	0.94	0.01	0.04	0.00	572.70	0.00	307.70	0.00	10.60
873	800	2.5	400000	0.86	0.08	0.04	0.00	554.40	0.03	304.90	0.01	17.70
874	800	2.5	600000	0.89	0.04	0.04	0.00	564.00	0.02	309.10	0.01	22.00
875	800	2.5	800000	0.98	0.05	0.04	0.00	598.00	0.04	307.70	0.00	20.80
876	800	2.5	1000000	0.84	0.10	0.04	0.00	552.40	0.04	308.30	0.00	26.70
877	800	2.5	1200000	0.93	0.00	0.04	0.00	568.60	0.01	311.30	0.01	33.00
878	800	2.5	1400000	0.79	0.15	0.04	0.00	533.00	0.07	308.80	0.01	50.30
879	800	2.5	1600000	0.80	0.14	0.04	0.00	538.50	0.06	311.10	0.01	39.90
880	800	2.5	2000000	0.93	0.00	0.04	0.00	573.90	0.00	306.90	0.00	46.80
881	800	1.25	5000	1.01	0.06	0.05	0.25	588.20	0.02	320.30	0.02	191.70
882	800	1.25	10000	1.01	0.06	0.05	0.25	578.20	0.04	327.70	0.04	136.50
883	800	1.25	20000	1.00	0.05	0.04	0.00	590.20	0.02	311.30	0.01	128.50
884	800	1.25	50000	1.00	0.05	0.04	0.00	596.80	0.01	319.80	0.01	154.00
885	800	1.25	100000	0.98	0.03	0.04	0.00	605.60	0.01	313.30	0.01	155.00
886	800	1.25	200000	0.92	0.03	0.04	0.00	595.00	0.01	309.60	0.02	183.30

887	800	1.25	400000	0.96	0.01	0.04	0.00	599.70	0.00	312.40	0.01	183.30
888	800	1.25	600000	0.97	0.02	0.04	0.00	600.10	0.00	313.70	0.01	186.70
889	800	1.25	800000	0.94	0.01	0.04	0.00	597.90	0.01	313.60	0.01	151.50
890	800	1.25	1000000	0.95	0.00	0.04	0.00	602.00	0.00	311.80	0.01	201.70
891	800	1.25	1200000	0.95	0.00	0.04	0.00	598.40	0.00	314.30	0.00	178.30
892	800	1.25	1400000	0.94	0.01	0.04	0.00	597.50	0.01	312.60	0.01	241.70
893	800	1.25	1600000	0.95	0.00	0.04	0.00	598.40	0.00	313.30	0.01	195.00
894	800	1.25	2000000	0.95	0.00	0.04	0.00	601.20	0.00	315.40	0.00	313.30
895	900	10	5000	1.49	0.33	0.10	0.11	416.60	0.14	258.90	0.28	0.00
896	900	10	10000	0.80	0.29	0.06	0.33	367.40	0.01	229.70	0.13	0.10
897	900	10	20000	0.66	0.41	0.06	0.33	322.30	0.12	205.10	0.01	0.10
898	900	10	50000	0.82	0.27	0.07	0.22	343.80	0.06	208.70	0.03	0.10
899	900	10	100000	1.03	0.08	0.08	0.11	356.90	0.02	202.60	0.00	0.30
900	900	10	200000	0.97	0.13	0.08	0.11	357.50	0.02	199.80	0.01	0.60
901	900	10	400000	1.01	0.10	0.08	0.11	355.50	0.03	204.20	0.01	1.40
902	900	10	600000	0.96	0.14	0.08	0.11	350.30	0.04	201.50	0.00	2.20
903	900	10	800000	1.20	0.07	0.09	0.00	370.90	0.02	203.70	0.01	2.80
904	900	10	1000000	0.69	0.38	0.06	0.33	315.90	0.13	194.00	0.04	4.10
905	900	10	1200000	0.65	0.42	0.06	0.33	312.70	0.14	191.10	0.06	4.30
906	900	10	1600000	1.15	0.03	0.09	0.00	367.70	0.01	204.30	0.01	6.10
907	900	10	2000000	0.96	0.14	0.08	0.11	348.30	0.05	199.90	0.01	8.10
908	900	10	3000000	1.16	0.04	0.09	0.00	367.40	0.01	202.90	0.00	12.40
909	900	10	4000000	1.00	0.11	0.08	0.11	354.40	0.03	199.50	0.01	17.10
910	900	10	5000000	1.12	0.00	0.09	0.00	364.80	0.00	202.40	0.00	20.70
911	900	5	5000	3.05	0.23	0.15	0.17	624.90	0.09	371.80	0.03	0.50
912	900	5	10000	2.70	0.31	0.14	0.22	565.10	0.18	387.00	0.07	0.50
913	900	5	20000	3.23	0.18	0.16	0.11	590.50	0.14	395.00	0.09	0.50
914	900	5	50000	2.78	0.29	0.14	0.22	566.80	0.18	366.40	0.01	0.70
915	900	5	100000	2.42	0.39	0.12	0.33	559.60	0.19	369.70	0.02	1.00
916	900	5	200000	4.40	0.12	0.20	0.11	719.10	0.05	378.20	0.05	1.90
917	900	5	400000	2.74	0.30	0.14	0.22	582.70	0.15	348.30	0.04	3.50
918	900	5	800000	3.79	0.04	0.18	0.00	674.20	0.02	362.90	0.00	7.10
919	900	5	1200000	4.12	0.05	0.19	0.06	696.00	0.01	367.20	0.01	12.00
920	900	5	1600000	3.62	0.08	0.17	0.06	642.00	0.07	360.70	0.00	15.10
921	900	5	2000000	4.13	0.05	0.19	0.06	696.00	0.01	365.30	0.01	19.00
922	900	5	3000000	3.88	0.02	0.18	0.00	681.60	0.01	361.40	0.00	28.40
923	900	5	4000000	3.81	0.03	0.18	0.00	672.80	0.02	361.60	0.00	40.00
924	900	5	6000000	3.94	0.00	0.18	0.00	687.90	0.00	361.80	0.00	58.80
925	900	2.5	5000	3.62	0.09	0.16	0.06	665.80	0.11	405.50	0.01	10.40
926	900	2.5	10000	3.69	0.07	0.16	0.06	712.60	0.04	388.90	0.05	10.00
927	900	2.5	20000	3.60	0.10	0.15	0.12	688.70	0.08	400.00	0.02	10.40
928	900	2.5	50000	3.71	0.07	0.16	0.06	740.30	0.01	399.00	0.02	10.70
929	900	2.5	100000	3.33	0.16	0.14	0.18	696.90	0.06	401.50	0.02	11.80
930	900	2.5	200000	3.14	0.21	0.14	0.18	659.20	0.12	399.50	0.02	13.50
931	900	2.5	400000	2.83	0.29	0.12	0.29	635.50	0.15	397.70	0.03	18.80
932	900	2.5	800000	2.85	0.28	0.12	0.29	635.90	0.15	395.00	0.03	28.00

933	900	2.5	1200000	3.81	0.04	0.16	0.06	758.50	0.02	402.10	0.02	37.70
934	900	2.5	1600000	3.85	0.03	0.16	0.06	760.50	0.02	403.20	0.01	45.90
935	900	2.5	2000000	4.01	0.01	0.17	0.00	768.50	0.03	407.60	0.00	67.80
936	900	2.5	2400000	3.98	0.00	0.17	0.00	745.30	0.00	408.60	0.00	71.00
937	900	1.25	5000	3.86	0.11	0.16	0.14	686.30	0.04	398.10	0.03	208.33
938	900	1.25	10000	3.52	0.01	0.15	0.07	671.60	0.06	403.00	0.02	178.33
939	900	1.25	50000	3.57	0.02	0.14	0.00	708.60	0.01	410.70	0.00	173.33
940	900	1.25	100000	3.46	0.01	0.14	0.00	715.20	0.00	405.60	0.02	190.00
941	900	1.25	200000	3.50	0.00	0.14	0.00	717.00	0.00	408.90	0.01	178.33
942	900	1.25	400000	3.54	0.01	0.14	0.00	721.90	0.01	410.70	0.00	221.67
943	900	1.25	600000	3.52	0.01	0.14	0.00	718.80	0.00	412.50	0.00	258.33
944	900	1.25	800000	3.49	0.00	0.14	0.00	713.90	0.00	412.10	0.00	220.00
945	900	1.25	1000000	3.50	0.00	0.14	0.00	718.20	0.00	413.60	0.00	276.67
946	900	1.25	1200000	3.52	0.01	0.14	0.00	717.60	0.00	414.00	0.00	233.33
947	900	1.25	1400000	3.51	0.01	0.14	0.00	719.30	0.01	413.00	0.00	356.67
948	900	1.25	1600000	3.56	0.02	0.14	0.00	725.20	0.01	414.90	0.01	265.00
949	900	1.25	2000000	3.49	0.00	0.14	0.00	715.60	0.00	412.20	0.00	316.67
950	1000	10	5000	0.16	0.07	0.01	0.00	402.50	0.13	327.40	0.29	0.20
951	1000	10	10000	0.15	0.00	0.01	0.00	462.20	0.00	253.40	0.00	0.80
952	1000	5	5000	0.27	0.60	0.01	0.67	492.10	0.30	470.10	0.10	0.40
953	1000	5	10000	0.46	0.32	0.02	0.33	833.40	0.18	360.80	0.15	0.70
954	1000	5	20000	0.50	0.26	0.03	0.00	616.70	0.12	393.00	0.08	1.50
955	1000	5	50000	1.02	0.50	0.04	0.33	1087.80	0.55	373.60	0.12	0.70
956	1000	5	100000	1.47	1.16	0.06	1.00	938.20	0.33	500.10	0.18	1.00
957	1000	5	200000	1.25	0.84	0.05	0.67	953.10	0.35	477.20	0.12	1.70
958	1000	5	400000	1.12	0.65	0.05	0.67	984.30	0.40	437.90	0.03	3.50
959	1000	5	500000	1.08	0.59	0.05	0.67	964.80	0.37	425.90	0.00	4.60
960	1000	5	600000	1.17	0.72	0.05	0.67	1129.50	0.61	399.10	0.06	6.40
961	1000	5	800000	1.17	0.72	0.05	0.67	1110.90	0.58	397.10	0.07	8.30
962	1000	5	1200000	1.19	0.75	0.05	0.67	1116.90	0.59	405.80	0.05	11.00
963	1000	5	1600000	0.69	0.01	0.03	0.00	703.10	0.00	426.00	0.00	13.90
964	1000	5	2000000	0.64	0.06	0.03	0.00	686.20	0.02	423.30	0.01	17.90
965	1000	5	3000000	0.68	0.00	0.03	0.00	703.50	0.00	425.50	0.00	26.30
966	1000	2.5	5000	0.46	0.02	0.02	0.00	746.80	0.11	352.10	0.18	9.30
967	1000	2.5	10000	0.44	0.02	0.02	0.00	723.70	0.07	352.90	0.18	8.50
968	1000	2.5	20000	0.55	0.22	0.02	0.00	742.40	0.10	411.30	0.04	9.00
969	1000	2.5	50000	0.71	0.58	0.03	0.50	802.80	0.19	430.30	0.00	8.90
970	1000	2.5	100000	0.69	0.53	0.03	0.50	764.20	0.13	456.00	0.06	10.00
971	1000	2.5	200000	0.67	0.49	0.03	0.50	797.10	0.18	437.20	0.02	11.40
972	1000	2.5	400000	0.68	0.51	0.03	0.50	846.80	0.25	437.90	0.02	16.10
973	1000	2.5	800000	0.66	0.47	0.03	0.50	838.40	0.24	444.10	0.03	24.30
974	1000	2.5	1200000	0.47	0.04	0.02	0.00	679.90	0.01	443.00	0.03	48.40
975	1000	2.5	1600000	0.50	0.11	0.02	0.00	691.40	0.02	442.40	0.03	46.60
976	1000	2.5	2000000	0.45	0.00	0.02	0.00	675.30	0.00	430.30	0.00	61.80
977	1000	1.25	5000	0.66	0.05	0.03	0.00	785.20	0.03	444.10	0.01	185.00
978	1000	1.25	10000	0.70	0.11	0.03	0.00	747.60	0.07	439.10	0.02	152.30

979	1000	1.25	20000	0.61	0.03	0.03	0.00	747.30	0.07	429.50	0.04	149.20
980	1000	1.25	50000	0.65	0.03	0.03	0.00	763.80	0.05	439.20	0.02	134.20
981	1000	1.25	100000	0.66	0.05	0.03	0.00	786.90	0.03	439.10	0.02	171.70
982	1000	1.25	200000	0.65	0.03	0.03	0.00	784.30	0.03	451.40	0.00	165.80
983	1000	1.25	400000	0.62	0.02	0.03	0.00	792.70	0.02	453.80	0.01	195.00
984	1000	1.25	600000	0.60	0.05	0.03	0.00	775.00	0.04	454.70	0.01	186.70
985	1000	1.25	800000	0.62	0.02	0.03	0.00	807.30	0.00	448.80	0.00	173.30
986	1000	1.25	1000000	0.62	0.02	0.03	0.00	794.40	0.02	453.70	0.01	216.70
987	1000	1.25	1200000	0.62	0.02	0.03	0.00	791.80	0.02	453.80	0.01	208.30
988	1000	1.25	1400000	0.64	0.02	0.03	0.00	807.30	0.00	456.90	0.02	261.70
989	1000	1.25	1600000	0.64	0.02	0.03	0.00	808.20	0.00	455.40	0.01	233.30
990	1000	1.25	2000000	0.63	0.00	0.03	0.00	807.50	0.00	449.30	0.00	290.00

8.4 Appendix D

The table below presents the Method B models analytically

$DV_{0.5}$	*Method B Model (Mesh C)*	R^2
35	$N_{p,cr} = (6.03 \times 10^{-4} + 1.94 \times 10^{-3} devPF)^{-2}$	99.8%
50	$N_{p,cr} = (6.75 \times 10^{-4} + 5.97 \times 10^{-3} devPF)^{-2}$	99.0%
70	$N_{p,cr} = (6.73 \times 10^{-4} + 2.89 \times 10^{-3} devPF)^{-2}$	97.8%
80	$N_{p,cr} = (8.51 \times 10^{-4} + 1.03 \times 10^{-2} devPF)^{-2}$	92.8%
100	$N_{p,cr} = (8.02 \times 10^{-4} + 2.57 \times 10^{-2} devPF)^{-2}$	95.6%
125	$N_{p,cr} = (6.56 \times 10^{-4} + 1.02 \times 10^{-2} devPF)^{-2}$	95.7%
150	$N_{p,cr} = (8.70 \times 10^{-4} + 9.94 \times 10^{-3} devPF)^{-2}$	99.6%
200	$N_{p,cr} = (1.10 \times 10^{-3} + 2.16 \times 10^{-2} devPF)^{-2}$	99.2%
250	$N_{p,cr} = (1.59 \times 10^{-3} + 2.79 \times 10^{-2} devPF)^{-2}$	100.0%
300	$N_{p,cr} = (1.32 \times 10^{-3} + 9.89 \times 10^{-3} devPF)^{-2}$	70.8%
350	$N_{p,cr} = (8.39 \times 10^{-4} + 4.97 \times 10^{-2} devPF)^{-2}$	96.1%
400	$N_{p,cr} = (2.03 \times 10^{-3} + 7.01 \times 10^{-2} devPF)^{-2}$	99.5%
500	$N_{p,cr} = (2.51 \times 10^{-3} + 1.44 \times 10^{-2} devPF)^{-2}$	97.9%
600	$N_{p,cr} = (4.16 \times 10^{-3} + 5.01 \times 10^{-3} devPF)^{-2}$	55.1%
700	$N_{p,cr} = (2.36 \times 10^{-3} + 8.25 \times 10^{-4} devPF)^{-2}$	95.9%
800	$N_{p,cr} = (2.09 \times 10^{-3} + 2.99 \times 10^{-3} devPF)^{-2}$	91.8%
900	$N_{p,cr} = (1.94 \times 10^{-3} + 2.29 \times 10^{-2} devPF)^{-2}$	82.1%
1000	$N_{p,cr} = (1.00 \times 10^{-2} + 6.21 \times 10^{-2} devPF)^{-2}$	99.9%
$DV_{0.5}$	*Method B Model (Mesh M)*	R^2
35	$N_{p,cr} = (7.43 \times 10^{-4} + 5.60 \times 10^{-3} devPF)^{-2}$	89.2%
50	$N_{p,cr} = (6.62 \times 10^{-4} + 5.92 \times 10^{-3} devPF)^{-2}$	97.8%
70	$N_{p,cr} = (4.62 \times 10^{-4} + 7.44 \times 10^{-3} devPF)^{-2}$	97.6%
80	$N_{p,cr} = (1.00 \times 10^{-3} + 1.00 \times 10^{-2} devPF)^{-2}$	99.4%
100	$N_{p,cr} = (7.69 \times 10^{-4} + 4.61 \times 10^{-3} devPF)^{-2}$	99.5%
125	$N_{p,cr} = (7.32 \times 10^{-4} + 1.63 \times 10^{-2} devPF)^{-2}$	89.9%
150	$N_{p,cr} = (1.03 \times 10^{-3} + 2.21 \times 10^{-2} devPF)^{-2}$	94.8%
200	$N_{p,cr} = (1.56 \times 10^{-3} + 1.88 \times 10^{-2} devPF)^{-2}$	97.4%
250	$N_{p,cr} = (1.29 \times 10^{-3} + 4.88 \times 10^{-2} devPF)^{-2}$	96.2%

300	$N_{p,cr} = (2.00 \times 10^{-3} + 2.20 \times 10^{-2} devPF)^{-2}$	87.5%
350	$N_{p,cr} = (2.03 \times 10^{-3} + 7.01 \times 10^{-2} devPF)^{-2}$	98.9%
400	$N_{p,cr} = (1.66 \times 10^{-3} + 8.34 \times 10^{-3} devPF)^{-2}$	92.7%
500	$N_{p,cr} = (2.43 \times 10^{-3} + 3.45 \times 10^{-2} devPF)^{-2}$	98.7%
600	$N_{p,cr} = (6.39 \times 10^{-4} + 9.33 \times 10^{-3} devPF)^{-2}$	93.4%
700	$N_{p,cr} = (2.88 \times 10^{-3} + 1.23 \times 10^{-2} devPF)^{-2}$	94.8%
800	$N_{p,cr} = (4.54 \times 10^{-3} + 1.75 \times 10^{-1} devPF)^{-2}$	74.1%
900	$N_{p,cr} = (5.42 \times 10^{-3} + 2.15 \times 10^{-2} devPF)^{-2}$	97.8%
1000	$N_{p,cr} = (1.61 \times 10^{-3} + 1.42 \times 10^{-2} devPF)^{-2}$	90.3%
$DV_{0.5}$	***Method B Model (Mesh F)***	***R^2***
35	$N_{p,cr} = (5.89 \times 10^{-4} + 3.17 \times 10^{-3} devPF)^{-2}$	98.6%
50	$N_{p,cr} = (8.74 \times 10^{-4} + 2.06 \times 10^{-2} devPF)^{-2}$	96.6%
70	$N_{p,cr} = (5.29 \times 10^{-4} + 1.81 \times 10^{-2} devPF)^{-2}$	96.5%
80	$N_{p,cr} = (7.49 \times 10^{-4} + 8.45 \times 10^{-3} devPF)^{-2}$	99.2%
100	$N_{p,cr} = (7.00 \times 10^{-4} + 1.03 \times 10^{-2} devPF)^{-2}$	97.8%
125	$N_{p,cr} = (7.28 \times 10^{-4} + 4.09 \times 10^{-2} devPF)^{-2}$	95.2%
150	$N_{p,cr} = (9.55 \times 10^{-4} + 1.11 \times 10^{-2} devPF)^{-2}$	99.7%
200	$N_{p,cr} = (9.65 \times 10^{-4} + 6.70 \times 10^{-2} devPF)^{-2}$	98.9%
250	$N_{p,cr} = (9.89 \times 10^{-3} + 9.36 \times 10^{-2} devPF)^{-2}$	86.3%
300	$N_{p,cr} = (1.73 \times 10^{-3} + 6.20 \times 10^{-2} devPF)^{-2}$	95.3%
350	$N_{p,cr} = (3.82 \times 10^{-3} + 3.58 \times 10^{-2} devPF)^{-2}$	89.2%
400	$N_{p,cr} = (2.86 \times 10^{-3} + 4.67 \times 10^{-2} devPF)^{-2}$	75.0%
500	$N_{p,cr} = (2.20 \times 10^{-3} + 7.67 \times 10^{-2} devPF)^{-2}$	96.5%
600	$N_{p,cr} = (3.29 \times 10^{-3} + 4.97 \times 10^{-2} devPF)^{-2}$	80.2%
800	$N_{p,cr} = (2.86 \times 10^{-3} + 2.95 \times 10^{-2} devPF)^{-2}$	41.6%
900	$N_{p,cr} = (1.29 \times 10^{-3} + 1.06 \times 10^{-2} devPF)^{-2}$	99.6%
1000	$N_{p,cr} = (2.67 \times 10^{-3} + 2.22 \times 10^{-2} devPF)^{-2}$	98.2%
$DV_{0.5}$	***Method B Model (Mesh VF)***	***R^2***
35	$N_{p,cr} = (6.76 \times 10^{-4} + 5.10 \times 10^{-3} devPF)^{-2}$	95.1%
50	$N_{p,cr} = (6.91 \times 10^{-4} + 7.86 \times 10^{-3} devPF)^{-2}$	96.7%
70	$N_{p,cr} = (6.24 \times 10^{-4} + 1.21 \times 10^{-2} devPF)^{-2}$	96.3%
80	$N_{p,cr} = (6.97 \times 10^{-4} + 8.50 \times 10^{-3} devPF)^{-2}$	97.9%
100	$N_{p,cr} = (7.39 \times 10^{-4} + 1.01 \times 10^{-2} devPF)^{-2}$	97.8%
125	$N_{p,cr} = (2.77 \times 10^{-3} + 1.21 \times 10^{-2} devPF)^{-2}$	64.1%
150	$N_{p,cr} = (2.31 \times 10^{-3} + 6.81 \times 10^{-2} devPF)^{-2}$	79.1%
200	$N_{p,cr} = (2.14 \times 10^{-3} + 3.67 \times 10^{-2} devPF)^{-2}$	92.1%
250	$N_{p,cr} = (9.88 \times 10^{-4} + 1.48 \times 10^{-1} devPF)^{-2}$	91.8%
300	$N_{p,cr} = (1.92 \times 10^{-3} + 1.79 \times 10^{-2} devPF)^{-2}$	95.2%
350	$N_{p,cr} = (2.66 \times 10^{-3} + 6.91 \times 10^{-2} devPF)^{-2}$	96.5%
400	$N_{p,cr} = (2.78 \times 10^{-3} + 8.31 \times 10^{-2} devPF)^{-2}$	96.2%
500	$N_{p,cr} = (2.66 \times 10^{-3} + 3.44 \times 10^{-2} devPF)^{-2}$	84.9%
600	$N_{p,cr} = (1.83 \times 10^{-3} + 2.11 \times 10^{-2} devPF)^{-2}$	96.4%
700	$N_{p,cr} = (2.86 \times 10^{-3} + 1.46 \times 10^{-1} devPF)^{-2}$	89.6%
800	$N_{p,cr} = (5.77 \times 10^{-3} + 6.30 \times 10^{-1} devPF)^{-2}$	76.8%
900	$N_{p,cr} = (2.07 \times 10^{-3} + 1.17 \times 10^{-1} devPF)^{-2}$	99.9%

1000	$N_{p,cr} = (3.29 \times 10^{-3} + 6.14 \times 10^{-2} devPF)^{-2}$	80.9%

8.5 Appendix E

Below is the SPSS report from the Method C statistical analysis.

Variables Entered/Removed[a]

Model	Variables Entered	Variables Removed	Method
1	devD10, DV50, Cell, devPF3, devMC3, devD32[b]	.	Enter

a. Dependent Variable: sqrtNp

b. All requested variables entered.

Model Summary

Model	R	R Square	Adjusted R Square	Std. Error of the Estimate
1	.780[a]	.608	.604	.002135082971224

a. Predictors: (Constant), devD10, DV50, Cell, devPF3, devMC3, devD32

ANOVA[a]

Model		Sum of Squares	df	Mean Square	F	Sig.
1	Regression	.003	6	.001	124.592	.000[b]
	Residual	.002	481	.000		
	Total	.006	487			

a. Dependent Variable: sqrtNp

b. Predictors: (Constant), devD10, DV50, Cell, devPF3, devMC3, devD32

Coefficients[a]

Model		Unstandardized Coefficients		Standardized Coefficients		
		B	Std. Error	Beta	t	Sig.
1	(Constant)	.001	.000		3.666	.000
	DV50	4.628E-6	.000	.399	13.747	.000

	Cell	-5.592E-5	.000	-.056	-1.908	.057
	devPF3	.000	.000	-.039	-.712	.477
	devMC3	.003	.001	.198	3.258	.001
	devD32	-.003	.002	-.089	-1.343	.180
	devD10	.026	.002	.645	12.672	.000

a. Dependent Variable: sqrtNp